PUB-5457

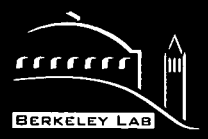

ERNEST ORLANDO LAWRENCE BERKELEY NATIONAL LABORATORY

Superbend Conceptual Design Report

Advanced Light Source Division

April 1999

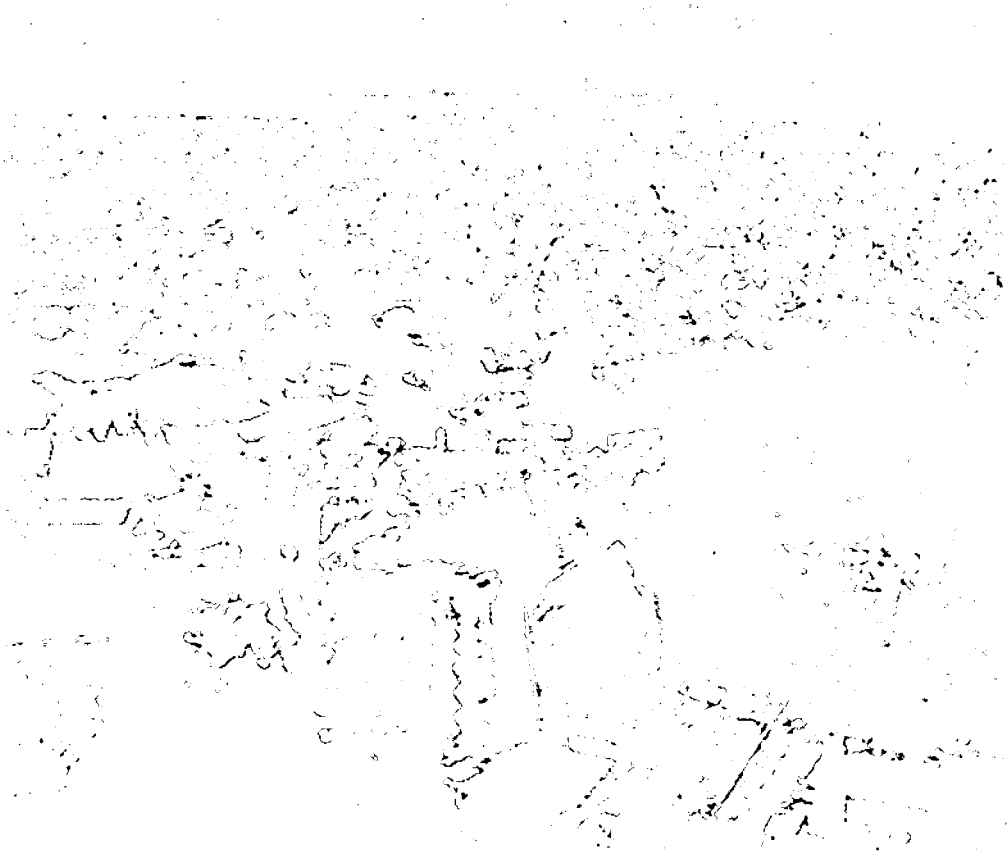

DISCLAIMER

SUPERBEND

Conceptual Design Report

Advanced Light Source
April 15, 2000

This work was supported by the Director, Office of Science. Office of Basic Energy Sciences under U.S Department of Energy Contract No. DE-AC03-76SF00098 and Industry Contract BG9928300.

TABLE OF CONTENTS

SUMMARY

The Superbend magnets described herein are bending (dipole) magnets are high-field superconducting magnets, with nominal peak field 0T and on-axis field $\int Bdz = 1.08$ T-m.

The superbend magnets will greatly expand the ALS's photon energy range. Three superbend magnets will replace conventional bends in sectors 4, 8, and 12 of the ALS storage ring. They will provide at existing beamport locations six photon fans having a critical energy of 12 keV for 12 new beamlines.

The conceptual design report includes sections on:

1.0 SCOPE
2.0 PARAMETER DEFINITION AND REVIEW PROCESSES
3.0 ACCELERATOR PHYSICS AND OPERATIONAL ISSUES
4.0 SUPERBEND DIPOLE SPECIFICATIONS
5.0 DIPOLE MAGNETIC MEASURMENTS AND FIDUCIALIZATION
6.0 VACUUM CHAMBER MODIFICATIONS
7.0 CONTROLS
8.0 POWER SUPPLIES
9.0 MAGNET AND CRYOSTAT DIAGNOSTICS
10.0 ACCELERATOR TEST PLANS
11.0 UTILITIES

The cost estimate and associated fabrication schedules for the superbend magnets, associated quadrupole magnets, power supplies, diagnostics, vacuum chamber modifications, control system, diagnostics, and installation are found elsewhere.

SUPERBENDS PROJECT BASELINE SCOPE

1.1 General

This document shall serve to define the core scope of the Superbend Project.

The scope includes the design, test, fabrication and installation of three super conducting dipole magnets to replace the center bend magnets in sectors 4, 8 and 12. These magnets shall produce a peak field of 6 Tesla which will generate a 10^0 bend in the electron beam. The magnets shall be cooled by a cryocooler and shall utilize Dewars as a back up system.

The scope includes design, fabrication, testing and installation of 6 QDA magnets (one on either side of each new super bend magnet) which will replace the defocusing component of the removed center bend magnets.

The scope includes the design, procurement and installation of a separate power supply for each pair of QFA magnets that are immediately upstream and downstream of the new super bend magnet.

The scope includes development of a magnet measurement system and performing magnet measurements on the new quadrupoles and the super conducting dipole magnets.

The scope includes the design, purchase and installation of all utilities, controls and diagnostics necessary to install and operate the above noted equipment.

1.2 Conventional facilities

Provide layout and detail drawings along with all components and modifications to existing facilities, necessary to provide for the successful installation and operation of 3 Superbend magnets in the ALS SR at sectors 4, 8 & 12. This will include either modifying or providing new, Roof shielding blocks at each location along with any facility modifications necessary to provide for 2 new Quadrupole magnets at each location along with cryogenic components in support of the Superbend cryostat.

1.3 Superconducting dipoles

1.3.1 Preliminary Design

- **Test cryostat fabrication**

  This is under design and fabrication at Wang NMR – original price was $30,000. Increases are due to purchase of HTS leads and increased testing time at Wang NMR.

- **Cryocooler I purchase**

  Price of Sumitomo SRDK-415DW is $45,000 (out the door price).

- **Cryostat testing**

  This is the cryogenic system and HTS lead testing that will be done to verify the suitability of the design for use in the ALS. Wang included 2 weeks of preliminary testing in their proposal, and it is necessary to perform significantly more testing than this to make sure we have the cryogenics system in hand.

- **Superbend suspension strap test**

  We feel a long-term creep test is needed to ensure that the magnet remains in proper position. If creep is a problem, external adjustment may be necessary. Purchase at least 3 straps, as close as possible to the final configuration for long-term creep tests. Need to purchase fittings and spherical bearings to accurately mock up the actual configuration. Testing will be constant load (dead weight type testing would be the best)

- **HTS leads purchase**

  We include the purchase of 2 more pair of HTS current leads for additional testing at LBL. These would be to replace items that failed in testing, leads that are redesigned because of the testing results, or additional leads to look at another HTS approach

- **Conceptual redesign effort at Wang NMR**

  Because of interferences with the ALS vacuum chamber, beamlines and other elements, the cryostat and suspension strap design must be modified,. Also, there is redesign (add fiducials on the cold mass and possible observation ports in the vacuum vessel) necessitated by the alignment requirements. Another item under consideration is to allow for rapid magnet readjustment by external adjusters.

1.3.2 Detailed Design

- **R&D prior to design review**

  This is for Cryostat test planning, preparation of magnet design document, planning meetings, etc.

- **Test cryostat/leads testing**

  Testing at Wang and LBL to verify that we understand the heat loads, cooling capability of the cryocooler, and HTS lead performance.

- **Reviews & meetings**

  Extra effort spent in presentation preparation, making presentations, follow-up to review comments, etc.

- **Prototype magnet & cryostat design**

  Engineering effort needed to document the engineering requirements necessary for procurement to proceed. Areas are magnet, cryogenics, alignment, and structural.

- **Prototype liaison**

  Engineering and designer effort needed to provide technical oversight to Vendor during the prototype fabrication and vendor testing verification.

- **Prototype testing**

  The engineering and designer effort needed to plan, carryout, and document the prototype cryogenics and HTS lead testing at LBL. Also, to provide cryogenics support during the period of magnetic measurements.

- **Design modifications**

  The engineering and designer effort needed to translate prototype test results into design requirements changes for the production magnets.

- **Production liaison**

  Engineering and designer effort needed to provide technical oversight to Vendor during the fabrication of the three production magnets and verification of Vendor testing.

- **Production testing**

  The engineering and designer effort needed to plan, carryout, and document the cryogenics and HTS lead testing of the three production magnets at LBL. Also, to provide cryogenics support during the period of magnetic measurements.

- **Magnet installation assistance**

  The engineering and designer effort needed to assist in the installation of the Superbend magnets. (This is incidental assistance, not the main effort).

- **External cryogenics design**

  The engineering and designer effort needed to design, specify, and prepare procurements documentation for the ancillary cryogenic equipment needed to operate the Superbend magnets in case of cryocooler failure.

- **External cryogenics liaison**

  Engineering and designer effort needed to provide technical oversight to Vendor(s) during the fabrication of the cryogenic support hardware purchased in 1.3.4 below.

- **External cryogenics installation oversight**

  Engineering and designer effort needed to provide technical oversight in the installation of the cryogenic support equipment purchased in 1.3.4 below.

1.3.3 Magnet/cryostat fabrication

1.3.3.1 Prototype magnet

- **Magnet & cryostat**

  We foresee tighter requirements on the Superbend for magnet and yoke fabrication, alignment, compliance with pressure vessel safety than are allowed for in the present conceptual design, resulting in an estimated price of $125,000 for the prototype.

- **Cryocooler II**

  We assume cryostat tests will show the Sumitomo 415 to be adequate for the Superbend Prototype.- $45,000.

1.3.3.2 Production magnets

- **Magnet & cryostat**

  We estimate a price of $125,000 for each production magnet, and assume that 3 production units will be purchased.

- **Cryocooler III**

  We assume that the Sumitomo 415 will be adequate for the Superbend Prototype - $45,000 each, 3 required. We plan to have 5 cryocoolers, 3 that are in use on the ALS, one that is being reconditioned at the manufacturer, and one that is a spare at LBL.

1.3.4 External cryogenics fabrication

LN Dewars, Piping, and Valves - This is our estimate of the hardware needed to connect LN to the 3 Superbend locations in case of cryocooler failure. Piping and valves will be preinstalled with the LN Dewar positioned outside the shielding blocks. This will allow for rapid connection of LN, and ease of maintenance.

LHe Dewars, Piping, and Valves - This is our estimate of the hardware needed to connect LHe to the 3 Superbend locations in case of cryocooler failure. Piping and valves will be preinstalled, with the LHe Dewar positioned outside the shielding blocks. This will allow for rapid connection of LHe, and ease of maintenance.

1.3.5 Survey & alignment

- **Prototype**

  LBL will need to provide Survey and Alignment personnel to assist Vendor in getting the magnet in the proper position and correlated with external fiducials on the cryostat vessel

- **Production**

  LBL will need to provide Survey and Alignment personnel to assist Vendor in getting each production magnet in the proper position and correlated with external fiducials on the cryostat vessel.

1.3.6 Magnet/cryostat testing

1.3.6.1 Prototype magnet

- **Area preparation**

  Test Area Preparation – This is the estimated expense of setting up the area to test the Superbend prototype magnet.

- **Cryogenics testing**

  This is for the manpower and equipment needed to thoroughly test the prototype Superbend cryogenic and HTS Leads.
  After the tests to characterize the short-term cryogenic and magnetic performance are completed, the prototype will be subjected to a series of long term cryogenic and magnetic measurements tests to make sure the long-term behavior is understood and suitable for use in the ALS.

- **Magnetic measurements**

  Static magnetic integral multipole measurements will be performed on a total of four super-bend dipole magnets as a check on performance, to a characterize individual differences between the four, and to relate magnet fiducials to the magnetic field. In addition, simple Hall probe and eddy current measurements will be performed on the first unit. If accelerator physics studies indicate that detailed 3d field maps are required, this activity must be re-scoped.

  Integral multipole measurements will use the coil that was used for the SB4 test magnet. Some software development will be required to prepare the Metrolab magnetic measurement system for these measurements. Multipole measurements will be used to define the horizontal and vertical integral magnetic center. A procedure must be developed and fixtures designed and fabricated to relate the magnetic center to magnet fiducials. Integral multipole measurements will also be used to define the angular orientation of the dipole field. This will require purchase of an appropriate instrument to accurately measure the coil angular orientation relative to level.

  Simple Hall probe measurements will provide a profile of B_y along the centerline. These measurements will be done manually with probe placement controlled to ~1 mm.

1.3.6.2 Production magnet testing

- **Area preparation**

  Test Area Preparation – This is the estimated expense of setting up the area to test the Superbend production magnets. Need struts, etc.

- **Cryogenics testing**

  This is the total manpower and equipment needed to thoroughly test each production Superbend cryogenic and HTS Leads.

  After the tests to characterize the cryogenic and magnetic performance are completed, as many production magnets as possible will be subjected to a series of long term cryogenic and magnetic measurements tests to make sure the long-term behavior is understood and suitable for use in the ALS.

1.4 Quadrupoles

The super-bend project will require the construction and installation of six new quadrupole magnets. These magnets will be based upon the ALS storage ring QD design, and will utilize existing core laminations and fabrication and assembly fixtures wherever possible. In addition to fabrication and assembly, the scope of this activity includes integral multipole measurements and fiducialization.

The tasks required for completion are itemized below.

- Magnet fabrication and assembly
  - Locate and identify existing QD components.
    - Laminations
    - Die
    - Coil winding fixtures and molds
  - Core stacking fixutre
  - Assemble drawing package
  - Develop fabrication and assembly plan
    - Coils
    - Cores
    - Coil core assembly and wiring
  - Procurement(s)/JO(s)

- Magnet measurements and fiducialization
  - ➢ Develop and test data acquisition program
  - ➢ Design fiducialization procedure
  - ➢ Design and fabricate fixtures
  - ➢ Measurements and fiducialization

1.5 Photon Stops

Provide calculations, layout and detail drawings along with all components necessary to replace the existing Storage Ring Photon Stops and blank off flanges with new components that will be adequate to withstand the increased heat load from the 6T Superbend magnet at ALS SR at sectors 4, 8 & 12. Develop and implement a plan to provide adequate equipment protection for a beam missteer of 3 mr at the center of the Superbend magnet.

1.6 Power Supplies

1.6.1 Power supply specifications for Superbend magnet

To accommodate the various ALS beam operation energies, the super conductive magnet current will increase or decrease over a range of about 240 to 300 Amperes linearly. The maximum current slew rate of this operation is 3A/sec. The power supply will be designed to operate continuously without a super conductive magnet persistence circuit. A protection circuit will be provided as a part of the super bend magnet, to discharge the coil energy, in case of the magnet quenches. This protection circuit is constructed as an integral part of the super conductive magnet. The power supply design will incorporate internal circuitry to protect against possible damage to the power supply (or magnet) when AC power failure occurs unexpectedly. The power supply specifications are given in chapter 8.

- **Power supply control**

The existing power supplies at the ALS are controlled with an analog signal of ± 10V. The proposed power supplies for the super bend magnets can be controlled in the same fashion. If however digital control is preferable then this method can be implemented as required.

- **Power supply location**

Space is available for instrumentation and power supplies needed for three super bend magnet. AC power is available and LCW is available. A preliminary drawing

of the instrumentation rack space is shown on figure 1 (not available on this E-mail).

- **Current measurements**

The current will be measured with a current transducer of Danfysik type 860R. The maximum current range of this device is 40 to 600 Amperes in which the accuracy is specified to 50 ppm. The stability is in the order of 1 ppm/°C

1.6.2 Power supplies for QDA and QFA magnets

The power supply requirements on the quadrupoles (QFA and QDA) will be the same as they are on the existing quadrupoles (QFA & QD) installed at the ALS. The power supply output voltage and current ranges are 54 Volt for the QFA and 40 Volt for the QDA while the maximum current for both supplies is 130 A. The stability requirements for these supplies is 1 part in 10,000.

1.6.3 Number of power supplies needed

Power Supply function	Number of supplies needed per section	Total number of supplies needed including spares
Superbend magnet	1	4
QFA	2	8
QFD	2	8

1.7 Controls/diagnostics

- **Superbend magnetic field**

Two Hall probes capable of measuring 6 T field will be installed in or near the main dipole field of the magnet. The probes will be attached to the cryostat and will be available during magnetic measurements. Two probes are installed because of the difficulty and cost associated with replacement of a defective unit once the cryostat and magnet have been installed in the storage ring. We will use Group 3, model DTM-151 Teslameters with LPT-141 Hall probes. The probes are calibrated by GMW Associates (Group 3 representatives) against an NMR instrument in a uniform field of 6T. Calibration data are contained in an EPROM installed in the probe connector. The Teslameter will be read by the control system via the GPIB at 10 readings per second. Superbend power supply operation may be referred to the measured field instead of the usual control system magnet current set point.

- **Superbend magnet coil temperature**

  Two cryogenic temperature sensors accurate from 3.5 to 325° K will sense the superconducting coil temperature. One sensor will be a spare. These sensors must function in a high magnetic field and some degree of ionizing radiation. Cernox (Lake Shore) temperature sensors are suitable. The Lake Shore model 218 Temperature Monitor reads up to eight sensors at about 1 Hz. It displays corrected temperature readings and provides GPIB connection to external computers for external monitoring. In addition, the monitor provides temperature set-point alarms that will be used to interlock the magnet coil power supply. The intention is to prohibit energizing the magnet coils if they are not in the superconducting state (at about 11° K or below). These temperature sensors will be fully evaluated in the test cryostat.

- **High TC leads**

  The voltage drop across the high TC leads will be monitored continuously and archived along with other ALS system data. Ideally, the voltage drop will be zero if the leads are superconducting. There are two reasons why the voltage drop may increase. [1] The high temperature end of the HTC leads may warm and lose superconductivity. [2] The HTC leads may deteriorate over time and require replacement. Case [1] should not be fatal to the leads although it will result in lost beam. If the voltage drop exceeds a specified level, the magnet coil power supply will be shut off to prevent lead destruction. This means we must have an interlock to disable the power supply, and we must dissipate the stored energy in the magnet while not inducing a quench or producing excessive power in the HTC leads. The acceptable time constant for absorption of magnet energy in an external load is 100 seconds. At this rate the voltage produced across the magnet coils will not forward bias the cold diodes in the internal quench protection circuitry. We assume the HTC leads can be cooled quickly and normal ALS operation resumed.

  If the leads have become defective (case [2]), then the cryostat and magnet will be replaced.

- **Cryogenic level sensing**

  The level of liquid helium in the lower Dewar will be sensed by a commercially available superconducting helium level monitor (AMI model 135 or equivalent). The helium level will be monitored in the ALS control system via a GPIB interface to the instrument. If the helium level becomes too low, the instrument will sound an alarm to alert operators.

  Liquid nitrogen level will be measured with an AMI model 185 (or equal) cryogenic liquid level sensor. These instruments detect liquid level by capacitance measurement in a cryogenic probe. External monitoring and alarms will be handled as above. We expect some of the nitrogen will be frozen solid. It is not

known at this time if the probe will continue to function properly in frozen nitrogen.

These instruments will be fully evaluated in the test cryostat.

- **Cryostat pressure**

The super insulation in the cryostat will function well only if the cryostat is evacuated. We will install a conventional ion gauge on the cryostat to measure pressure. The heat from the ion gauge filaments must be isolated from the cryostat via a vacuum pipe to prevent a heat load on the cryopump. A set-point alarm will alert operators if the cryostat pressure rises or if the ion gauge fails.

- **Magnet coil voltage**

Two leads connected across each superconducting coil will be monitored by the control system. The extra leads are for redundancy. The voltage across the coils will normally be zero if the current is not changing. The coil inductance and the di/dt will determine any voltage we measure. During ramping conditions or during a magnet quench the voltage may exceed the dynamic range of control system digitizers. External circuits will attenuate the voltage to a safe value. It is not now expected that we will use this voltage for an interlock, but we could trip the quench prevention circuits if the voltage becomes too high for any reason. During magnet testing this voltage will be monitored to characterize the magnet coil inductance in a variety of circumstances. These data could be useful if we have difficulties with a magnet (for example a shorted turn).

- **Errant photon beam interlock (EPBI)**

The photon beam produced by the Superbend magnets can damage the vacuum chamber if the electron beam orbit through the magnet is vertically distorted. Beam position monitors (all ready in place) on both sides of the Superbend will be used to detect excessive vertical orbit shifts and will cause the stored beam to be aborted. Special beam position monitor electronics have been designed to protect the vacuum chamber from missteered insertion device beam. With slight modifications these electronics will serve as Superbend photon beam interlocks.

- **Cryostat testing**

The ALS electrical engineering group will support the cryostat test program with data acquisition systems and software applications.

1.8 Installation

- **Mechanical Installation**

  Provide layout and detail drawings along with all components and modifications to existing facilities, necessary to develop a process to successfully, *in situ* machine the Storage Ring Vacuum chambers at sectors 4, 8 & 12 so that the Superbend Cryostat can be properly installed and aligned around the storage ring chamber.

  Provide plans and schedules along with layout and detail drawings as well as components and modifications to existing facilities, necessary to successfully install all components associated with 3 Superbend magnets at Storage Ring Sectors 4, 8 & 12.

- **Electrical installation**

  The electrical installation consists of installing three standard 19" double electrical racks in the Storage Ring Sectors 4, 8, and 12. Overhead wireway and ladder tray will be installed to connect these racks to the existing AC power and signal cable facilities. An electrical cable right of way inside the Storage Ring shielding will be made by core drilling through the Storage Ring inner concrete shield wall in sectors 4, 8, and 12 and sawing an 18" wide trench across the Storage Ring walkway in these three sectors. In addition to the QFA, QDA and Super Bend magnet power supplies, a number of additional electrical chassis for power distribution, computer control and equipment protection will be installed in the 19" racks.

PARAMETER CHANGES AND REVIEW PROCESSES

2.1 ALS Project Change Authorization Procedure

2.1.1 Purpose

The purpose of this procedure is to define how the Change Authorization form is to be completed and to define the limits of the Change Authorization process.

2.1.2 Process

The Change Authorization form can be initiated by anyone on the project who identifies a change in the scope, schedule or budget that would affect a project baseline beyond the threshold limits noted below. The completed form must be approved by the Project Lead Engineer, Project Manager, and Project Leader. The form is then given to the Project Coordinator for assignment of a change number, logging and distribution.

At the start of the project the Project Lead Engineer, Project Manager, Project Leader and Project Coordinator will work together with the project team to develop a project core scope document (defining the important deliverables for the project), project baseline schedule (including milestones) and a project Total Estimated Cost (TEC). These items will then be approved by ALS Management and will define the project baseline against which all changes will be made.

2.1.3 Thresholds

The Change Authorization form must be filled out and approved before any of the following thresholds are exceeded:

1) An increase of $25K or more to any of the WBS level 2 categories. This increase will be deducted from the approved contingency funds for the project.

2) A delay in the completion of any of the baseline milestones greater than 1 month.

3) Any change to the project core scope document.

4) Any change to the project TEC or to the project completion date must be approved by ALS Management.

2.2 Superbend Change Authorization Form

Superbend Project Change Authorization

ALS Planning and Administration

Change Number: _____

Change Originated By: _____

Change Description

Change Justification

Schedule Change (current and revised milestone dates)
(See Attached)

Budget Change Description

Approvals

Project Lead Engineer	R. Schlueter	Date
Project Manager	J. Krupnick	Date
Project Leader	D. Robin	Date

cc: A. Paterson

2.3 Superbend Project Detailed Budget Revisions

Change Number: _____

Change Originated By: _____

	Current Budget ($K)	Proposed Budget ($K)	Change
1.1 Project Management	78		
1.2 Conventional Facilities	122		
1.3 Dipole	1759		
1.4 Quadrupoles	226		
1.5 Photon Stops & Blanks	193		
1.6 Power Supplies	446		
1.7 Controls &Diagnostics	300		
1.8 Installation	200		
1.9 Contingency	653		
Total	3977		

2.4 Review processes

Superbend reviews associated with critical project milestones are incorporated into the master schedule:

- The project team was formed and Superbend kickoff occurred in September 1998.
- A physics review (chair: S. Krinsky) was conducted in December 1998, validating accelerator physics related Superbend specifications and high-level dipole strategic design decisions.
- A superbend and quadrupole power supply review (chair: R. Keller) was held April 20, 1999, which validated specifications s for superbend and quadrupole magnet power supplies so we could proceed with procurement.
- A superbend quadrupole review (chair: J. Tanabe) was held in May 6, 1999. The superbend quadrupole construction/procurement/operation plan was validated so we could proceed with quadrupole magnet construction/procurement.
- A pre-prototype procurement superbend magnet review (chairs: R. Scanlan and K. Robinson) was held July 7-8 1999. The superbend cost and schedule were critiqued and the technical design affirmed in preparation for prototype magnet procurement.
- A pre-prototype fabrication superbend dipole design review of Wang by LBL was conducted in November 1999. This formed the basis for finalization of the design package prior to letting the dipole first article contract.
- A status review will be held in April 2000 to give Lab management a project update and assess progress.
- A pre-production procurement superbend magnet review will be held in the Fall 2000 to assess performance of the prototype superbend dipole magnet and implications for production units.
- A pre-ALS installation review will be conducted in 2001 to review all 4 Superbend magnets, associated quadrupole, controls, and subsystem performance testing before installation of Superbends into the ALS storage ring.

ACCELERATOR PHYSICS AND OPERATIONAL ISSUES

3.1 Introduction

In this section we discuss the relevant accelerator physics and operational issues connected with operating the ALS with superbends in order to motivate the tolerances on the superbends. We begin with a description of the storage ring and how it will be modified to include superbends. Then we discuss the operational requirements and how they drive the tolerances. We conclude with a summary table of the tolerances.

3.2 Modifying the storage ring to include Superbends

The magnetic lattice of the Advanced Light Source storage ring consists of 12 sectors. An overview of the storage ring is shown in Figure 1. Each of the 12 sectors has a triple bend achromat structure. A typical sector without Superbends is shown in the top of Figure 2. These sectors will be referred to as normal sectors. The basic idea of the Superbend project is to modify 3 of the 12 sectors in the ring (4, 8 and 12) to include Superbends. A Superbend sector is shown in the bottom of Figure 2. These sectors will be referred to as Superbend sectors.

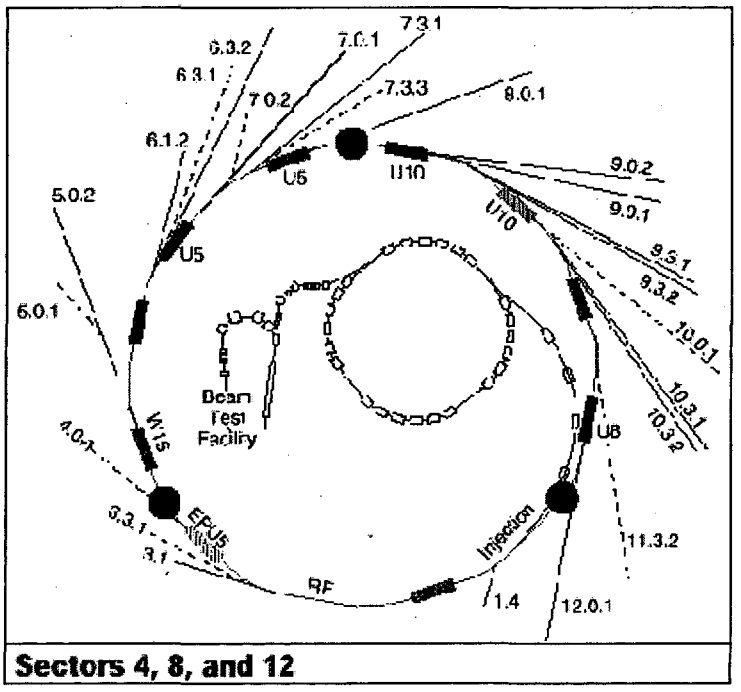

Figure 1. Overview of the ALS with with the location of the superbends marked.

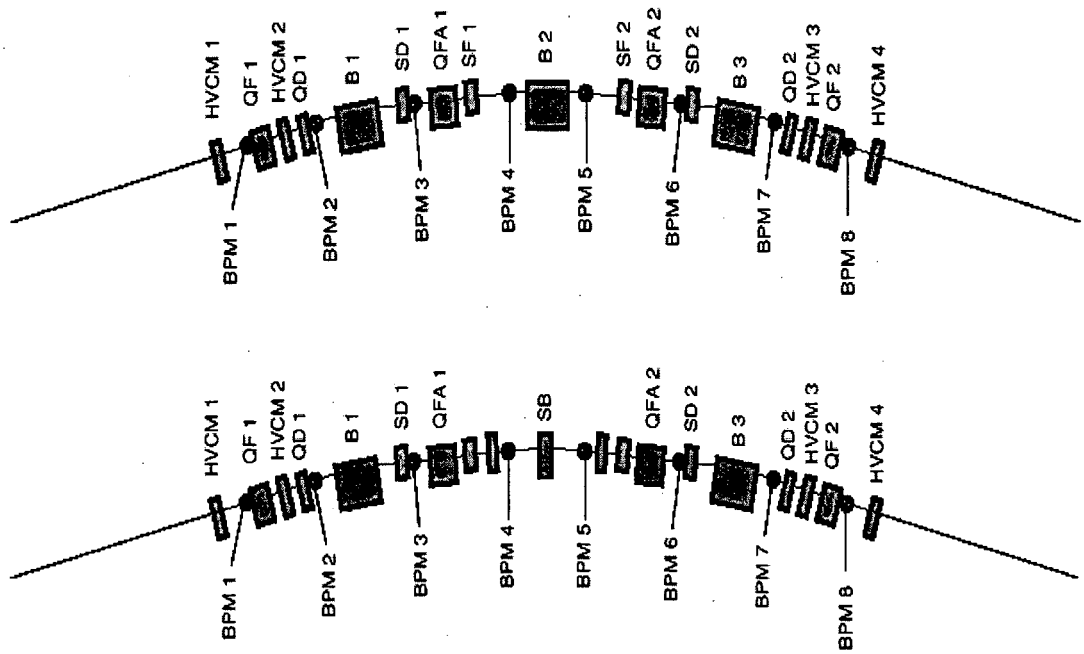

Figure 2. Layout of a normal sector (top) and Superbend sector (bottom). To modify a normal bend sector to become a superbend sector the second combined function bend, B2, is removed and replaced with a superbend, SB, and two quadrupoles, QDA1 and QDA2.

3.2.1 Nine new magnets

Several steps are taken to modify a normal sector to become a Superbend sector. The central bend of the triple bend achromat is removed and replaced by a Superbend and 2 quadrupoles (QDAs). The normal bend that is removed is a combined function bend. So in addition to having a dipole field component, the normal bend has a strong quadrupole field component that the Superbend magnet does not have. Ideally we wish to make the lattice functions of the Superbend sectors identical with the lattice of the normal sectors. In this way we preserve the 12-fold periodicity in the ring which reduces nonlinear resonance excitation and improves the dynamics.

The reason that the QDA quadrupoles are placed in the lattice is to compensate for the missing focusing of the Superbends making the sectors more similar. In total with all 3 Superbend sectors modified we will have removed 3 normal bend magnets and installed 3 Superbend magnets and 6 QDA quadrupoles.

3.2.2 Twelve new power supplies

Several issues need to be considered when determining whether the superbends and quadrupoles should be powered individually or in pairs. From the accelerator physics standpoint it is desirable to power each of the superbends separately so

that one has the flexibility to adjust each magnet individually to maintain a good orbit. As discussed in section 7 small differences in field between the superbends will result in large orbit distortions.

With regards to the quadrupoles there were several issues that were considered when choosing the number of power supplies. From the accelerator physics point of view it is desirable to have the flexibility of adjusting each superbend sector individually to compensate for focusing differences between the superbends. So at a minimum one would like 2 power supplies --- one for each QFA pair and one for each QDA pair in each Superbend sector. Therefore at a minimum there would be 6 new quadrupole supplies. One also would like the possibility to have some adjustment on each quadrupole for beam-based alignment. However one can use shunts for this.

Besides these accelerator physics requirements there are other concerns such as cost that need to be considered. At present all of the QFAs are powered on 1 supply. We decided that from a cost standpoint we would power the QFAs in each sector as pairs and install shunts for the beam-based alignment. (In fact we have already purchased the shunts.) However we decided that we would power all the QDAs individually. There is not a strong reason to have the QDAs powered individually or in pairs with shunts. One advantage of powering the QDAs individually is that would make the QDA power supplies would be identical to the QD power supplies that already exist. This reduces the number of quadrupole families.

So in summary each of the Superbends and the QDAs will be powered on individual power supplies. When modifying the sectors we will decouple the QFAs in the Superbend sectors from the QFAs in the normal sectors. In each Superbend sectors the 2 QFAs will be powered on one supply. So in total we will have 12 new power supplies (3 Superbend, 3 QFA and 6 QDA).

3.3 Reference frame and the ideal beam trajectory

3.3.1 Frames of reference

The mechanical design of Superbend magnet is described in Egon Hoyer's section and the three-dimensional fields of the Superbend are described in Clyde Taylor's section. As can be seen in these sections the frame of reference that most naturally lends itself to expressing the fields of the Superbend is the Cartesian reference frame. As discussed Clyde Taylor's section, the Superbends have a strong integrated sextupole field. This sextupole field can be used to define the transverse and magnetic center of the magnet. We define the transverse magnetic center (both horizontal and vertical) as the location where there is no integrated quadrupole field.

In accelerator physics one often uses a curvilinear frame of reference that is defined with respect to the ideal beam trajectory. A comparison of the two frames is shown in Figure 3. In section 4 we describe how the Superbend is modeled with respect to the different frames of reference

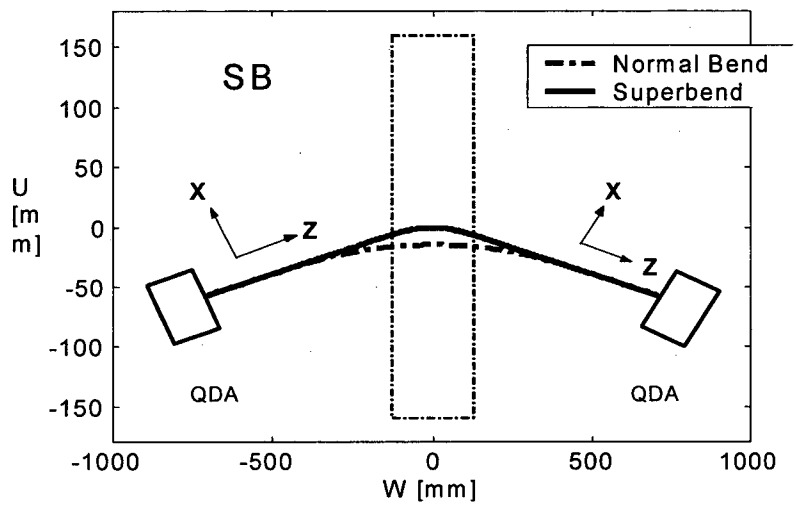

Figure 3. Reference frames and the ideal trajectory for a particle in a normal sector (dashed) and one in a Superbend sector (solid).

3.3.2 The ideal beam trajectory

The ideal beam trajectory for a particle in a Superbend sector is shown in Figure 3. In the Superbend sector the design trajectory of the ideal particle passes through the magnetic center of the upstream (left) QDA quadrupole. When the 'ideal' particle arrives at the longitudinal center of the superbend it is also at the transverse center of the superbend and has been bent by 5 degrees. When the 'ideal' particle arrives at the longitudinal center of the superbend it will be 14mm horizontally outward of the ideal normal dipole trajectory (difference between the solid and dashed line in Figure 3). When the 'ideal' particle arrives at the downstream QDA it will have been bent by a total of 10 degrees. The 'ideal' particle then passes through the center of the downstream (right) QDA quadrupole.

The length of the trajectory of an 'ideal' particle in a superbend sector is 1.64mm longer than the trajectory in a normal sector. So for 3 Superbend sectors the orbit length is about 5 mm longer than the orbit length in the lattice without the Superbends. This means that operation with the Superbends will require that the RF frequency of the machine be approximately 12 KHz lower than the value that we presently operate with. So in addition to the storage ring both the booster and the linac will also need to be operated at 12 KHz lower frequency.

3.4 Modeling the Superbends

For most of the results that are shown we use a simplified model of the Superbend. The model assumes that within the body of the magnet the transverse fields in the curvilinear coordinates can be expressed in a two-dimensional multipole field expansion. In this model the assumption is made that within the body of the magnet there is no variation in the transverse fields with the longitudinal coordinates. The fringe field of the model is modeled with a hard edge fringe field whose edges are parallel in the Cartesian reference frame. This model is called an isomagnetic model.

By using this model we assume that the following two approximations are valid:

1. We can ignore the sigita of the magnet (i.e. assume that the fields with respect to the curvilinear and the Cartesian frames are the same)
2. We can greatly approximate the fringe field (the area where there is a longitudinal variation of the field).

For most issues these approximations are reasonable. Because we are allowed to make these simplifications in the model we are able to make the same simplifications in the field measurements. This will be discussed in section 3.7.2.4.

The length, L, and dipole strength, B, of the isomagnetic Superbend model is determined through the following constraints:

1. The total angle of curvature has to be 10 degrees $(BL) / (B\rho) = (2\pi)/36$
2. The integral of the square of B has to be the same for the isomagnetic and actual magnet.

This results in the following values for L and B:

L = 247 m

B = 3.54 T at 1.5 GeV and 4.48 T at 1.9 GeV

3.5 Constructing the linear lattice

3.1 Lattice matching

The goal for matching the magnetic lattice is to minimize the distortion of the lattice functions from the lattice without Superbends. The lattice can be matched in several ways. We chose a nominal matching scheme which we used for the tracking calculations. For this nominal lattice we matched the lattice in the following way: 8 constraints are met by adjusting 8 parameters. The constraints and parameters are shown in Figure 4. The resulting lattice functions for the normal

and Superbend sectors are shown in Figure 5. Table 1 lists the lattice parameters for this lattice.

CONSTRAINTS (8):	**PARAMETERS (8 'Families'):**
GLOBAL: 2 betatron tunes (ν_x, ν_y) 2 chromaticities (ν_x', ν_y'), LOCAL (Center of the straight section): 1 horizontal dispersion (η_x=0), 3 derivatives — dispersion and betatron functions ($\eta_x' = 0$, $\alpha_x = 0$, $\alpha_y = 0$)	*IN THE NORMAL SECTORS:* 1 QF 1 QD *IN THE SUPERBEND SECTORS:* 1 QF 1 QD 1 QDA *IN ALL SECTORS:* 1 QFA 1 SF 1 SD

Figure 4. List of the constraints and parameters that is used to fit the "nominal" lattice.

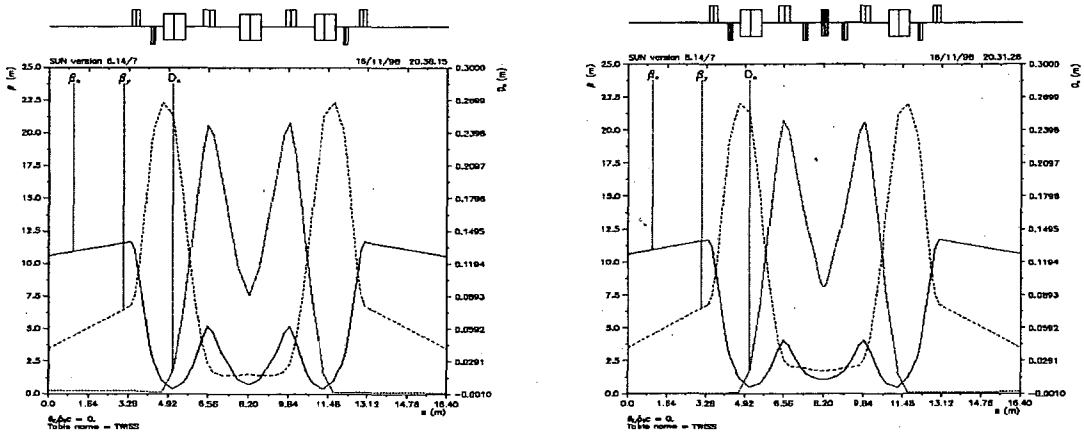

Figure 5. Twiss parameters for the normal and Superbend sectors fitted to zero dispersion in the straight section.

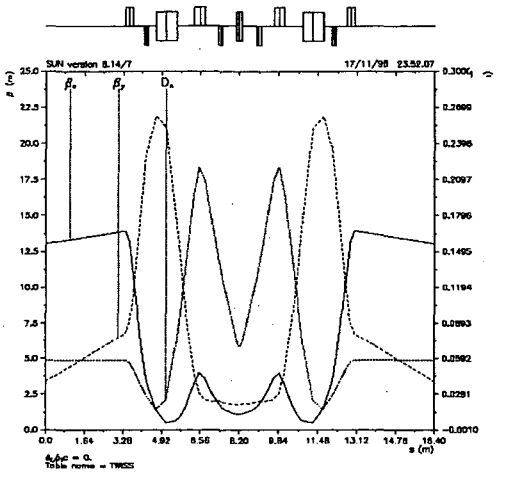

Figure 6. Twiss parameters for a Superbend sectors fitted to 6 cm of dispersion in the straight section.

We wish to point out two things about the match. First we did not adjust the QFA magnets in the Superbend sectors differently than in the normal sectors. Therefore we may have not realized the optimal condition for the dynamics. Second we adjusted the dispersion to be zero in the straight section. As we discuss below in the impact on the parameters, adjusting the dispersion to be slightly positive in the straight section will reduce the horizontal emittance. To adjust the lattice to include finite dispersion in the straight sections is realized by slightly adjusting the quadrupole families. The lattice for a Superbend sector that is adjusted to have 6 cm of dispersion in the straight section is shown in Figure 6.

The lattice parameters are given in Table 1. As displayed in the table the emittance and energy spread increase with the introduction of the superbends. By adjusting the lattice to have positive dispersion in the straight section one can largely recover the emittance. In concert with the users a study was made looking at the impact on the synchrotron light users from a change in parameters [1]. It should be mentioned that we have operated the storage ring during one machine studies shift with nonzero dispersion. However there has not been much experience operating in this mode. More work both theoretical and experimental needs to be done to see if this mode of operation is acceptable.

	No S-Bends ($_x = 0$)	**3 S-Bends** ($_x = 0$)	**3 S-Bends** ($_x = 6$cm)
Energy	1.9 GeV	1.9 GeV	1.9 GeV
$_x$	5.5 [nm rad]	13 [nm rad]	7.5 [nm rad]
$_E$	0.08%	0.10%	0.10%
E /turn	232 KeV	281 KeV	281 KeV

Table 1: Storage ring parameters with no superbends ($_x$=0), 3 superbends ($_x$=0), and 3 superbends ($_x$= 6cm)

3.6 Operational requirements

Operational requirements of the ALS drive the performance of the superbends. In a qualitative sense it is important that we:

1. Provide the desired source brightness and flux for the superbend users
2. Provide a sufficiently good injection efficiency
3. Do not degrade the lifetime
4. Have sufficiently fast energy ramping
5. Have sufficiently small orbit motion

These operational needs impact the tolerances on:

1. The dipole field
2. Higher-order multipole field components
3. Magnet alignment
4. Magnet ramping speed
5. Power supply jitter and magnet vibration

One now needs to quantify the above requirements and tolerances. Dipoles such as the superbends are broadband sources of radiation that are not very sensitive to the critical field. As a result the requirements on the absolute field are fairly loose. We have placed the following tolerance on the absolute field: At the location of the beam ports (2.6 and 7.4 degrees) the field must be within 5% of the design field.

At 1.9 GeV, the field = 4.9 Tesla +/- 5% at 2.6 and 7.4 degrees.

At 1.5 GeV, the field = 3.9 Tesla +/- 5% at 2.6 and 7.4 degrees.

Let's quantify the other operational requirements of the ALS. In order to have no significant impact on operation it is important that the following requirements be met.

3.6.1 Injection

In the ALS we inject beam into the machine horizontally displaced from the stored beam. The separation between the injected and stored beam is measured by continually injecting beam into the ring and then moving in a beam scraper until the injection capture rate is impacted. From the position of the scraper one can measure the amplitude of the oscillation of the injected beam. Typically the injected beam is approximately 10 mm away from the stored beam. We have been able to move the stored beam close enough to the injection septum so that we have injected beam with the scraper in at 7 mm. So for injection it is possible to capture beams with a 7 mm horizontal aperture (Ideally we would feel more comfortable with a 10 mm aperture.) Therefore one requirement for injection is

that there be an on-energy dynamic aperture that is larger than 7 mm in order to capture beam.

3.6.2 Lifetime

Need a "dynamic" momentum acceptance that is greater than 2.0% in order that there be no reduction in the lifetime at 1.9 GeV. If the "dynamic" momentum acceptance is greater than 2.0% the total momentum acceptance will be determined by the rf-bucket (which is 2%) and therefore there will be no reduction in lifetime due to the Superbends at 1.9 GeV.

We also require that the total distortion of the horizontal and vertical -fun ction be less than 5% rms in order not to strongly impact the dynamic aperture. This requirement on the acceptable value of beta-beating and its impact on lifetime is less easy to determine than requirement on the momentum acceptance. The value of 5% is reasonable based upon our experience with the present machine.

3.6.3 Induced orbit distortion

It is desirable to be able to store beam without powering any of the corrector magnets. In order to comfortably store beam without the correctors turned on we require that the superbends should not introduce a horizontal orbit distortion of more than 2 mm at a_x = 11m and a vertical orbit distortion of more than 0.2 mm at a_y = 4m.

3.6.4 Orbit jitter

We require that the horizontal orbit jitter introduced by the superbends be less than 3 m rms and the vertical orbit jitter be less than 1 m rms for frequencies >0.01 Hz. This requirement stems from the fact that at present this is the type of beam motion that we are experiencing at frequencies > 0.01 Hz. We do not want to make operation with the superbends significantly noisier. We require that the horizontal orbit jitter introduced by the superbends be less than 20 m rms and the vertical orbit jitter be less than 2 m rms for frequencies < 0.01 Hz. This requirement stems from the fact that we would like to keep the orbit drift down to $1/10^{th}$ of an rms beam size in both planes. The rms beam sizes are 200 m horizontally and 20 m vertically at 1.5 GeV with 1% coupling.

3.6.5 Energy Ramping

We require that the introduction of the superbends does not greatly increase the length of the injection cycle.

Ideally we would like the possibility of ramping the superbends from 1.5 GeV to 1.9 GeV in 20 seconds in order that they can match the maximum ramping speed of the normal bend magnets. Note: This is not a hard requirement but a desire in the event that we try to improve the overall ramping rate.

3.7 Tolerances

From the operational requirements presented in section 6 one can derive some of the tolerances on the magnet. In particular it is possible to derive the tolerances on the following quantities:

1. Integrated and Absolute field
2. Multipole field content
3. Magnet alignment
4. Field jitter: power supply jitter and magnet vibration
5. Ramping speed and magnetic field reproducibility

3.7.1 Integrated and absolute field

The requirement on the integrated field is that the dipole must bend the beam by 10 degrees. For a given beam energy the integrated field is then determined:

$$\int_0^L Bds = \frac{2\pi}{36} \times \frac{E[GeV]}{0.3} \qquad (1)$$

= 0.873 Tm at 1.5 GeV

= 1.105 Tm at 1.9 GeV

If the integrated field of one of the magnets is different from the ideal value this will give rise to a horizontal angular kick which will in turn give rise to both a change in the horizontal orbit as well as a change in the beam energy. One can adjust the superbend power supply to get the proper integrated field. We must insure that we have the precision to set the field of the superbend to within the specified tolerances.

The angular kick, $_x$, from a bend whose relative difference in integrated field from ideal (BL/BL_0) is

$$\Theta_x = \frac{\Delta BL}{BL_0} X \frac{2\pi}{36} \qquad (2)$$

The resulting change in beam orbit due to $_x$ is

$$x(s) = \frac{\theta_x \sqrt{\beta_x(s)}\sqrt{\beta_x(0)}}{2\sin \pi\nu_x} \cos\left(\psi_x(s) - \pi\nu_x\right) - \frac{\theta_x \eta_x(s)\eta_x(0)}{\alpha L_0} \tag{3}$$

where $_x$ is the horizontal tune, L_0 is the orbit length, x(s) is the observation point, (s) is the beta-function at the observation point, (0) is the beta-function at the kick point, (s) is the beta-function at the observation point, (0) is the beta-function at the kick point, and (s) is the phase advance between the kick point and the observation point.

The resulting change in the beam energy due to θ_x is

$$\frac{\Delta E}{E} = \frac{\theta_x \eta_x(0)}{\alpha L_0} \tag{4}$$

The requirement that is the tightest and drives the tolerance on the setability of the bend field is the requirement on the beam orbit. We wish to have the ability to set the bend field so that the contribution to the orbit distortion from all 3 bends would be no worse than 20 m peak-to-peak in the straight section. If we power the 4 supplies (the 3 superbends and 1 normal bend) in different random combinations and look at the largest orbit distortion in any straight section we find that the maximum amplitude is 2.5 times the maximum amplitude generated by any one superbend. So this means that we can allow one superbend to generate 20/2.5 = 8.5 m of orbit distortion.

Assuming an x(s) of 8.5 m of orbit distortion one can use equations 7.2 and 7.3 to determine the maximum BL/BL_0 that can be tolerated. In the case of the ALS we typically operate with a $_x$ g reater or equal to 0.25. The horizontal - functions at the kick and observation points are

$$\beta_x(s) = 11\text{m}$$
$$\beta_x(0) = 0.8\text{m}$$

We wish to solve for the minimum $_x$ which gives x(s) = 8.5 microns. The maximum values of $x(s)$ comes when setting $\cos\left(\Psi_x(s) - \pi\nu_x\right)$ in equation 3. This gives

$$\theta_x = 4.5\mu\text{rad}. \tag{5}$$

This tells us that we can allow 4.5 rad of kick. We know that each superbend bends the beam by 2 /36 = 0.17 radians. That gives a I/I = $4.5\text{x}10^{-6}/1.7\ \text{x}10^{-1}$ = 1/38000 of the bend current at 1.5 GeV. If we wish to specify this as a function of max current of the supply, which corresponds to an energy of 2.4 GeV, then we have the requirement that

$$\frac{\Delta I}{I_{\max}} < \frac{1}{60000} \tag{6}$$

This implies that we need at least 16 bit resolution on the bend power supply.

In terms of long term (<0.01 Hz) drift we require the beam be stable to at least one beam sigma (~20 μm). Therefore for long term stability the requirements on the power supply is that the relative current change within a fill (up to 12 hours) be

$$\frac{\Delta I}{I_{\max}} < \frac{1}{60000} \tag{7}$$

We should note here that the machine be running with slow horizontal and vertical orbit feedback. Therefore if the tolerance is not met the orbit feedback will correct most of the error. However it is best to be in a situation where one does not have to rely on the feedback system to meet the user requirements.

3.7.2 Multipole content and particle tracking studies

The tolerable magnet multipole content is determined through tracking studies of the dynamic aperture (both injection and momentum aperture studies). For particle tracking we used a 6-D symplectic integrator [2]. In the model the magnets are isomagnetic and the cavity is a thin lens. Realistic physical apertures are included (± 25mm horizontal and ± 4mm vertical in the straight section) which matches those of the real ring. We also included quadrupole field errors that we typically see in operation — distributed normal quadrupole errors that give rise to about a 5% rms horizontal and vertical betabeating and distributed skew quadrupole errors that give rise to about a 1% emittance coupling.

Initially we included the following multipole content for the superbends.

Tolerance:

Sextupole: $B_3/B_1=32 \times 10^{-4}$ at 1 cm

Decapole: $B_5/B_1 = 2 \times 10^{-4}$ at 1 cm

These were the greater of the calculated or measured systematic multipoles for the SB4 prototype magnet.

For tracking we set the chromaticities to zero and set the tunes to 14.25 horizontally and 8.2 vertically. These tunes were chosen after doing a quick scan of the tune space.

3.7.2.1. Periodicity breaking and the betatron tunes

In the ALS as in most other 3rd generation light sources the main source of nonlinearity are the high field chromatic sextupoles. The focusing between sex-

tupoles is linear with amplitude. At the sextupoles the particles experience an nonlinear kick that is quadratic with amplitude.

Most of the 3rd generation light sources are designed with a high degree of periodicity. Periodicity helps to suppress nonlinear resonance excitation. The condition for resonance excitation is

$$N_x \nu_x + N_y \nu_y = P \times Q \tag{8}$$

where N_x, N_y, Q, and P are integers with P being the degree of periodicity of the lattice. The order of the resonance is $|N_x| + |N_y|$. One can see that as one increased the degree of periodicity, P, the number of low order resonances decreases. Thus having a high degree of periodicity results in a cleaner tunespace. This can be seen in Figure 7 where we have plotted all allowed resonances up to 5th order for a lattice with 12-fold periodicity (left) and 3-fold periodicity (right). Therefore one can guess that including 3 superbends in the lattice and reducing the periodicity from 12 to 3 will reduce the usable tunespace.

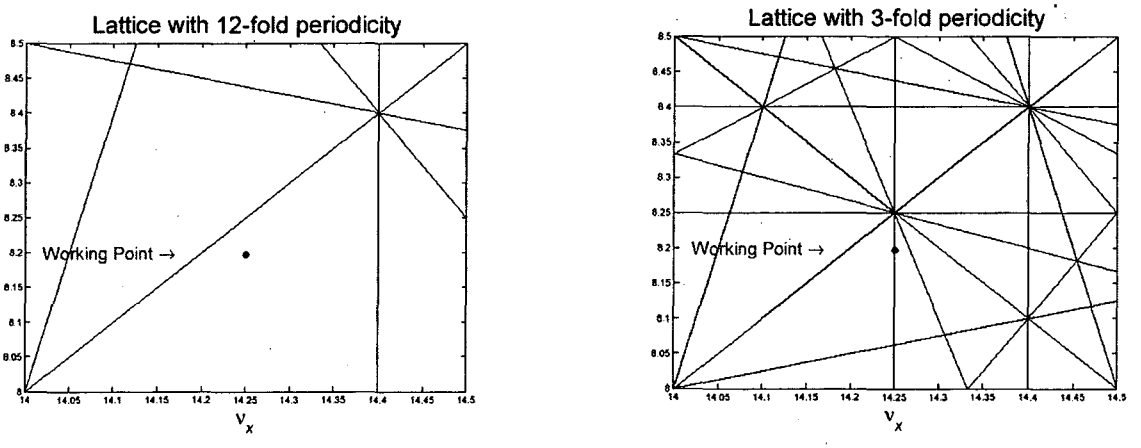

Figure 7. All "allowed" resonances up to 5th order for a lattice with 12-fold periodicity (left) and 3-fold periodicity (right).

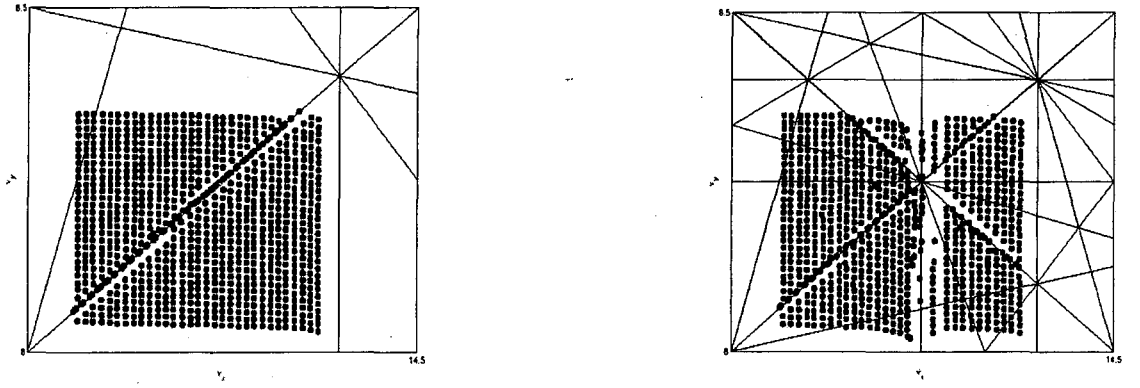

Figure 8. Tunescans for a lattice with 12-fold periodicity and a lattice with 3-fold periodicity.

To choose a working point we performed tunescans with a frequency post processor. The procedure was the following: First the betatron tunes were set. Then a particle was launched with an initial offset of 10 mm horizontally and 1 mm vertically and tracked for 1024 turns or until lost. If the particle survives 1024 turns the frequency post processor computes the fundamental frequencies for that particle. The procedure is then repeated for many different tunes. In total the machine is adjusted to 900 tunes (on an evenly spaced grid of 31x31 tunes between $_x$ = 14.1 to 14.4 and $_y$ = 8.1 to 8.4). The results can be seen in Figure 8.

In the case of no superbends one only sees the influence of the $2_x - 2_y =$ 1 2 resonance. In the case of 3 evenly spaced superbends one sees that there are more resonances excited. In particular one sees a 4th order resonance, $4_x =$ 57, that is strongly excited and also several coupled resonances which cross at the $_x$ = 14.25 and $_y$ = 8.25. In these regions the motion of large amplitude particles is chaotic. However even in the case of 3 superbends evenly spaced there still seems to be large regions in tunespace where it is possible to operate. This is not true in the case of 3 superbends located asymmetrically around the ring. In that case the periodicity goes from 3 to 1 and the tunescans were greatly distorted with many missing points.

It is important to mentions that the tuneshift with amplitude is negative in both planes. Therefore operating with a horizontal tune of 14.25 and a vertical tune of 8.20 allows one to operate safely away from (below) the coupling resonance and (left) of the fourth order resonance. Based upon the tunescans for the 3 evenly spaced superbends, a working point was chosen ($_x$ = 14.25 and $_y$ = 8.2) for more detailed tracking studies.

3.7.2.2 Injection studies

For injection studies particles were launched on energy at the injection point with initial conditions of

$$(x = x_i,\ p_x = 0,\ y = y_i \text{ and } p_y = 0,\ \Delta E/E=0 \text{ and } ct = \tau = 0)$$

and tracked without synchrotron oscillations for 512 turns or until lost.
The results with and without superbends is shown in Figure 9. In the figure we had plotted a dot at both -7 mm and -10 mm. The minimum aperture that we need for injection is 7 mm. We presently inject with a 10 mm separation between the stored and injected beam.

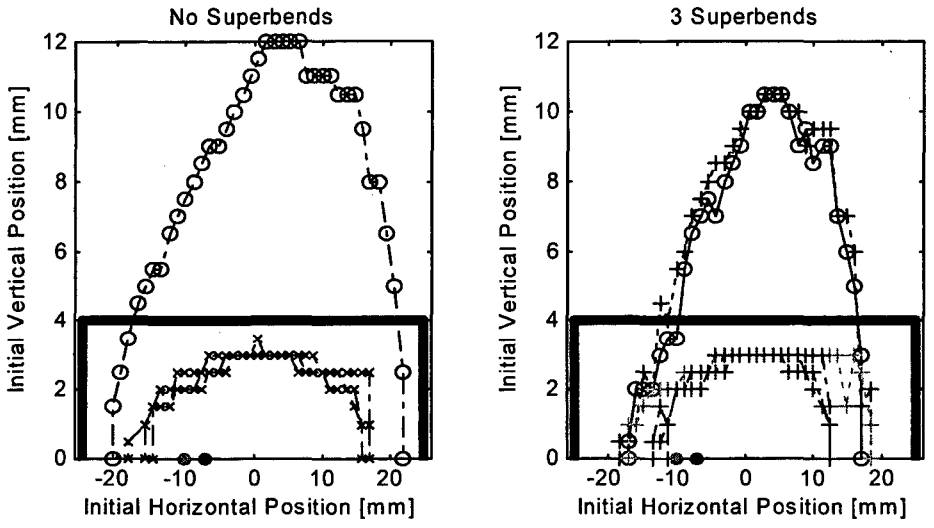

O idea
\+ SB. multipole er-
\+ SB. multipole errors + physical aper-
x normal quad +skew quad, + physical aper-
\+ SB. Multipole errors + normal quad +skew quad, + physical aper-

normal injection offset (-10 mm)
minimum injection offset (-7 mm)

Figure 9. Initial on-energy tracking studies for the lattice without superbend (left) and with superbends (right).

The case without Superbends as shown on the left side of the figure the aperture without errors and physical apertures is slightly greater than 20 mm horizontally. When we added a physical aperture and errors, the aperture reduces to about 15 mm with for all error seeds. The case with Superbends as shown on the right side of the figure. With no errors, physical apertures or systematic multipole errors, the horizontal dynamic aperture is about 18mm. If we add systematic multipole errors the aperture does not change. If we then include both a physical aperture and random quadrupole errors the aperture reduces to 11 mm. So even though there is a reduction in the dynamic aperture it seems that one can still inject into the lattice with some margin.

We suspected that the reduction in dynamic aperture is a result of having perturbed the ring's natural 12-fold periodicity. This is done in two ways: First we change the linear phase advance between the existing sextupoles and second we introduce a "new" sextupole in the lattice. In fact the integrated sextupole strength is quite large. It is about half the strength of a chromatic sextupole (SF or SD). In principle both effects (linear perturbation and systematic sextupoles) can impact the dynamic aperture.

Already with these results one can see something that is rather interesting. There is a reduction in the dynamic aperture of the ideal lattice when comparing no superbends and with superbends. What is curious was that after that reduction, including the systematic sextupole errors did not further impact the dynamic aperture. One might think that placing such a strong sextupole field in a 3-fold symmetric pattern around the ring would impact the dynamic aperture. We suspected the reason there was no significant impact was due to the fact that the superbends are located in a region where the β-functions are small in both planes.

In order to test that assumption the following simulation was made. To isolate the effect of the systematic sextupoles we took an ideal lattice without superbends and placed an integrated sextupole in the normal bends which would be replaced by superbends and tracked the lattice. The results are shown in Figure 10. We find that if we look then at the dynamic aperture with no systematic sextupole as compared with the aperture with 1 times and 2 times the strengths of the "expected" systematic sextupole the dynamic aperture remained nearly the same. This was to say that we could even double the systematic sextupole without seeing any appreciable change in the aperture.

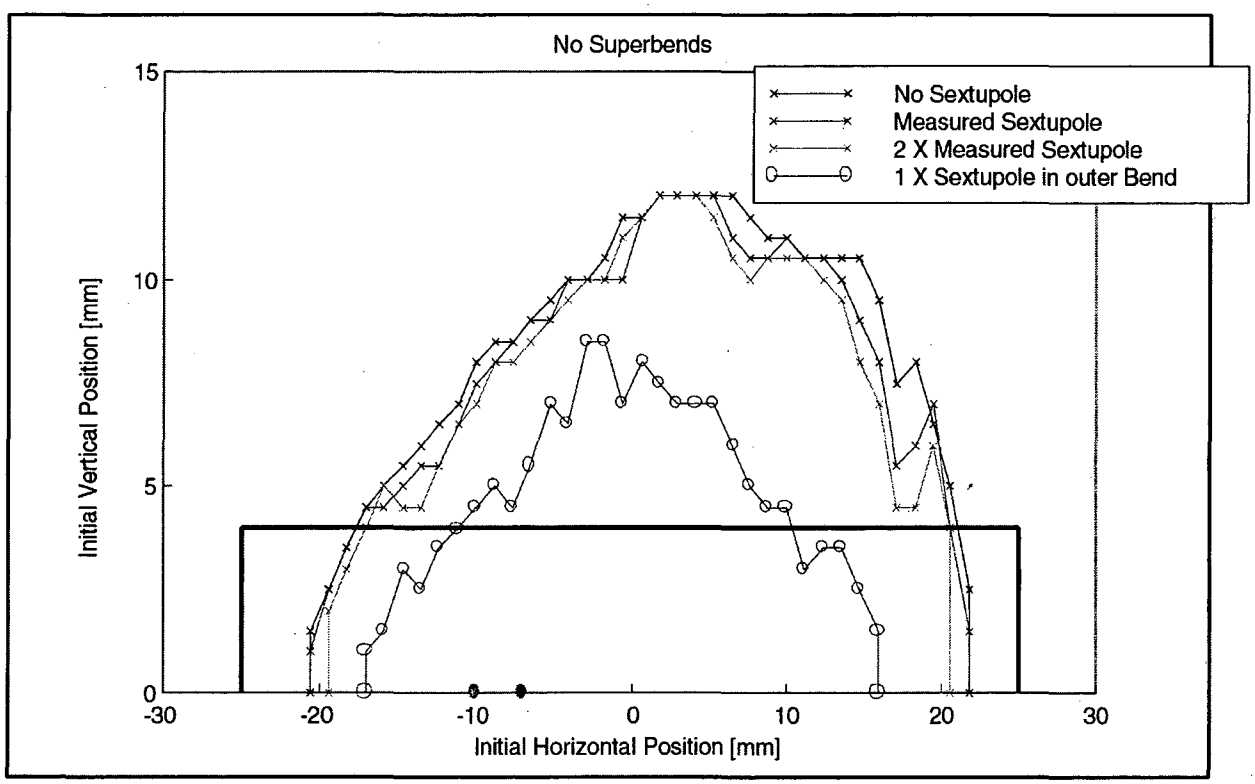

Figure 10. Effect if the systematic sextupole distributed in a 3-fold periodic pattern.

As a sanity check we moved the systematic sextuple to 3 outer bends located periodically around the ring. In these bends the β-function is large vertically. With only 1 times the systematic sextupole strength the dynamic aperture is re-

duced significantly. So it appears that the fact that the superbends are located in a region where the β-function is small is the reason that we can tolerate a large sextupole strength.

Due to the fact that we saw no impact on the dynamic aperture when the systematic sextupole strength was doubled we decided to repeat the tracking studies with twice the systematic multipole content and also included some random sextupole errors.

The new values for the systematic multipole content that was chosen was

Sextupole: $B_3/B_1 = 60 \times 10^{-4}$ at 1 cm

Decapole: $B_5/B_1 = 2 \times 10^{-4}$ at 1 cm

and for random errors of

Sextupole: $B_3/B_1 = \pm 3 \times 10^{-4}$ (peak-to-peak) at 1 cm

The new tracking results with gradient errors can be seen in Figure 14.

There is no significant impact on the dynamic aperture over what was shown with the smaller multipole errors.

3.7.2.3 Momentum Aperture Studies

In the ALS the dominant cause of particle loss is through intrabeam or Touschek scattering. The Touschek scattering process is shown in Figure 11. In the case of Touschek scattering two particles in the bunch which are undergoing transverse oscillations collide with each other. One particle looses some momentum and the other particle gains some momentum. If the amount of momentum gained or lost is sufficiently small, the motion of the particle will be stable and will slowly damp down to the center of the bunch. If the momentum gained or lost is too large, the particle motion can become unstable and/or hit a physical aperture.

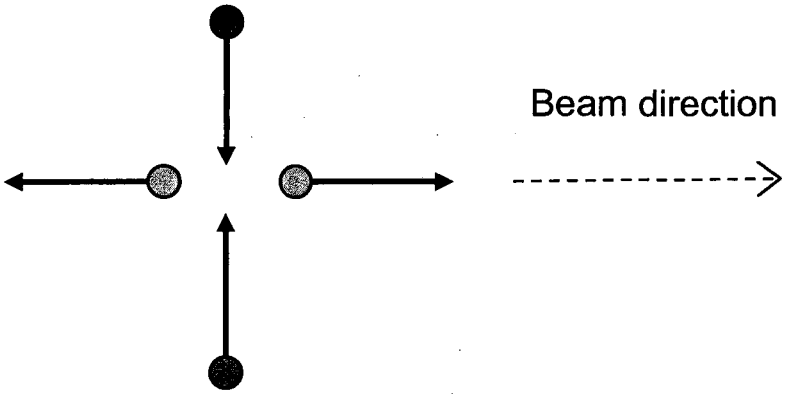

Figure 11. Touschek scattering process.

The momentum acceptance, , is determined by the largest amount of momentum that can be gained or lost and the particle will still survive. The Touschek lifetime is roughly a function of the square of the momentum acceptance and is given below.

$$\frac{1}{\tau_{Tous}} \propto \frac{1}{E^3} \frac{I_{bunch}}{V_{bunch}} \frac{1}{\sigma'} \frac{1}{\varepsilon^2}$$

where E is the beam energy, I_{bunch} is the electron bunch current, V_{bunch} is the volume of the electron bunch, and σ' is the horizontal divergence of the electron beam.

The momentum acceptance is determined by one or more of the following three things:

1. The rf bucket
2. The physical aperture
3. The dynamic aperture

The momentum acceptance is a function of the longitudinal position in the ring where the scattering occurs and may be limited by different effects. For instance particles scattered in the straight section where the dispersion function is small may have a larger momentum acceptance that is limited by the rf bucket. Particles scattered in the arcs may have a smaller momentum acceptance that is limited by the physical or dynamic aperture. This is because particles that scatter in the arcs where there is a large dispersion function will have large induced transverse motion that may cause them to hit the transverse dynamic or physical aperture before the rf bucket is reached.

The induced amplitude to lowest order is a function of $\boldsymbol{H}\delta^2$ where $\boldsymbol{H}$ is

$$\boldsymbol{H} = \gamma \eta^2 + 2\alpha \eta\eta' + \beta \eta'^2$$

In the case where the dispersion function, η, and its derivatives are adjusted to zero in the straight section, the $\boldsymbol{H}$ function is zero. The $\boldsymbol{H}$ function is a maximum and constant between the bends in the arcs. The H function is plotted in Figure 12.

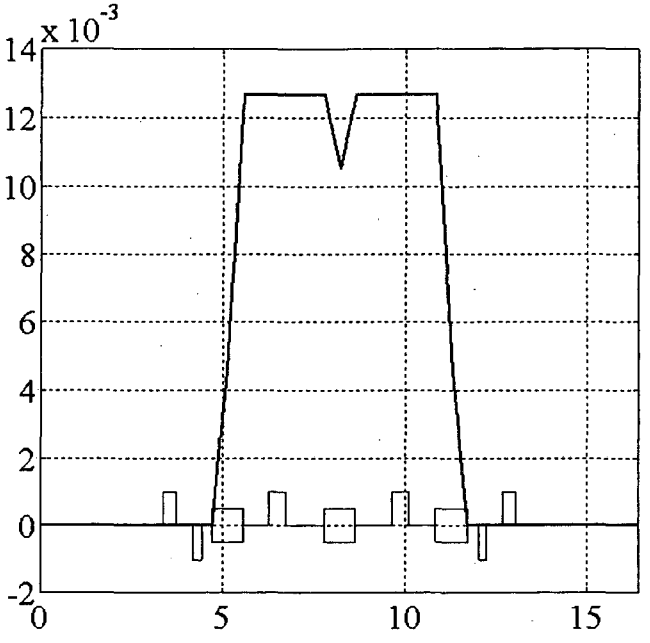

Figure 12. H function as a function of length along the sector.

The height of the rf bucket provided by the accelerating voltage in the cavity is

$$\varepsilon_{rf} \simeq \sqrt{\frac{V_{rf}}{\alpha h E}}$$

where *Vrf* is the rf-voltage, is the momentum compaction factor, *h* the harmonic number and *E* the nominal beam energy. The rf-bucket for the ALS running at an energy of 1.9 GeV and with a peak voltage of 1 MV is roughly 2 %. Therefore we would like to insure that the dynamic and physical aperture do not limit the momentum acceptance to a level below 2%.

Tracking studies allow us to predict where the where the momentum acceptance will be limited by the dynamic and physical aperture. In order to determine the dynamic momentum acceptance we do something artificial in the tracking studies so that the rf bucket is large enough that it is not the limiting aperture. We increase the cavities rf voltage, *Vrf*, which increases the bucket height. We also decrease the cavities rf frequency in direct proportion to the increase in the rf voltage. By doing this we keep the synchrotron tune constant.

For momentum aperture studies, particles were launched off energy at the injection point with initial conditions of

(x = x_i, p_x = 0, y = 1mm and p_y = 0, E/E= $_i$ and ct = = 0)

and tracked without synchrotron oscillations for 512 turns or until lost.

For the momentum aperture studies we initially tracked lattices with systematic multipole errors for SB4 only:

Sextupole: $B_3/B_1=32 \times 10^{-4}$ at 1 cm

Decapole: $B_5/B_1 = 2 \times 10^{-4}$ at 1 cm

The results with the initial multipole values can be seen in Figure 13. On the left on finds the aperture for the lattice with no superbends. On the right is the aperture with superbends. There vertical axis is horizontal amplitude. The horizontal axis is initial energy offset. Three normal and skew quadrupole error seeds are shown for each case.

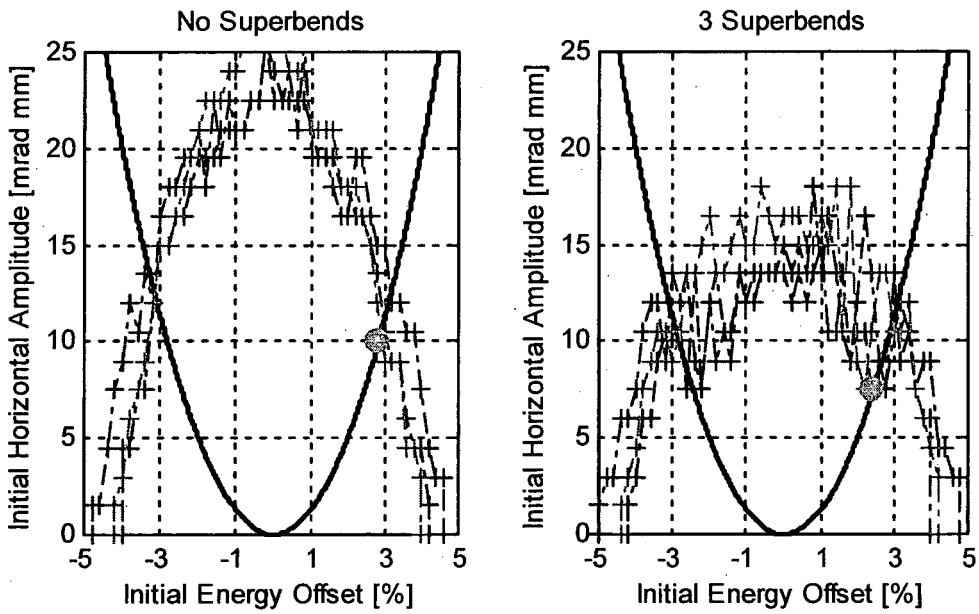

Figure 13. Initial momentum aperture studies for the lattice without Superbends (left) and the lattice with Superbends (right). Linear lattice errors and realistic physical apertures are included in the tracking.

There is also a solid line plotted which gives the induced amplitude as a function of energy for a particle who is scattered in region 2. The intersection of the solid line with the aperture gives the "dynamic" momentum acceptance. We find that in the case without superbends the momentum acceptance is limited at 2.8%. In the case with superbends the momentum acceptance is limited at 2.4%. So there is some reduction of the momentum acceptance but at 1.9 GeV the dynamic momentum acceptance is still larger then that determined by the rf-bucket.

In the second set of tracking we increased the sextupole multipole content and added a random sextupole error values. The new values for the sextupole was chosen was

Sextupole: $B_3/B_1 = 60 \times 10^{-4} \pm 3 \times 10^{-4}$ at 1 cm

The results of the tracking are shown in Figure 14. We find that the aperture is still larger than 2% for all 3 seeds. So this multipole content seems to be reasonable.

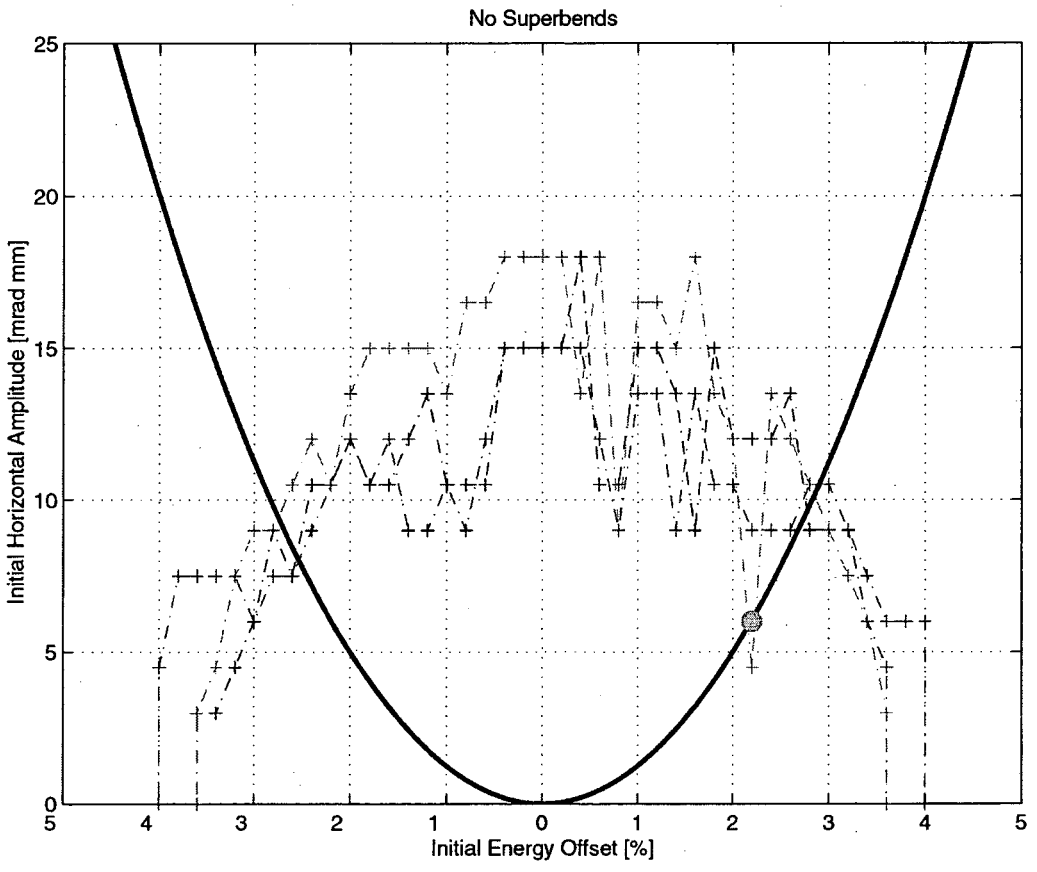

Figure 14. Momentum aperture studies for the lattice with 3 superbends with larger sextupole errors.

3.7.2.4 Effect of the full 3-D field map

How good is the isomagnetic model as a representation of the superbend? As seen in Figure 15, the Superbend fields are far from isomagnetic. There is a strong variation in field along the length of the orbit. We investigated the impact of the full 3-D fields on the beam dynamics. This work was done with Etienne Forest of KEK and Shlomo Caspi. We will outline the procedure and present the results of that study.

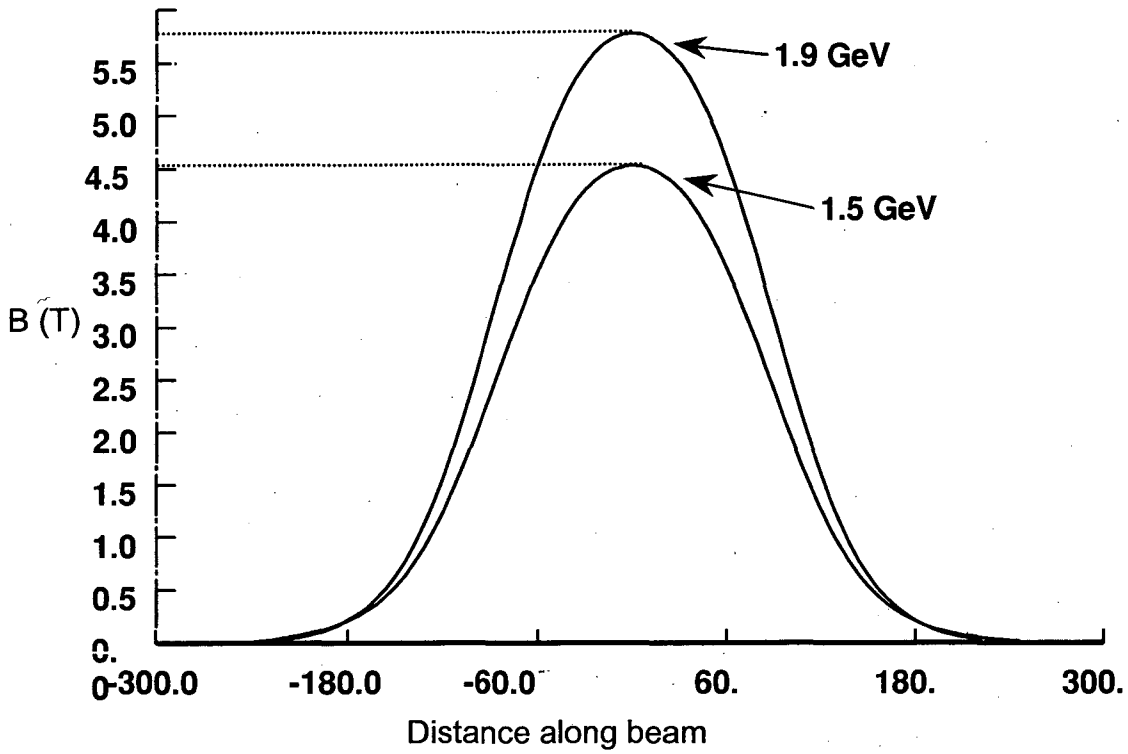

Figure 15. The longitudinal field profile for the superbends.

The first step was to express the field of the magnet in a 3-D field harmonic representation. This was done by using a TOSCA model for the magnet and calculating the fields with the magnet on a cylindrical surface of 1 cm in radius passing through the transverse center of the magnet. From field points the field was then fitted to an analytical multipole expansion. The representation for the field was 3-D field representation of Caspi, Helm, and Laslett [3].

Now having an analytical representation for the field, it was possible to track particles through the magnet. Tracking was done using the Differential Algebra or Truncated Power Series Algebra (DA or TPSA) package of Martin Berz in order to generate a transfer map (Taylor series) through the Superbend around the design orbit.

Once this transfer map was generated it was symplectified order by order [4]. Next the map was inserted into the tracking code and evaluated implicitly using a generating function.

After the lattice was constructed a one-turn map for the ring was constructed and the tunes and chromaticity were adjusted to be the same as for the isomagnetic model. Then the fitted model was tracked. The results can be seen in Figure 16.

The tracking results are for 3 lattices with different linear errors seeds. For each seed the results are presented for the isomagnetic and 3-D model of the superbend. We see that the results are nearly the same. We also saw no significant difference in the off energy tracking results comparing the isomagnetic model and the 3-D model of the superbend. Therefore we conclude that the isomagnetic model for the lattice is sufficient for the tracking. (This may not be too surprising considering the previous result showing the insensitivity to the strength of the higher order field multipoles.) We can also conclude that from a dynamics point of view integrated multipole measurements are adequate for the superbends.

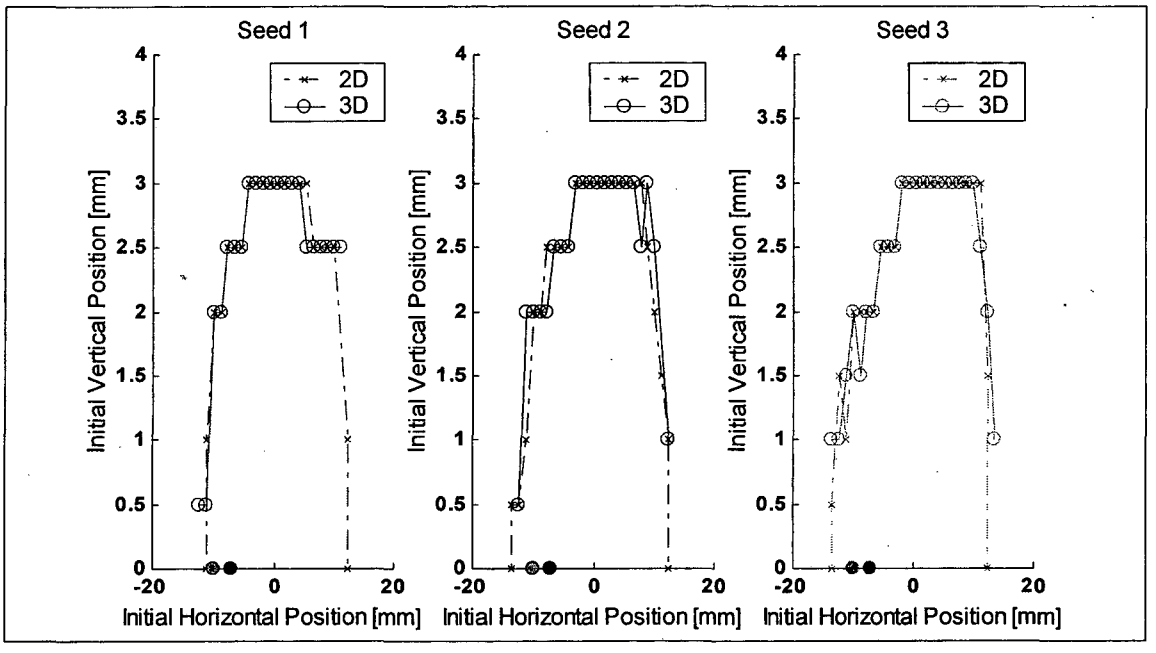

Figure 16. A comparison of on-energy tracking for a lattice where the superbends have been modeled using an isomagnetic magnet model versus a full 3-D field map.

So to summarize the tracking results:

1. The reduction in the dynamic aperture is primarily due to the perturbation of the linear lattice functions reducing the periodicity of the ring from 12 to 3.

2. Higher order multipole components have little impact on the aperture presumably due to the superbends located in a position of low β.

3. There is no significant difference in the dynamics between an isomagnetic model with integrated multipoles and a model with an accurate 3-D representation of the fields.

Based upon these results we provide the following tolerances on the sextupole and higher order integrated multipole fields.

Tolerance:

Sextupole: $B_3/B_1 = 60 \times 10^{-4} \pm 3 \times 10^{-4}$ at 1 cm

Decapole: $B_5/B_1 < 2 \times 10^{-4}$ at 1 cm

3.8 Alignment

Misalignment of the Superbends generates several effects:

1. A longitudinal misplacement will result in a horizontal orbit distortion.
2. A horizontal misplacement will result in both a horizontal orbit distortion and vertical -beating (periodicity breaking).
3. A vertical misplacement will result in vertical orbit distortion and coupling.
4. A roll of the magnet will result in vertical orbit distortion.

3.8.1 Longitudinal position of the superbends

One can estimate the effect of a longitudinal magnet position error in the following way. Suppose I move the magnet that bends the beam by an angle θ by an amount s. The resulting orbit distortion is just.

$$\Delta x(s) = \frac{\theta\sqrt{\beta_x(s)}}{2\sin(\pi\nu_x)}\left(\sqrt{\beta_x(0)}\cos\left(\psi_x(s) - \pi\nu_x\right) - \sqrt{\beta_x(\Delta s)}\cos\left(\psi_x(s) - \pi\nu_x - \psi_x(\Delta s)\right)\right) \quad (9)$$

where $_x(0)$ is the horizontal -function at the original location of the bend, $_x(s)$ is the horizontal -function at the new location of the bend, $_x(s)$ is the horizontal phase advance from the original location of the bend to the observation point, s, $_x(s)$ is the horizontal phase advance from the original location of the bend to the new location of the bend, and $_x$ is the horizontal tune.

If we assume $_x(0)$ approximately equal to $_x(s)$ and that $_x(s)$ is small then we can rewrite equation (8.1)

$$\Delta x(s) = \frac{\theta\sqrt{\beta_x(s)}\sqrt{\beta_x(0)}}{2\sin\left(\pi\nu_x\right)}\left(\psi_x(\Delta s)\sin\left(\psi_x(s) - \pi\nu_x\right)\right) \quad (10)$$

Lets assume that $_x$=0.25, =2 /36, $_x$(0)=1.5m, $_x$(s)=0.001. Then if one magnet is moved longitudinally by 1mm at a $_x$ = 1.5m then at an observation point where (s) = 11m, the maximum x is about 350 m. This means that if all 3 magnets were displaced by up to 1 mm longitudinally the distortion to the horizontal orbit would still be less than 1mm. This seems reasonable considering that the total error allowed is 2 mm.

Tolerance:

Error in longitudinal position = ±1mm from ideal.

3.8.2 Horizontal position of the superbends

A horizontal misplacement of the magnet will result in both a horizontal orbit distortion as well as horizontal and vertical -beating (periodicity breaking). The requirement that sets the tightest limit on the horizontal location is the requirement to keep the vertical -beating under 5%.

As mentioned in section 3.1 the superbends will have a strong integrated sextupole field, *Sl*. The transverse magnetic center of the magnet is defined as the position where the integrated quadrupole field is zero. The design trajectory is such that when the particle trajectory is bent by 5 degrees the beam is going through the magnetic center of the dipole.

A variation in the transverse position, *x*, will result in -beating through variations in the quadrupole feeddown focusing from each magnet. The quadrupole feeddown, *Kl*, from each magnet is just

$$Kl = 2Sl\Delta x \tag{11}$$

The resulting -beating from one magnet is given as

$$\frac{\Delta\beta_y}{\beta_y} \approx \Delta Kl \times \beta_y(0) = 2 \times \Delta x \times Sl \times \beta_y(0) \tag{12}$$

where (0) = 1.5m and *Sl* = 10m^{-2}. In order to keep the vertical -beating under 2% from one Superbend the limit on position is 0.5mm. This means that if all 3 magnets were misaligned by less than 0.5mm the total -beating would be under 5%.

Tolerance:

Error in horizontal position = ±0.5mm.
Note: This is not an absolute tolerance but a magnet to magnet tolerance.

3.8.3 Vertical position of the superbends

A variation in the vertical placement will result in vertical orbit distortion and coupling. The requirement that sets the tightest limits on the vertical alignment of the superbends is the coupling and the requirement to keep the skew quadrupole feeddown to the level of the other sextupoles in the ring in order not to increase

the coupling. The contribution to the coupling from a skew quadrupole, *Kl*, is proportional to $Kl \times \sqrt{\beta_x \beta_y}$ where $_x$ and $_y$ are the -functions at the location of the skew quadrupole. The skew quadrupole component from a sextupole is *Kl* = *2Sly*, where *y* is the deviation in the orbit to the vertical center as defined by the sextupole.

We set the tolerance on *y* such that we keep the quantity $Sly\sqrt{\beta_x \beta_y}$ at the same level as that of the other sextupoles (see Table 2)[5]. Therefore the vertical misalignment of the magnet should be less than 400 m.

Family	*Sl* (m^{-2})	$\sqrt{\beta_x \beta_y}$ (*m*)	*y* (μm)	$Sly\sqrt{\beta_x \beta_y}$
SF	11	2.3	150	0.004
SD	8	4.1	150	0.005
Superbend	10	1.1	400	0.0045

Table 2. Comparison of the skew quadrupole feeddown components as a function of vertical beam offset for SF, SD, and the Superbends.

Tolerance:

Error in vertical position = ±0.4mm from ideal.

3.8.4 Roll of the superbends

A variation in magnet roll will result in vertical orbit distortion. The tolerance on the roll is determined by the requirement that the contribution to the vertical orbit distortion should be less than 200 m at a $_y$ of 4 m. The vertical kick $_y$ from a 10 degree horizontal bending magnet that is rotated by $_r$ radians is

$$\theta_y = \frac{2\pi}{36}\theta_r \tag{13}$$

The resulting orbit distortion y is then

$$\Delta y = \theta_y \frac{\sqrt{\beta_y(0)}\sqrt{\beta_y(s)}}{2\sin(\pi\nu_y)}\cos\left(\psi_y(s) - \pi\nu_y\right). \tag{14}$$

where $_y(0)$ is the vertical -function at the location of the bend, $_y(s)$ is the vertical -function at the observation point, $_y$ (s) is the vertical phase advance from the original location of the bend to the observation point s, and $_y$ is the vertical tune.

Let us assume that $_y$=0.2, $_y$ (0)=0.8m, $_y$ (s)= 4m. By keeping the roll angle to less than 250 rad insures that the contribution to the vertical orbit distortion from the roll of all 3 superbends will be less than 200 m.

Tolerance:

Error in roll < ±250 rad

3.9 Field jitter and vibration tolerance

The objective is to keep the contribution to the orbit motion from all the superbends below 3 m rms horizontal and 1 m rms vertical in the frequency range of (0.01 to 1000 Hz). This puts the following limits on the integrated motion due to vibration and power supply jitter.

Tolerance:

1. Longitudinal motion < 3 m (rms)
2. Horizontal motion < 5 m (rms)
3. Vertical motion < 5 m (rms)
4. Rolling motion < 2 rad (rms)
5. Power supply ripple, $\Delta I/I_{max} < 1/200{,}000$

These results can be derived from the formulas given is the previous subsections.

3.10 Energy ramping: speed and magnetic field reproducibility

Presently the ALS operates primarily at 2 electron beam energies: 1.5 GeV and 1.9 GeV. In fact most of the user operation (> 70%) is at 1.9 GeV. At both energies beam is injected into the storage ring with a beam energy of 1.5 GeV. For 1.9 GeV operation the beam energy is ramped in the storage ring from 1.5 GeV to 1.9 GeV. After the beam has decayed to about ½ its initial current, the remaining current is ramped down to 1.5 GeV. The ring is topped up to full current and the beam is ramped back up for users. This process is called the injection cycle.

The injection cycle begins when beam is taken away from users (close the photon shutters) and ends when we give beam back to users (open the photon shutters).

The full injection process or cycle is shown in Figure 17. The injection cycle takes about 11 minutes (a little longer if we are operating in 2 bunch mode where there is a parasitic bunch cleaning step). The process is as follows. First the beam is

taken away from users and the insertion device gaps are opened. The beam energy is then ramped down to 1.5 GeV. After reaching 1.5 GeV the beam current is topped off from 200 to 400 mA. The beam is then ramped up to 1.9 GeV, the orbit is corrected. Finally the insertion device gaps are closed and the beam is given back to users. Of that 11 minutes about 4 minutes is used for energy ramping (2 minutes to ramp down and 2 minutes to ramp up).

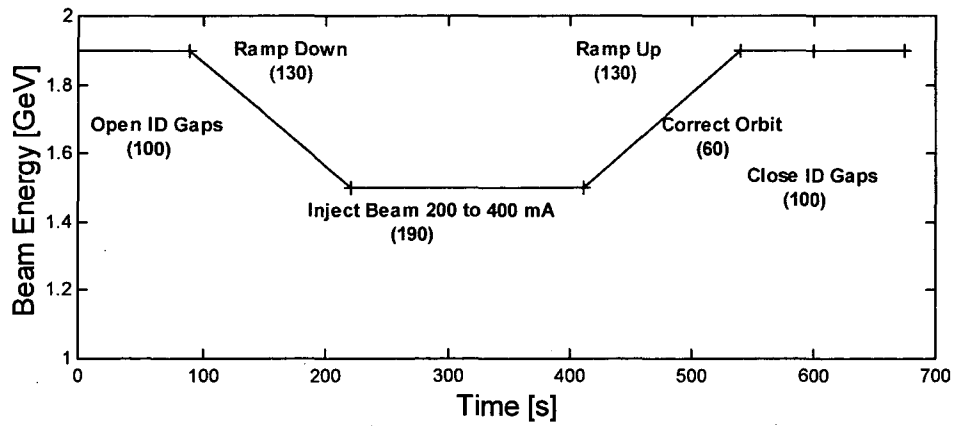

Figure 17. The injection cycle.

3.10.1 The injection cycle

It is important that the length of the injection cycle does not lengthen significantly when the machine is operating with the superbends. Therefore both the ramping and filling stages should not lengthen. For a good injection rate both the orbit needs to be reproducible and the dynamic aperture needs to be large.

Now let's discuss at the requirements of the superbends during the ramping stage of injection. Let's begin the discussion by examining what happens during the present ramping process. Field measurements correlating field to power supply current were made for the dipoles after they were constructed. Presently Superbends ramping is based upon magnet currents (not directly on field). This involves a lookup table and requires that establish a conditioning state such that the field-to-current is reproducible.

At present there are 52 main magnet families or power supplies (1 bend, 49 quadrupoles, and 2 sextupole) as well as 164 corrector magnet power supplies that are ramped. The ramp is divided into a number of steps. At each step magnet current set points are sent out to all the power supplies from a high level control system application. Once the setpoints arrive at the low level local controllers, the power supplies start ramping. Due to limitations in the present control system, the set points arrive at the local controller only to within 0.1 seconds of each other. Therefore ramping within each step is only partly synchronized.

Partial synchronization of the ramping results in tune jitter within a step. However the tune jitter is sufficiently small such that the beam does not get lost (The more

steps the smaller the tune jitter). Empirically we have found that one requires at least 180 steps (and sometimes more) to minimize beam loss during the ramp. It is not desirable to arbitrarily increase the number of steps because this lengthens ramping times. This is because delays are included in each step to insure that all magnets have reached their set points. These delays are for the most part independent of the step size. At present with 180 steps the machine takes about 2 minutes to ramp from 1.5 GeV to 1.9 GeV. In principle if one could remove the delays it would be possible to ramp faster. The fastest possible ramping rate is limited by the storage ring bend power supply. The bends can ramp between 1.5 GeV and 1.9 GeV in only 20 seconds.

There is one major difference between ramping with superbends and ramping without superbends. Without superbends all the bends are the same and they are on one power supply. As a result all bends change their field in sync. Therefore changes in bend field result in changes in beam energy not changes in beam orbit. However operation with the superbends means that the bends are decoupled. The mismatches in field will result in orbit errors as well as energy errors (see for example equation 7.3).

During ramping we require that the horizontal orbit shifts should be less than ±2mm in the straight sections where the horizontal -function is $_x$ = 11m. If one wishes to base the ramp upon current and not field as is done in the present ramping case then one needs to have a good match between the current and field of both the superbend and the normal bend. This match should be good to within 0.1% in field in order that the orbit distortion is less than 2 mm.

The map of current to field of the superbend will be determined through magnetic measurements initially. These measurements will serve as a "first pass" at matching the integrated dipole field of the superbend with the normal bend. During operation the beam orbit will be used to refine the match. What is important that relying on lookup tables is that the field as a function of current is reproducible level of 0.1% or better.

Once we have an accurate lookup table for the superbend and the normal bend, there still will be orbit motion during the ramp resulting from the ramping of the normal and superbends being asynchronous within a step. If the ramp is divided into *Nsteps* and one superbend is off by as much as one step the angular kick, θ_x, would be

$$\theta_x = \frac{2\pi}{36}\left(1 - \frac{1.9}{1.5}\right)\left(\frac{1}{Nsteps}\right) \tag{15}$$

So the orbit distortion, x, from one superbend being off by one step would be

$$\Delta x(s) = \frac{\theta_x\sqrt{\beta_x(s)}\sqrt{\beta_x(0)}}{2\sin(\pi\nu_x)}\left(\cos\left(\psi_x(s) - \pi\nu_x\right)\right) - \frac{\theta_x\eta_x(s)\eta_x(0)}{\alpha L_0} \tag{16}$$

where $_x(0)$ is the horizontal - function at the location of the bend, $_x(s)$ is the horizontal - function at the observation point, $_x(s)$ is the horizontal phase advance from the location of the superbend to the observation point s, and $_x$ is the horizontal tune. Lets assume that $_x$=0.25, $_x$ (0)=1.5m, $_x(s)$=11m. If we also assume that *Nsteps* = 180 then the maximum orbit distortion from all 3 superbends being off by as much as 1 step from the normal bends is 2mm. So from an orbit distortion point of view 180 steps are adequate.

Therefore if the fields versus current are reproducible and the ramping rate of the superbends are fast enough we should be able to ramp in the same manner as we ramp presently with no lengthening in ramping time. If the fields are not reproducible we have two back up options. The first is to feedback on the orbit during the ramp. The second is to control the beam directly on field. We plan to install 2 Hall probes per superbend to monitor the Superbend field. They will also be useful for trouble shooting problems.

It is conceivable that we will need to do an orbit correction at the top and bottom of the ramp both for users and for injection. Since we only correct the orbit at the top of the ramp this will add a little bit of time to the injection cycle (possibly as much as one minute). Since most of the orbit distortion will be generated by the mismatch of the Superbend one can imagine that the first step in orbit correction is to correct the orbit just using the superbends. Having a setability of the field of less than 1/60,000 allows one to correct the part of the orbit distortion coming from the mismatch of the bends down to the ~20 micron level.

From energy ramping we have the following requirements

1. The slew rates of the superbends should be 3A/s to match the maximum ramp rate of the normal bends. This is desirable especially if we wish to speed up the ramp in the future.
2. Fields should be setable at a rate of 10 Hz or greater. (At present the control system is limited to 10 Hz.)
3. The reproducibility in the field should be better than 0.1% in order to insure that we can base the ramp solely on current.
4. The magnet-to-magnet shift in the transverse center should be less than 0.5 mm while ramping between 1.5 GeV and 1.9 GeV.

3.11 Summary of Tolerances

Quantity	Tolerance	Driver
Magnetic Field		
Field at 2.6° and 7.4°	4.9T ± 5% at 1.9 GeV 3.9T ± 5% at 1.5 GeV	Photon Brightness
Maximum integrated field	$Bl_1 \geq 1.17$ Tm	Possibility for 2.0 GeV operation
Integrated multipoles Sextupole Octupole and higher ($n > 3$)	$\left\|\frac{Bl_3}{Bl_1}\right\| < 60\times10^{-4}$ $\pm 3\times10^{-4}$ at r= 1cm $\left\|\frac{Bl_n}{Bl_1}\right\| < 2\times10^{-4}$	Dynamic aperture
Integrated field	$Bl_1 = 0.8727$ Tm ± 0.1% at 1.5 GeV $Bl_1 = 1.1054$ Tm ± 0.1% at 1.9 GeV	Horizontal orbit
Absolute Alignment		
Longitudinal position	1 mm	Horizontal orbit
Horizontal position	0.5 mm*	Vertical beta-beating
Vertical position	0.4 mm	Coupling
Roll	250 rad	Vertical orbit
Vibration		
Longitudinal motion	3 m for frequencies > 0.01 Hz	Fast horizontal motion
Horizontal motion	5 m for frequencies > 0.01 Hz	Fast horizontal motion
Vertical motion	5 m for frequencies > 0.01 Hz	Fast vertical motion
Rolling motion	2 rad for frequencies > 0.01 Hz	Fast vertical motion
Field Jitter		
Fast	1/200,000 for frequencies > 0.01 Hz	Fast horizontal motion
Slow	1/60,000 for frequencies < 0.01 Hz	Slow horizontal motion
Ramping		
Slew rate	20 seconds	Ramping speed of normal bends
Difference in integrated field between superbends and normal bends	At any step the difference in integrated field between the normal bends and any superbend should be better than 0.1%.	Horizontal orbit

*The horizontal position tolerance is not really an absolute tolerance but a magnet-to-magnet tolerance.

3.12 References

[1] Advanced light source note LSAP–265 (1999).

[2] Tracy II as symplectic integrator written by Hiroshi Nishimura, Etienne Forest and Johan Bengtsson.

[3] S. Caspi, M. Helm and L.J. Laslett, "3D Field Harmonics", LBL-30313, 1991.

[4] M. Xiao, T. Katayama and E. Forest, DA Method and Symplectification for a field Map generated matrices of Siberian Snakes for spin tracking, PAC 1999.

[5] R. Keller, T. Lauritzen, Survey and Alignment for the ALS Project at LBL Berkeley, LSAP Note #146.

SUPERBEND DIPOLE SPECIFICATIONS

4.1 Introduction

The Superbend Magnet is a high field, short pole length superconducting dipole magnet with a central peak field of 5.69 T. When three Superbend Magnets are installed in the ALS, replacing existing gradient magnets, they will provide nominal 4.97 T source points which will provide synchrotron radiation with a nominal critical energy of 11.9 keV.

The magnet has a cold iron "C" shaped core driven by two superconducting racetrack coils. The magnet assembly is installed in a cryostat such that the vertical high field region in the magnet gap penetrates the cryostat cutout, known as the "mouthpiece". The mouthpiece is sized so that the cryostat can be inserted around the existing ALS storage ring vacuum chamber and the high field region can then be centered on the beam orbit. The cryostat includes, in addition to the magnet, the coil leads, a helium vessel, a liquid nitrogen vessel/ cold shield, a cold mass support system, a cryocooler, a quench protection system and magnet current leads which are housed within the cryostat vacuum vessel. The Superbend Magnet installed in the ALS Storage Ring is shown in Figure 1.

4.2 Magnet design

The Superbend Magnet design embodies major components that include a magnet core, two superconducting coils, two coil current leads, a helium vessel, a liquid nitrogen vessel and shield, a cold mass support system, a cryocooler, a quench protection system, a cryostat vacuum vessel, an external support system and field clamps. These major components are shown in Figure 2.

The design requirements and design parameters for the Superbend Magnet are tabulated below. This is followed by the detailed description of the magnetic design, magnet core, coil conductor, coil, coil current leads, helium vessel, liquid nitrogen vessel/ cold shield, cold mass support system, cryocooler, quench protection system, vacuum vessel, external support system and field clamps.

4.3 Requirement parameters

The basic requirements on magnet location and position, field, field conditioning, field ramping, and field stability that drive the design of the Superbend Magnet are given here:

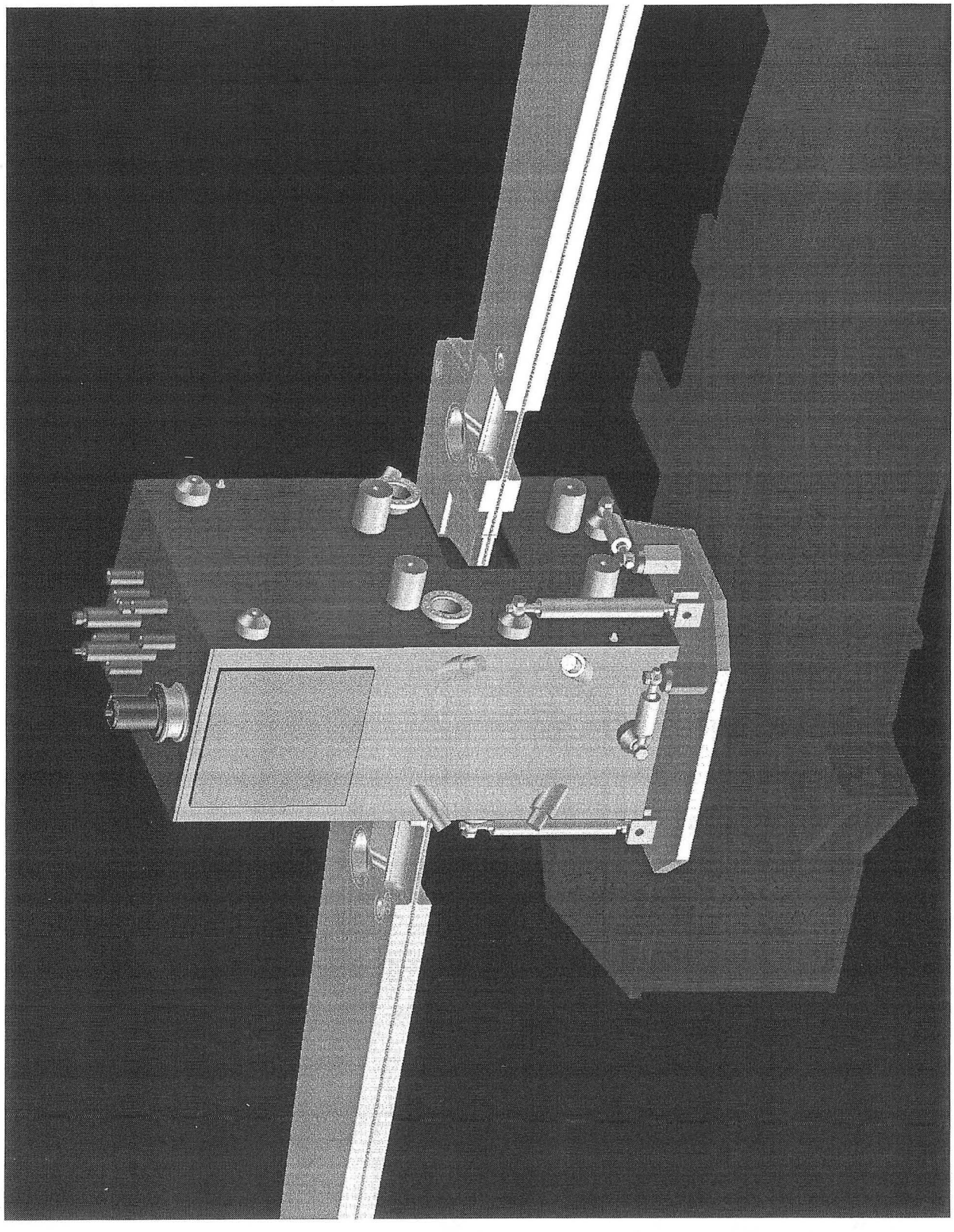

Figure 1. Superbend magnet installed in the ALS.

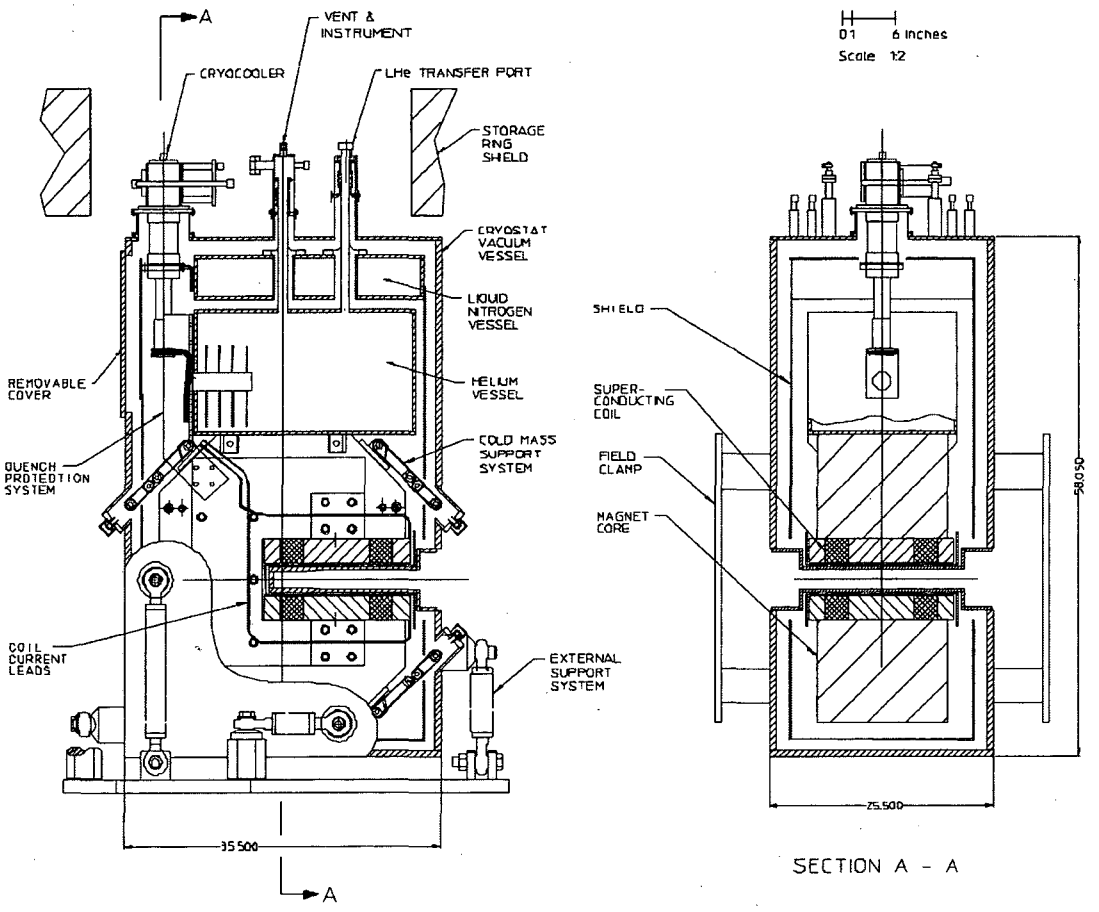

Figure 2. Superbend magnet.

4.3.1 Magnet locations and position

Curved Sectors	4, 8, 12
Magnets to be replaced	sr4 B2, sr8 B2, sr12 B2
Magnet centerline height above floor	1.400 m
Magnet transverse, longitudinal position	Same as the replaced magnets with the electron beam passing through the Superbend Magnet magnetic center.
Magnet yaw position	Entrance/exit electron beam trajectories must match existing gradient magnet entrance/exit electron beam trajectories and be symmetric about the magnet transverse centerline to provide 10 degrees of trajectory bend

Magnet pitch and roll	Nominally level with respect to gravity

4.3.2 Field requirements

Nominal maximum peak operating field	5.69 T (dB/dz = 0) with a nominal maximum operating current of 291 A
Nominal operating field at the electron beam orbit located +/- 2.4 degrees from the magnet center	4.97 T
Nominal operating field integral	1.1053 T m (10 deg. Bend @ 1.9 GeV)
Maximum peak cycling field (B_{maxc})	Field achieved when driving the magnet with 102% of the nominal maximum operating current
Nominal current margin	116% (338 A)
Conductor critical current	338 A @ 8.06 T & 4.3 deg K
Nominal multipole content @ r= 1 cm	B2/B1 = 7 X 10^{-4}
(based on SB4 tests)	B3/B1 = 32 X 10^{-4}
	B4/B1 = 1 X 10^{-4}
	B5/B1 = 2 X 10^{-4}
	B6+.../B1 = < 2 X 10^{-4}

4.3.3 Field conditioning requirements

Big loop conditioning	Cycle to maximum peak cycling field once per week at 3 A/s (B = 0 to B_{maxc} to B = 0) (52 cycles/yr or 1040 cycles/20 yrs)
Small loop conditioning	Cycle at every fill ($B_{1.9\ GeV}$ to $B_{1.5\ GeV}$ to $B_{1.9\ GeV}$)
	Every 8 hrs/multibunch operation – 90 % of the time
	Every 1.5 hrs/2 bunch operation – 10% of the time
	(1570 cycles/yr or 31,400 cycles/20 yrs)

Accelerator physics studies	Weekly operation Big loop – 3 cycles/wk (156 cycles/yr or 3120 cycles/20 yrs) Small loop – 20 cycles/wk (1040 cycles/yr or 20800 cycles/20yrs)
Cumulative field conditioning	
Requirements for 20 years	Big Loop – 4,160 cycles Small loop – 52,200 cycles

4.3.4 Field ramping requirements

Small loop

Form	Staircase
Lower current @ $B_{1.5\ GeV}$	207 A
Upper current @ $B_{1.9\ GeV}$	291 A
Maximum average ramping speed	0.8 A/s
Max. instantaneous ramping speed	3.0 A/s

Big loop

Form	Ramp
Starting current	0 A
Peak current (B_{maxc})	297 A
Maximum ramping speed	3.0 A/s

4.3.5 Field stability requirements

Short term (< 1 min)	+/- 3 micron rms max orbit displacement for all frequencies > 0.01 Hz dI/I_{max} 1 : 200 000
Long term (> 1 min)	+/- 20 micron max. orbit displacement @ 1.5 GeV for all 3 magnets dI/I_{max} 1 : 60 000

4.4 Design Parameters

4.4.1 Magnet core parameters

Magnet core material	Fully annealed AISI 1010 steel
Magnet pole gap	100.0 mm
Magnet pole height	67.05 mm
Magnet pole length (beam direction)	114 mm
Magnet pole width	180 mm
Magnet pole lamination thickness	23.0 mm (0.9055 inch)
Magnet pole weight (ea.)	36 lbs.
Magnet yoke length	380 mm
Magnet yoke width	700 mm
Magnet yoke height	820 mm
Magnet yoke lamination thickness	41.9 mm (1.65 in.)
Magnet yoke weight	2779 lbs.
Magnet core weight	2851 lbs.

4.4.2 Magnet pole tip construction tolerances

Pole height tolerance	+/- 0.050 mm
Pole width tolerance	+0.000/-0.50 mm
Pole length tolerance	+0.000/0.050 mm

4.4.3 Magnet pole tip positional tolerances (with respect to the theoretical magnet centerlines)

Direction	Tolerance
Vertical	+/- 0.089 mm (+/- 0.0035 inch)
Radial	+/- 0.280 mm (+/- 0.011 inch)
Longitudinal	+/- 0.280 mm (+/- 0.011 inch)
Roll (radial angular)	+/- 0.99 mrad
Pitch (longitudinal angular)	+/- 1.56 mrad
Yaw (pole rotation)	+/- 5.59 mrad

4.4.4 Magnet coil conductor parameters

Conductor material	Cu/NbTi
Copper/superconductor ratio	3.0
Number of superconductor filaments	330
Relative resistivity ratio	>200
Conductor size - bare	0.9 mm X 1.8 mm
Conductor size – insulated	1.00 +/- 0.02 mm X 1.90 +/- 0.02 mm
Conductor insulation	Formvar

4.4.5 Magnet coil parameters

Number of turns per layer	33
Number of layers	70
Total number of turns	2309
Conductor length (theoretical)/coil	1725 m

4.4.6 Magnet coil positional tolerances (with respect to the theoretical magnet centerlines)

Direction	Tolerance
Vertical	+/- 0.368 mm (+/- 0.0145 inch)
Radial	+/- 0.635 mm (+/- 0.025 inch)
Longitudinal	+/- 0.635 mm (+/- 0.025 inch)
Roll (radial angular)	+/- 2.84 mrad
Pitch (longitudinal angular)	+/- 3.81 mrad
Yaw (coil rotation)	+/- 12.70 mrad

4.4.7 Magnet coil lead parameters

Number	2
Manufacturer	American Superconductor, Inc.
Rating	350 amps @ 82 K

4.4.8 Liquid helium vessel parameters

Material	304L SS
Volume	85 liters
Test pressure	30 psia
Relief valve setting	8 psi gauge

4.4.9 Liquid nitrogen vessel and shield parameters

Material	Aluminum
Volume	35 liters
Test pressure	30 psia
Relief valve setting	8 psi gauge

4.4.10 Cold mass support system parameters

Number of supports	8
Strap material	S-2 Glass – epoxy composite
Link material	304 SS
Support design operational load	5910 lbs.
Support conditioning load	10,000 lbs.

4.4.11 Cryocooler parameters

Manufacturer	Sumitomo
Refrigeration unit model	SRDK-415DW
Cryocooler model	RDK-415DW
1^{st} stage cooling power	45 W@ 50 K
2^{nd} stage cooling power	1.5 W @ 4.2 K
Compressor model	CSW-71C
Compressor cooling requirement	Water - 7 liter/min

4.4.12 Quench protection system parameters

Activation voltage	20 V
Time constant	20 sec

4.4.13 Instrumentation

Temperature sensors	8
Sensor type	Cernox

4.4.14 Vacuum vessel parameters

Material	304L SS
Height	1474 mm
Length	648 mm
Radial width	902 mm
Inner radius mouthpiece vertical gap	42.2 mm
Outer radius mouthpiece vertical gap	54.9 mm
Test pressure	15 psia (external), 5 psi (internal)
Relief valve setting	2 psi gauge

4.4.15 External support parameters

Number of supports	6
Configuration	LBNL Drawing No. 25F1606
Pitch	1.058 mm/turn

4.4.16 Field clamp parameters:

Material	AISI 1010 steel
Thickness	0.75 inch
Distance from magnet core	260 mm

4.5 Design Description

4.5.1 Magnetic design

4.5.1.1 Superbend multipole requirements and mechanical tolerances

This section considers the effects of mechanical position tolerances of the poles and coils and their affect on the superbend magnetic multipoles. The resulting multipoles are compared to the requirements for storage ring operation. Table 1 below summarizes. The storage ring requirements.

Table 1. Normalized Multipole Requirements at r = 1 cm

$$|b_1/a_1| < 2.5\times10^{-4}$$
$$|b_2/a_1| < 6.0\times10^{-4}$$
$$\Delta|a_2/a_1| < 5\times10^{-4}$$
$$|a_3/a_1| < 6\times10^{-3}$$
$$\Delta|a_3/a_1| < 3\times10^{-4}$$

The Δ symbol indicates a requirement on magnet-to-magnet variation among the three superbend magnets.

Calculations of error multipoles corresponding to assembly tolerances are based upon a list of maximum expected coil and pole position errors, and coil perturbation sensitivity coefficients. The values used for coil and pole positions are based upon a judgment of achievable tolerances using careful assembly techniques. The coil perturbation sensitivity coefficients are also used to account for pole perturbations. We assume that a pole movement produces a qualitatively similar affect as a coil movement. For example, a small vertical motion of the coil is similar to a small vertical motion of the pole. Since the contributions to the multipole components are similar, the same sensitivity coefficients are used for pole perturbations.

The following tables are compilations of expected position errors and the effects on multipoles. The sensitivity coefficients, S_{b1}, etc., are in units of normalized multipole ($\times10^4$) per unit of error (mm or mrad). Multipole components are in units of 10^{-4} at 1 cm.

Table 2. Expected Skew Dipole

Error Type	Units	Error Value	S_{b1} (10^4)	$\|b_1/a_1\|$ (10^4)
Pole dy	mm	0.09	---	---
dx	mm	0.28	24.0	6.7
dz	mm	0.28	---	---
roll	mrad	0.99	-0.83	0.8
pitch	mrad	1.56	---	---
yaw	mrad	5.59	---	---
Coil dy	mm	0.37	---	---
dx	mm	0.64	24.0	15.4
dz	mm	0.64	---	---
roll	mrad	2.84	0.83	2.4
pitch	mm	3.81	---	---
yaw	mm	12.70	---	---

Table 3. Expected Skew Quadrupole

Error Type	Units	Error Value	S_{b2} (10^4)	$\|b_2/a_1\|$ (10^4)
Pole dy	mm	0.09	3.26	0.3
dx	mm	0.28	0.01	---
dz	mm	0.28	---	---
roll	mrad	0.99	-3.26	3.2
pitch	mrad	1.56	---	---
yaw	mrad	5.59	---	---
Coil dy	mm	0.37	3.26	1.2
dx	mm	0.64	0.01	0.1
dz	mm	0.64	---	---
roll	mrad	2.84	-3.26	9.3
pitch	mm	3.81	---	---
yaw	mm	12.70	---	---

Table 4. Expected Normal Quadrupole

Error Type	Units	Error Value	S_{a2} (10^4)	$\lvert a_2/a_1 \rvert$ (10^4)
Pole dy	mm	0.09	---	---
dx	mm	0.28	-3.26	0.9
dz	mm	0.28	---	---
roll	mrad	0.99	0.68	0.7
pitch	mrad	1.56	---	---
yaw	mrad	5.59	---	---
Coil dy	mm	0.37	---	---
dx	mm	0.64	-3.26	2.1
dz	mm	0.64	---	---
roll	mrad	2.84	0.68	1.9
pitch	mm	3.81	---	---
yaw	mm	12.70	---	---

Table 5. Expected Normal Sextupole

Error Type	Units	Error Value	S_{a3} (10^4)	$\lvert a_3/a_1 \rvert$ (10^4)
Pole dy	mm	0.09	-0.14	---
dx	mm	0.28	-0.01	---
dz	mm	0.28	---	---
roll	mrad	0.99	-0.14	0.1
pitch	mrad	1.56	---	---
yaw	mrad	5.59	---	---
Coil dy	mm	0.37	-0.14	0.1
dx	mm	0.64	-0.01	---
dz	mm	0.64	---	---
roll	mrad	2.84	-0.14	0.4
pitch	mm	3.81	---	---
yaw	mm	12.70	---	---

The multipole component b_1 can be corrected by adjusting the roll. The components a_2 and b_2 can be corrected by moving the magnet horizontally and vertically, respectively, in the presence of a strong sextupole. A normalized sextupole value of 3×10^{-3}, at $r = 1$ cm was assumed for position adjustment calculations. This value is based upon magnet analysis and confirmed by magnet measurements of SB4. Therefore the maximum expected error, and the corre-

sponding required adjustment, should be compared to the adjustment range. Table 6 below provides this comparison, where the expected error is calculated by adding individual components in quadrature and multiplying by $\sqrt{2}$ to account for two coils and poles for each magnet. The maximum allowance for adjustment by moving the full magnet and cryostat relative to the vacuum chamber is shown, with the additional range for adjusting the magnet inside the vacuum chamber shown in parentheses. However, internal adjustment will tighten the gap allowed for super-insulation, potentially reducing its effectiveness. Note that the roll and vertical (Δy) adjustments are not independent. If the magnet is adjusted for maximum roll, the vertical range is zero, and vise versa.

Table 6. Total Expected Errors, Required Adjustments

	Expected Error	Required Adjustment	Maximum Adjustment
$\lvert b_1/a_1 \rvert$	24.0	roll = 2.4 mrad	±7.3 (9.7) mrad
$\lvert b_2/a_1 \rvert$	14.0	Δy = 2.3 mm	±1.5 (2.0) mm
$\lvert a_2/a_1 \rvert$	4.3	Δx = 0.7 mm	±10 mm
$\lvert \Delta a_3/a_1 \rvert$	0.6	---	---

The results demonstrate that the range allowed for movement of the full cryostat assembly is sufficient to cancel the skew dipole and normal quadrupole, but not the skew quadrupole. A roll adjustment of 2.4 mrad will use up 0.5 mm of the vertical adjustment range, leaving 1.0 mm to adjust for skew quadrupole. The maximum expected variation in sextupole of 0.6 units is well below the required limit.

4.5.1.2 Eddy Current Effects

Eddy currents that are induced in any conductive superbend magnet system component must not exceed values that adversely impact field quality beyond the limits specified in the summary table of Section 3-11. Furthermore all structural superbend components must be of sufficient strength to withstand instantaneous forces and torques generated by these eddy currents.

The maximum slew rate specified in Section 3-10 for the superbends is 3A/s, so as to match the maximum ramp rate of the normal bends. This corresponds to a $\dot{B} = 600\,\text{G/s}$ in the superbends.

The eddy current induced per unit length along the arc s of any electrically conducting component in a dipole field B is given by

$$I'(s) = \sigma D x \dot{B}$$

where σ is the electrical conductivity of a component of thickness D at horizontal position x with respect to the magnet's vertical symmetry plane.

The multipole expansion for the field induced from a pair of filaments of current I at locations z and z^* in the gap region of height $2h$ between the poles of a dipole is

$$B^*(z) = \frac{\mu_0 I}{2hi} \sum_0 \frac{-1^{n+1}\alpha^n}{n!} \mathrm{Re}[b_n]; b_0 = 1/Tanh\alpha_0; \alpha = \frac{\pi}{2}\frac{z}{h}.$$

Integrating over the entire conductive component gives for the dipole component of the perturbation field:

$$B^*_{\Delta\_dipole} = \frac{-\mu_0}{2hi} \int_{s_{upper}} \mathrm{Re}[b_0]\sigma D \dot{B} dx .$$

Field perturbations due to eddy currents in all relevant conductive superbend system components were calculated via a code utilizing the expression developed above. The most critical components are the storage ring vacuum chamber, which is closest to the beam axis and the aluminum constraining ring, which, though farther away from the beam axis, is of a much larger cross-section. Other conductive components, *e.g.* the copper plate thermal conductors, the stainless steel vacuum cryostat, the pole laminations, and the LN shield induce negligible field perturbations because of either their relatively small cross-section, their relatively low conductivity, and/or their relatively large distance from the beam axis.

Eddy currents in the storage ring vacuum chamber with $\sigma_{Al} = 0.33/\mu\Omega cm$ and varying thickness of 5-15 cm give rise to field perturbations of magnitude 6 G. This is 1 part in 10,000 which is an acceptable, though not negligible, perturbation. The sextupole and other higher order components generated are negligible.

Alloy 5083 was chosen for the cold aluminum constraining rings because of its relatively low conductivity at cryogenic temperatures ($\sigma_{Al5083@4.2K} = 0.33/\mu\Omega cm$) relative to other alloys. These rings are much farther (10-18cm) from the beam axis, however their area ($40cm^2$) is relatively large. They give rise to field perturbations of magnitude 36 G. This is 6 parts in 10,000 which is still below the 0.1% requirement of Section 3-10.

4.5.2 Magnet core

The magnet requires a "C"-shaped iron core so that the magnet can be installed around the ALS storage ring vacuum chamber. This "C"-shaped core includes a "C"-shaped yoke and two racetrack shaped pole pieces. The nominal yoke di-

mensions 820 mm (32.28 inches) high, 700 mm (27.56 inches) wide and 380 mm (14.96 inches) thick. The pole piece plan, race track configuration, is 114 mm (4.488 inches) along the beam direction and 180 mm (7.087 inches) in the direction transverse to the beam. The core and pole are laminated with the laminations normal to the beam direction.

The yoke is laminated with 9 iron plates; material is 2.0 inch thick annealed AISI 1010 steel plates. The plates are machined to a thickness of 41.9 mm (1.65 inch) and a flatness of 0.005 inch, each side, prior to yoke fabrication. The pole pieces are also laminated and made from 1.0 inch annealed AISI 1010 steel plate, machined to 23.0 mm thickness (0.9055 inch) and a flatness of 0.001 inch, each side, prior to pole piece fabrication.

Yoke fabrication starts with the horizontal stacking of the thick plates that are interleaved with 0.003 inch thick S-2 glass cloth that are coated with high thermal conductivity epoxy coating, Stycast 2850FT and hardener 24LV, and room temperature cured with about 10 psi pressure. Next the parallel surfaces of the mouth of the C yoke, spacing 234.26 mm (9.223 inches), are machined to a dimensional tolerance of +/- 0.002 inch and a parallelism tolerance of 0.001 inch and the flatness of each surface to 0.001 inch. The four threaded holes for the two pole tips, the threaded holes for the coil support and the slots for the leads must be added. After machining the mouth of the yoke, the interlamination shorts must be removed. Then the slots for the outer bars, that tie the nine laminations together, are machined along with other required features. Welding of the bars to the laminations follows. The yoke assembly is shown in Figure 3.

Pole piece fabrication is similar to the yoke fabrication. The plates are stacked and interleaved with 0.003 inch thick S-2 glass cloth, epoxy coated with a high thermal conductivity epoxy coating, Stycast 2850FT and LV24 hardener, and the assembly is cured under about 50 psi pressure. The top and bottom faces of each pole are machined parallel to 0.001 inch and each face is to be flat to within 0.001 inch. Anticipated pole tip tolerances are given above in the Design Parameter Section [1]. After machining, the interlamination shorts must be removed. The pole assembly is shown in Figure 4.

The pole pieces are assembled to the yoke with 2 shoulder bolts each. The pole pieces are insulated from the magnet yoke with a 0.075 mm (0.003 inch) thick Kapton sheet. Anticipated pole tip positional tolerances are given in the Design Parameter Section [2].

After the magnet core is assembled, the pole surface must be referenced to the fiducials on the sides of the superbend magnet as shown in Figure 3. The estimated accuracy of transferring the pole surface dimensional information to the side fiducials is given below:

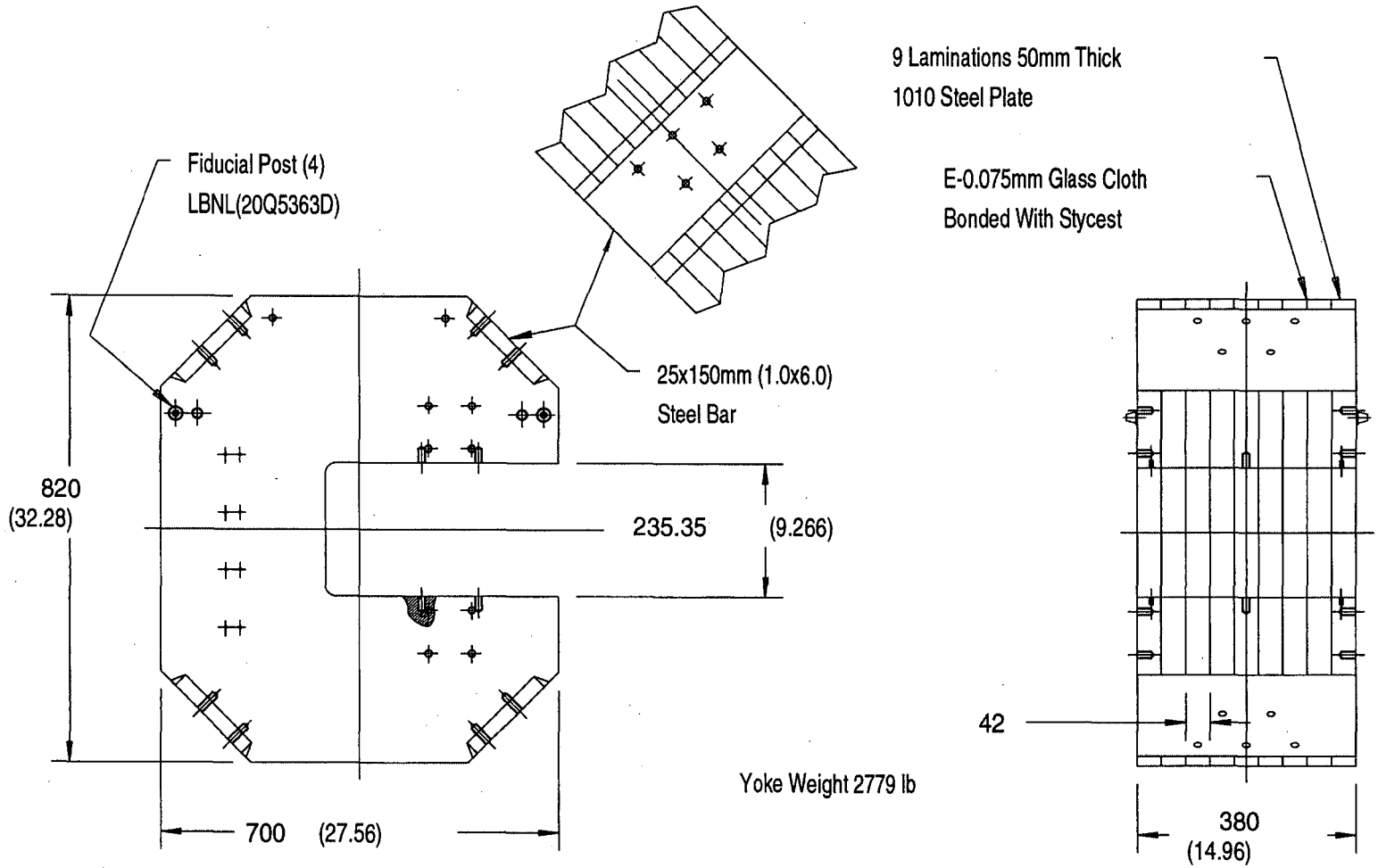

Figure 3. Superbend yoke assembly.

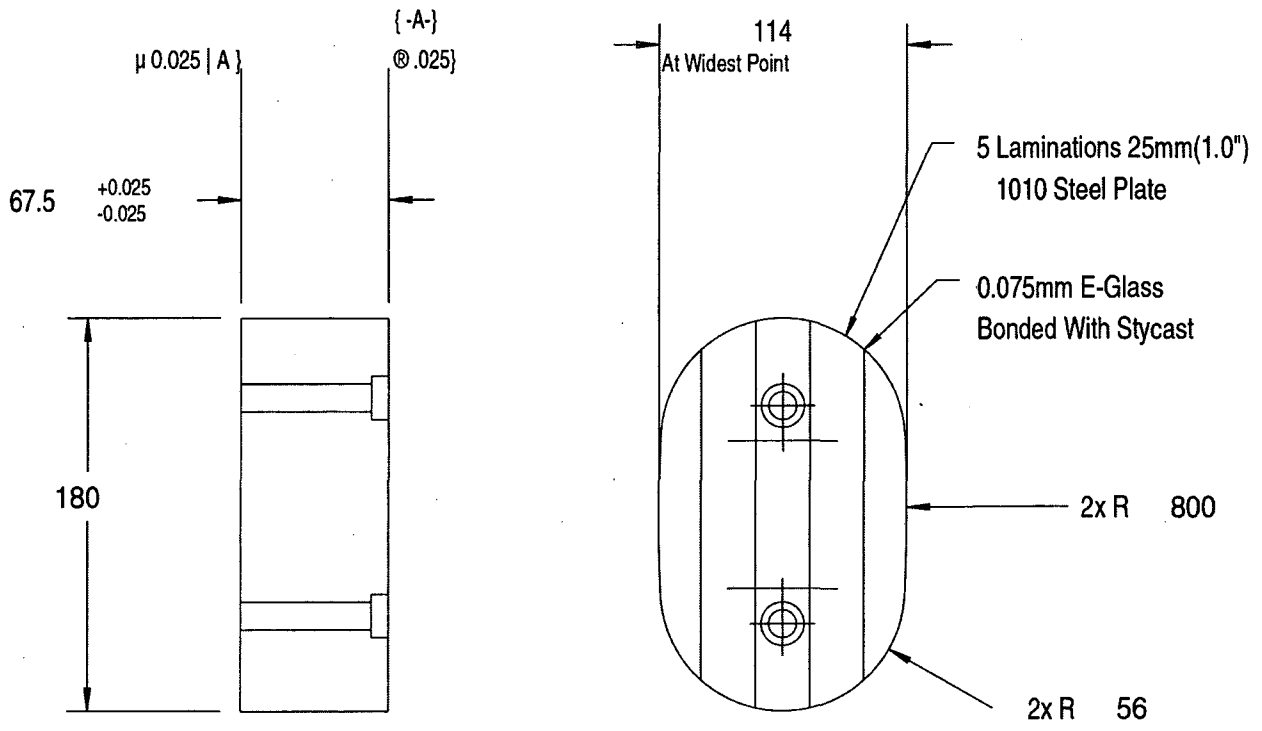

Figure 4. Superbend pole assembly.

Magnet Core – Magnet Core Fiducial Alignment (measuring) Error

Longitudinal	+/- 0.100 mm
Radial	+/- 0.100 mm
Vertical	+/- 0.100 mm
Pitch	+/- 0.50 mrad (based on a 400 mm fiducial spacing)
Roll	+/- 0.33 mrad (based on a 600 mm fiducial spacing)
Yaw	+/- 0.50 mrad (based on a 400 mm fiducial spacing)

When the magnet is energized to full field, the magnetic force pulling the pole tips together is estimated at 298,752 N (67,286 lbs) [3]. Under this loading, each pole tip will deflect 0,10 mm toward the midplane. Resulting stresses in the back leg of the yoke are 23.8 Mpa (3450 psi) compression and 18.3 Mpa (2660 psi) tension.

4.5.3 Magnet Coils

4.5.3.1 Conductor

The conductor material is a copper/superconductor (niobium-titanium alloy) in a nominal ratio of 3:1 [4]. The relative resistivity ratio (rrr) is specified as >200. The wire size (bare) is 0.9 mm by 1.8 mm and includes 330 superconductor filaments of 39 micron diameter with the bundle twisted with a 45 mm pitch. With insulation, Formvar, the conductor size is 1.00 +/- 0.02 mm by 1.90 +/- 0.02 mm. The required conductor length per coil is 1725 m.

4.5.3.2 Coil

The coil is wound on a 1 mm thick race tracked shaped spool with flanges that are configured so that the inner tube dimensions of the spool match the pole tip outline with a 0.005-inch gap all around as shown in Figure 5. Prior to winding two layers of 0.002-inch of MT Kapton & 0.003-inch mica paper is stuck to the inner tube; that is followed with a layer of 0.0025-inch S-2 glass cloth impregnated with Stycast 2850FT and LV24 hardener. The flanges are insulated with two layers of 0.002-inch MT Kapton, next to the copper flange and then 0.003-inch Mica paper is placed next to the Kapton. Next, the inner lead is dressed into position and then layer winding starts. Winding is done wet with the Stycast 2850FT and LV24 hardener with 33 turns per layer. After completing the winding of a layer a layer of 0.003-inch thick S-2 glass cloth is laid down. This process is repeated 70 times to complete the coil and the last layer has I less turn so the coil package ends up being a neat rectangular cross-section. Coil temperature and conductor resistance are monitored all during the winding to insure that turn-to-turn shorts do not develop. The outer radius is then insulated with a layer of 0.002-inch Kapton with 0.0025-inch E glass cloth and impregnated with Stycast 2850FT and LV24 hardener. The resistance and temperature of the completed coil are measured and recorded. Coil height 66.35 mm (2.612 +0.000/-0.20 inch) and radial thickness 80.55 mm (3.171 +0.000/-0.20 inch) are measured.

Because of the high magnetic forces, the coil is contained within a 5083-H321 aluminum structural ring. After the coil winding has been completed, the aluminum ring inner dimension is determined from the outer coil profile. The profile is cut so that a 0.50 mm (0.020-inch) gap is provided all the way around the coil

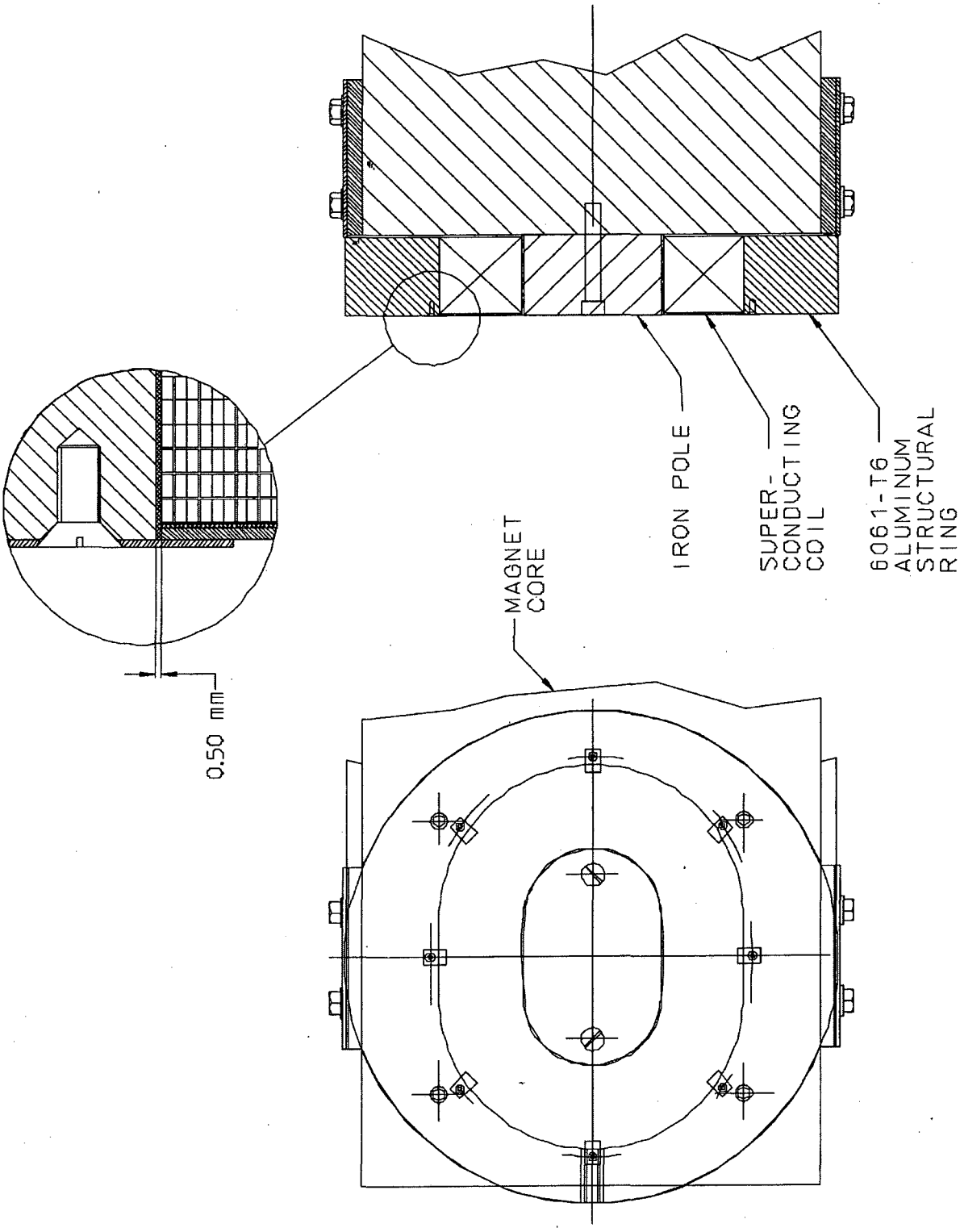

Figure 5. Superbend Coil.

when it is inserted into the ring. After coil insertion, the coil is bonded to the aluminum ring with 0.003-inch S-2 glass cloth and Stycast 2850FT and LV24 hardener. After completion of bonding, the coil-aluminum ring assembly is voltage checked, high potted to 1 kV with respect to the conductor.

Coil-aluminum ring assembly installation onto the magnet yoke involves preparing a gasket which goes between the coil assembly and the yoke, and then placing the coil-aluminum ring assembly onto the gasket and securing the assembly with 4 insulated bolts. The gasket consists of 3 sheets of 0.005-inch thick S-2 glass cloth which are bonded together, in place, with high thermal conductivity epoxy coating, Stycast 2850FT and 24LV hardener. Mold release is applied to the yoke, pole tip and coil to prevent the gasket from adhering to any of the parts. The estimated coil positional tolerances are given in the Design Parameter Section [2].

4.5.4 Coil Current Leads

The Superbend magnet system uses conduction cooled binary current leads, in which the high temperature section from room temperature to the thermal shield is pure copper and the lower section from the thermal shield to the superconducting magnet uses High Temperature Superconductor (HTS). Conduction cooled leads are a natural choice when cooling is provided by a closed-loop Gifford-McMahon cryocooler since there is no available cold helium gas stream that could be used to cool the current leads. Conduction cooled leads also have extreme simplicity of operation since a gas flow is not required.

The copper lead is optimized to minimize the heat load to the thermal shield. In this optimization, the proper length to diameter ratio is selected based on the temperature-dependent thermal conductivity and temperature-dependent electrical resistivity. For the Superbend, the copper lead is optimized for 320 A, which strikes a balance between the current at which the Superbend will be operated most of the time, 290 A, and the critical current, 336 A. Conduction cooled leads are stable and can be operated above their optimized value with little added heat input. The heat input to the thermal shield from the copper leads represents the single largest heat input to the thermal shield. This heat input essential drives the refrigeration requirement placed on the cryocooler.

The upper end of the copper lead is insulated from the vacuum vessel by means of a ceramic insulator. To ensure long-term trouble free operation, the vacuum seal around the insulator must be a metallic seal such as a Conflat. Under conditions of steady-state operation at 290 A the upper end of the lead will be frost-free because of joule heating. However, in extended periods of standby operation in which the current is off the leads will frost if they are exposed to atmospheric conditions. Frosting in itself is not a problem, but the cold temperature could cause the power cable insulation to crack and the melting ice could create

problems with adjacent electronics. To prevent such problems, a thermostatically controlled heater will be used to keep the lead end at room temperature. A 10 W heater on each lead should be adequate to keep the upper end warm when the current is off.

To ensure safety, the exposed leads will have an insulating cover to prevent accidental electrical contact. The ceramic insulator will have a voltage rating of at least 1000 V dc.

The low temperature end of the copper lead will be thermally anchored to the thermal shield and electrically connected to the upper end of the HTS section. The thermal anchor will ensure that the upper end of the HTS section will be less than 82 K. The thermal anchor will be able to withstand a test voltage of 1000 V dc for 1 minute in air at room temperature.

The HTS section is a commercially available lead made of BSCCO 2223 tapes in a silver alloy matrix, encapsulated in a epoxy-fiberglass rod for structural support. The HTS lead is specified to carry 350A at 82 K, with a heat leak into the 4K coil of 0.3 mW per pair at 290 A when the upper end is at 82 K. To prevent damage to the HTS material, low melting point solder such as Woods metal is used for making connections to the copper lead at the upper end and to the Nb-Ti conductor on the coil end. The connections are also bolted for long-term reliability.

Redundant voltage taps are attached to each end of the HTS section (and the connections on each end) for HTS lead quench detection. In case an excessive voltage drop is detected, action will be taken to rapidly drop the current passing through the leads.

4.5.5 Liquid Helium Vessel

The liquid helium vessel is required to maintain the coil in the superconducting state when the cryocooler is not operational. In normal operation, i.e. with the cryocooler operating, no liquid helium is consumed since the required low-temperature refrigeration is provided entirely by the cryocooler second stage.

With the cryocooler operating, the liquid helium in the vessel is cooled to about 3.5 K with a corresponding vapor pressure of 350 Torr. Because the liquid helium bath is below atmospheric pressure all valves and fittings that communicate with the vessel must be leak tight to prevent air from being pumped into the vessel. An air leak could pose a potential hazard since a plug could form that could prevent the vessel from venting in case of a pressure buildup caused by heating due to cryocooler shutdown, magnet quench, HTS lead quench, or loss of insulating and consequent vaporization of the liquid helium bath.

The liquid helium allows continued operation of the Superbend with an external supply of cryogenic fluids in case of cryocooler failure. The temperature and pressure of the liquid helium will rise to 4.3 K, 1.08 atm and refrigeration provided by utilizing the heat of vaporization. The liquid will be replenished as required from external storage dewars located outside the ALS Storage Ring shielding blocks using pre-installed transfer lines which penetrate the shielding. A superconducting-type liquid helium level sensor will be used to monitor the liquid level and operate valves on the storage dewar to automatically maintain the liquid helium at the proper level. A heat exchanger inside the liquid helium vessel ensures that the superconducting coil is thermally connected to the liquid helium bath and is thereby maintained at the proper temperature. The expected heat load to the 4K system with the cryocooler inoperative is 3 W, which consumes 4.2 l/hr. Since the on-board liquid is about 75 liters (90% of the 85 liter minimum vessel capacity), the Superbend will have a running time of 18 hours before an external liquid helium dewar must be installed and supply of liquid furnished to the liquid helium vessel.

The liquid helium vessel is constructed of 304L stainless steel, designed and manufactured to the intent of the ASME Boiler and pressure Vessel Code, Section VIII, Division 1, Appendix 13. The room temperature test pressure is 30 psig, with a relief valve/rupture disc setting of 8 psig. The expected maximum operating pressure is 1.2 psig.

The liquid helium vessel has two 304L stainless steel penetrations that allow filling, venting, and level sensing. Each of these penetrations has an outer diameter of 1 inch with a wall thickness of 0.020 inch. The penetrations are thermally anchored to the liquid nitrogen vessel to minimize heat input to the liquid helium vessel.

Except for the beam aperture region, the liquid helium vessel surfaces that are exposed to thermal radiation from surfaces of higher temperature are covered with a minimum of 10 layers of Multilayer Insulation (MLI) to reduce the heat flux due to thermal radiation. In the beam aperture region a minimum of 5 layers of MLI are applied. The MLI also limits the heat flux to the liquid helium vessel in case of accidental loss of insulating vacuum by providing a thermally insulating layer around the vessel.

4.5.6 Liquid Nitrogen Vessel and Shield

The liquid nitrogen vessel and shield act to limit the heat input to the 4 K components by intercepting heat due to radiation and conduction from room temperature. The conduction heating under normal operation is due to current leads, magnet supports, instrumentation wires, and helium vessel penetrations. When the cryocooler is off, there is significant heat input from the cryocooler. In normal

operation to liquid nitrogen is consumed since the required refrigeration is provided entirely by the cryocooler first stage.

With the cryocooler operating, the liquid nitrogen is cooled to about 50 K, where it is a solid with a vapor pressure of about 5 Torr. All valves and fittings must be leak tight to prevent air from being pumped into the liquid nitrogen vessel. An air leak could create a hazard if a plug formed which would prevent the vessel from properly venting due to a pressure increase cause by heating due to a cryocooler shutdown or loss of insulating vacuum.

The liquid nitrogen vessel allows for continued Superbend operation with external liquid in case of cryocooler failure. On cryocooler shutdown, the increased heat load will cause the solid nitrogen to melt and the liquid will rise to a temperature of 78 K and a pressure of 1.07 atm. The refrigeration is provided by boiling so the liquid must be replenished from an external storage dewar outside the ALS storage ring shielding using pre-installed transfer lines which penetrate the shielding. A capacitance-type liquid level gauge is used to monitor the liquid level and operate a supply valve to maintain the liquid at the proper level. The expected heat load to the liquid nitrogen vessel with the cryocooler off is 90 W, which leads to a consumption rate of 2 l/hr. Since the initial amount of liquid nitrogen is about 30 liters (90% of the vessel capacity of 35 liters), we can operate for 15 hours before an external liquid nitrogen source is required to be available.

The vessel is designed and manufactured to the intent of the ASME Boiler and pressure Vessel Code, Section VIII, Division 1, Appendix 13. The vessel is constructed of Aluminum alloy, type 6061 in order to have good thermal conductivity. The room temperature test pressure is 30 psig with a relief valve/rupture disc setting of 8 psig.

The vessel has four 304 stainless steel tubular penetrations for filling, venting, and level sensing, each having an outer diameter of 0.5 inch and a wall thickness of 0.035 inch. An aluminum-stainless steel transition piece made by explosive bonding allows the penetrations to be welded to the aluminum alloy vessel.

The liquid nitrogen vessel is thermally connected to an aluminum shield that completely encloses the 4 K components, including the throat area where the ALS vacuum chamber passes through the Superbend poles. The thermal shield is designed to have a peak temperature of 82 K when the cryocooler is inoperative and the Superbend is operated with cryogenic fluids. To minimize the heat load to the thermal shield, the outer surface of the shield is covered with a minimum of 30 layers of MLI, except in the throat region where 10 layers are used.

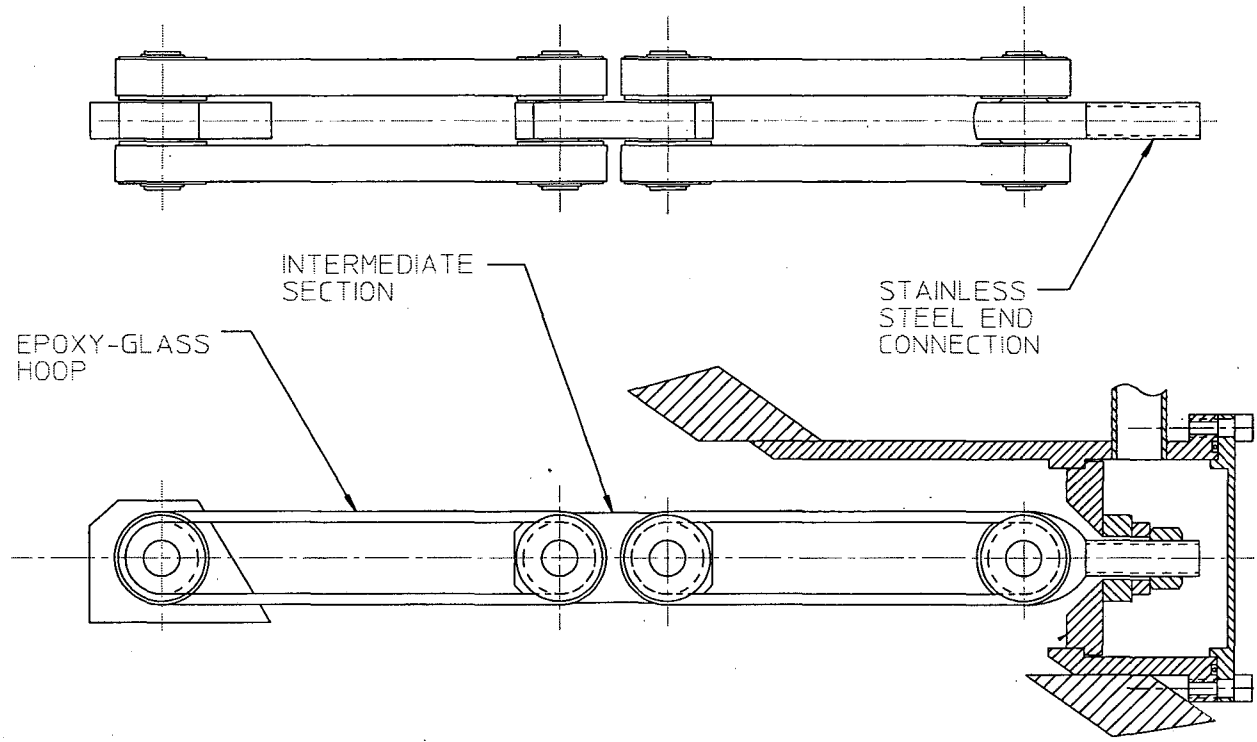

Figure 6. Superbend support strap assembly.

4.5.7 Cold Mass Support

The four degree Kelvin magnet is to be supported in the cryostat vacuum vessel with 8 straps arranged in a symmetrical configuration as shown in Figure 2. Each strap is made up of four epoxy-glass hoops, stainless steel end connec tions and an intermediate section, which intercepts the intermediate cryostat shield at 50-70 Kelvin, as shown in Figure 6

The epoxy-glass hoops are a WANG Inc. proprietary design; the hoops are wound from S-2 glass fiber and molded. \ WANG Inc reports that the yield strength and ultimate strength are nearly the same, 120,000 psi. The elastic modulus is 10 X 10^6 psi. To minimize creep, WANG Inc typically preloads the straps to 125% of the maximum working load for 24 hours prior to installation. The proposed cross section for the strap is 0.500 inches by 0.15 inches.

Strap loading, stress and deflections are summarized in the following table:

Table 7. Superbend Strap Loading, Deflection and Stress [5]

Condition	Nominal Loading		Design Loading (125% of Nominal)		
	Load (lbs)	Deflection (mils)	Load (lbs)	Deflection (mils)	Stress (psi)
Initial strap load - Installation of magnet in cryostat – average strap load	1840	8.6	2300	10.8	7660
Strap preload	1070	5.0	1340	6.3	4460
Strap cooldown loading	2270	10.6	2270	10.6	7570
Total strap operational loading	5180	24.2	5910	27.7	19700
Strap transport Loading (2g)	3680		3680		12300
Total strap operational loading+ transport loading (cryostat cold)	8860		9590		31970
Strap initial load + preload + transport loading (cryostat warm)	6590		7320		24400

The initial strap loading is based on a cold mass weight of 3329 lbs.

Strap conditioning preload is 10,000 lbs. (~125% of 7320lbs).

The weak link of the support strap is the rod end. A rod end was tested and failed at 18,000 lbs. For operational loading, this gives a factor of safety of 3; for transporting the Superbend magnet warm, the factor of safety is 2.5.

4.5.8 Cryocooler

The refrigeration for the Superbend magnet system will be provided by a 2-stage Gifford-McMahon cryocooler manufactured by Sumitomo Heavy Industries. The unit, model SDR-415, has a specified first stage refrigeration capacity of 45 W at 50K and a specified second stage capacity of 1.5 W at 4.2 K.
The expected Superbend heat loads are summarized in the Table 8 and compared with the specified refrigeration capacity of the Sumitomo cryocooler.

The Sumitomo SRD-415 provides a 240% contingency for 4 K refrigeration, which promotes a high level of confidence in our ability to maintain the Superbend coils in the superconducting state. The 50 K refrigeration, however, has a much lower level of contingency. A general rule of thumb is to have a 25% contingency on refrigeration capacity to handle heat loads that are higher than expected because of fabrication tolerances and errors.

Table 8

Source	Heat Load To 50 K (W)	Heat Load To 4 K (W)
Current leads	27.0	0.25
Thermal radiation	6.7	0.03
Magnet support straps	1.1	0.06
Tubes to LN reservoir	1.9	0.00
Tubes to LHe reservoir	0.9	0.06
SS cooldown Tubes	0.8	0.04
Instrumentation wires	0.1	0.001
Total	38.5	0.44
Cryocooler capacity	45	1.5
Contingency (%)	17	240

Two factors are important in assessing whether the Sumitomo SRD-415 cryocooler has sufficient first stage capacity for use in the ALS Superbends. The first is that the predominant 50 K heat load is due to the current leads. As mentioned earlier, the leads are conduction cooled so the heat load is known to a rather high degree of accuracy since it is dependent on well-characterized properties such as thermal conductivity and electrical resistivity of copper. Thus for the Superbends we probably can tolerate a level of contingency less than the conventional 25%. The second item is that the refrigeration of the first stage may be conservatively specified. In preliminary tests of the cryocooler [a], and company pre-shipment acceptance tests [b], we found that a heat load of 45W to stage 1 could be accommodated with the stage heated to approximately 42 K. In our tests a heat load of 60 W could be accommodated by Stage 1. We therefore judge the Sumitomo SRD-415 to be well suited to the Superbend magnet system.

The Sumitomo SRD-415 is UL-approved according to their Standard for Commercial Refrigerators and Freezers [c]. The system consists of a compressor package, the cold head, and flexible metal tubing connecting them.

The compressor is a scroll-type unit in which oil is injected into the working fluid (helium gas) for lubrication and cooling. The oil is removed in two stages, a knockout stage to remove oil droplets and a charcoal adsorber to remove the oil mist before it is supplied to the remote cold head which is located on the magnet cryostat. The compressor motor requires 9 kVA of 200 V, 3 phase power. The maximum recommended flow rate of cooling water is 2.6 gpm with an inlet pressure between 30 and 100 psi. The compressor and ancillary equipment are contained in a rectangular cabinet with dimensions 18" wide, 20" deep, and 27" high. The weight of the compressor package is 265 lbs. The manufacturer recommends that LBL replace the charcoal adsorber after 20,000 hrs of operation to prevent contamination of the regenerators.

The cold head is shown in Figure 7. The cold head refrigerator section, from the O-ring flange down, must be treated as a cryogenic component in order to utilize the maximum cooling capability of the cryocooler. The connection areas are OFHC copper for high thermal conductivity and the material in between them is austenitic stainless steel to minimize parasitic heat loads. In operation, the helium supply gas pressure ranges from 285 to 340 psig and the return gas pressure ranges from 70 to 85 psig.

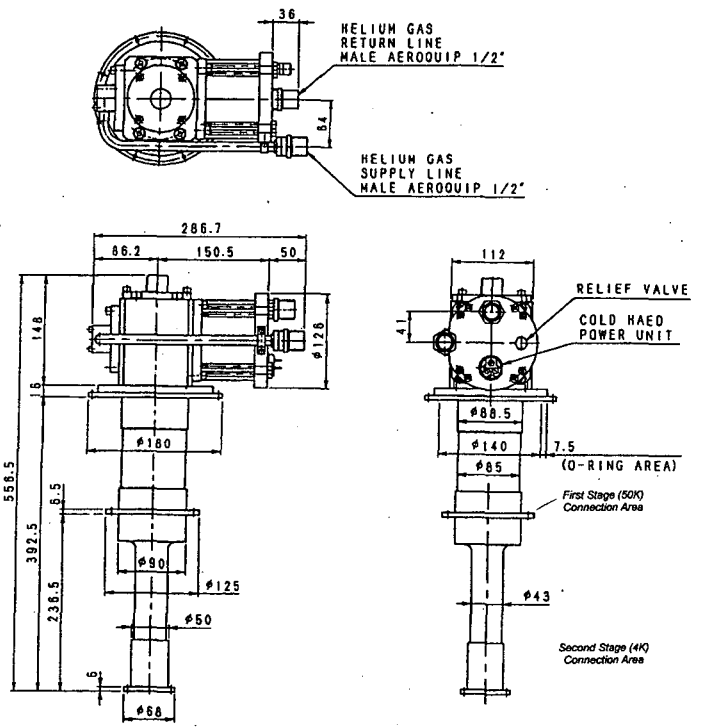

Figure 7. Cold head refrigeration section

Refrigeration is produced in the coldhead by isentropic expansion of the pressurized helium. The return pressure is considerably higher than the critical pressure, so no liquid is produced in the cold head. A motor at the room temperature end of the cold head drives a 2-stage regenerator up and down in synchronization with inlet and outlet gas valves. The combination of gas valves and moving regenerator allows the gas to be cooled by isentropic expansion, exchange heat with the regenerators, and generate the required refrigeration. The motor drives the regenerator at a frequency of 1.2 Hz. The cold head can be operated in any orientation, but a loss of 15% capacity can be expected at the worst orientation. The manufacturer recommends that the cold head be reconditioned at the factory every 10,000 hrs to replace the seals in the moving parts.

The flexible metal lines which connect the compressor to the cold head also function as surge volumes to dampen the pressure pulses caused by the opera-

tion of the inlet and outlet valves on the cold head. In order to avoid damage, the flexible metal lines must not be bent to a radius less than 12 inches.

Care must be taken to ensure that the cryocooler be connected to the Superbend system with a sufficiently high thermal conductivity in order to minimize the temperature drop to the Superbend magnet.

The temperature increase across the connection from the cryocooler first stage to the Liquid Nitrogen reservoir must be no greater than 6 K. This allows the thermal shield to be maintained at a temperature of 50K or less which results in a desirable upper end temperature for the HTS leads and ensures that the heat load to the 4 K cold mass is within the capability of the cryocooler. In addition to a sufficient copper cross section in the connection (his requires that that a sufficient compressive load be placed across the interface and the surface contact area be enhanced by incorporating a thin Indium foil, 0.005 inch thick, or a layer of Apieson N or Cry-Con grease. The mechanical load should place an interfacial stress on the order of 7 N/mm^2 (1000 psi) or higher.[e]

4.5.9 Quench Protection System

The Superbend quench protection system consists of passive and active devices which protect the superconducting coils and the High Temperature Superconducting (HTS) leads from potentially damaging excessive temperatures. Figure 8 shows the magnet system electrical schematic which includes current leads, superconducting coils, cold protection diodes, and voltage taps. The electrical signals from the voltage taps are connected to the Quench Protection Monitoring System which is not shown.

In case of magnet quench, a normal zone is created due to heat input from sources including: conductor motion, epoxy cracking, cryocooler malfunction, or beam-related incident. The normal zone grows in volume and develops an increasing internal electrical resistance. The resultant increasing voltage eventually causes the cold diodes to conduct. This provides a resistive path for the current and limits the voltage seen by the power supply to less than 30 V. In this approach, the stored magnetic energy is shared between the coil and the diode, but most of the energy is absorbed by the coil windings.

The upper and lower coil voltages (pins 3-4 and 5-6) are monitored by the Quench Detection Monitor and the difference between them is determined. If the trip level (current value 100 mV) is exceeded, the ac input to the magnet power supply is turned off and contactor C1 is closed and contactor C2 is opened. This ensures that current is turned off to the quenched system as fast as possible to prevent unnecessarily increasing the heat input to the system.

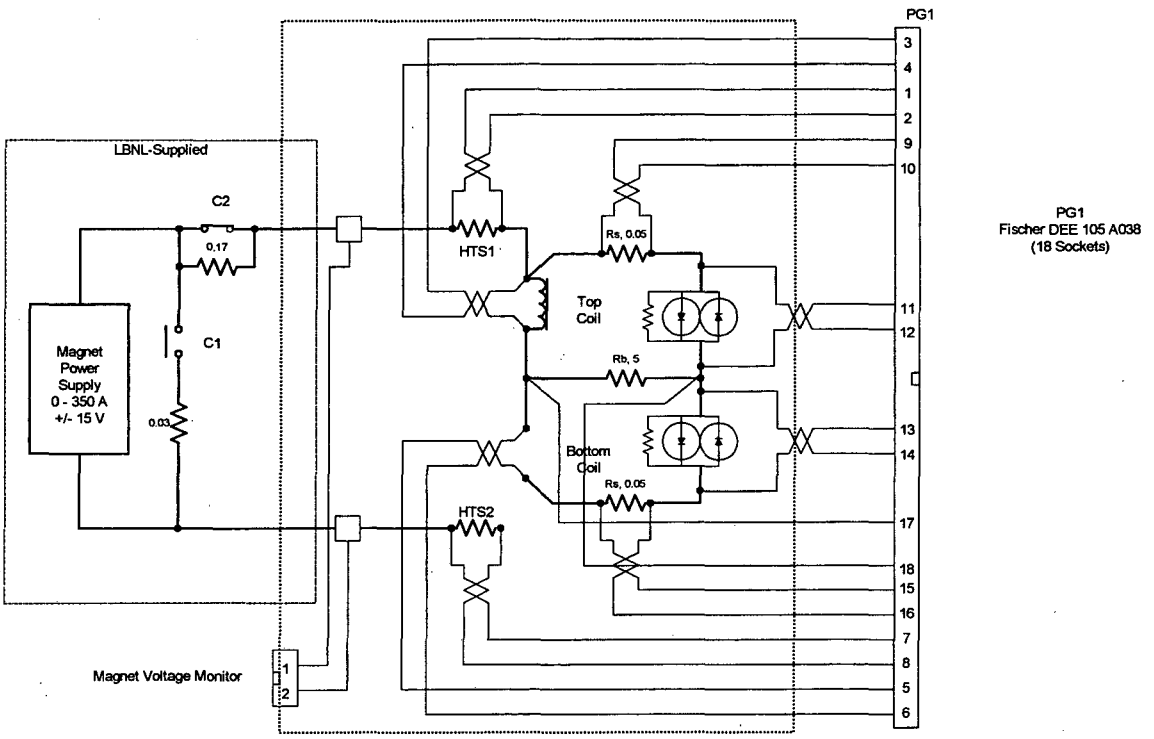

Figure 8. Magnet system electrical schematic.

The voltage drop across the HTS leads is available to the monitoring system at pins 1-2 and 7-8. If either HTS lead voltage drop exceeds the trip level (current trip value is 10 mV) the ac input to the power supply is removed, contactor C1 closes, and contactor C2 opens. This places approximately 60 volts across the cold diodes which causes them to conduct. The magnet current will very rapidly transfer from the external path though the HTS leads to the internal path through the conducting diodes. This protects the HTS leads from damage. If this action causes the superbend magnet to quench, the energy dissipation is the same as for the case of a quenching magnet; some energy absorbed by the diodes, but most of the energy absorbed by the windings. If the action does not result in a quench, then the magnet will be discharged by the diodes and the stored magnetic energy will be absorbed entirely by the diode assembly.

4.5.10 Instrumentation

A set of diagnostics are provided for interlocks and protection. In addition to the coil and HTS lead voltage taps mentioned in the section on the Quench Protection System, voltage taps are provided across the upper and lower coil diode stacks, the upper and lower 0.05 Ω sense resistors, and across the 5 Ω balance resistor. These voltage taps allow one to ensure that the diode system is functioning properly, and to pinpoint the problem if they are not working properly.

Cernox-type temperature sensors are used to verify that the system is at the proper temperature. Temperature sensors are installed at 8 locations on each magnet system:

T1 - cryocooler first stage,
T2 - cryocooler second stage
T3 - warm end of upper coil (positive) HTS lead
T4 - warm end of lower coil (negative) HTS lead
T5 - upper coil
T6 - lower coil
T7 – yoke cooling inlet
T8 – yoke cooling outlet

4.5.11 Vacuum Vessel

The cold mass is to be contained within a 304L stainless steel vacuum vessel as shown in Figure 9. The nominal wall thickness of the chamber is 1.0 inch and the mouth plates thicknesses are 0.25 – 0,50 inch thick [6]. The chamber is to be designed and fabricated in accordance with the ASME Pressure Vessel Code.

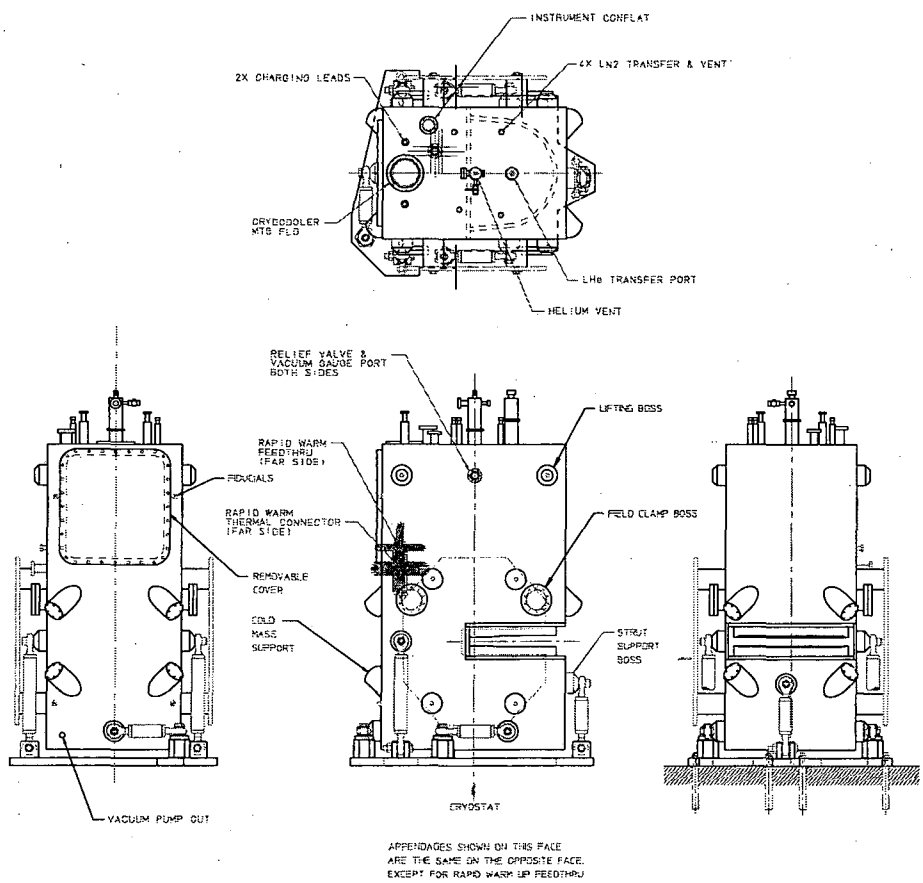

Figure 9. Superbend magnet vacuum vessel.

The following appendages and penetrations are to be provided in the vacuum vessel:

Description	No. Required	Size
1. Crane lifting points	4	4.0 inch boss with 3/4 – 10 UNC female thread
2. Strut support points	6	4.0 inch boss with 1 – 8 UNC female thread
3. Fiducial posts	4	20Q5363D
4. Alignment ports	4	4.0 inch tube 6.0 inch ConFlat
5. Access port	1	TBD
6. Cryocooler port	1	TBD
7. LHe transfer port	1	TBD
8. LHe vent & instrumentation port	1	TBD
9. LN2 transfer port	1	TBD
10. LN2 vent & instrumentation port	1	TBD
11. Instrumentation ports	2	TBD
12. Field clamp supports	8	4.0 inch round with 3/4 – 10 UNC female thread
13. Hall probe slots	2	machined slot
14. Support strap penetrations	8	4.0 inch O.D. x 2.5 inch I.D. tube with a double o-ring cover

The space allocation between the magnet pole tips and the vacuum vessel is critical. The space budget for the insulation and 50 K shield are shown in the details of the mouthpiece region in Figure 10 [7].

With an ALS Storage Ring vacuum chamber maximum thickness at the mouthpiece location of 2.030 inch (2.020 +0.010/-0.030 inch), and the Superbend Magnet vacuum vessel mouthpiece minimum outer opening of 2.160 inch, the space available for installation on either side of the ALS Storage Ring vacuum chamber is 0.065 inch (1.7 mm). This space is also available for adjustment of the Superbend Magnet after installation is complete.

An estimate has been made on possible magnet motion when going from atmospheric pressure and room temperature to vacuum and 4 degree Kelvin:(based on WANG estimate of motion) which is as follows:

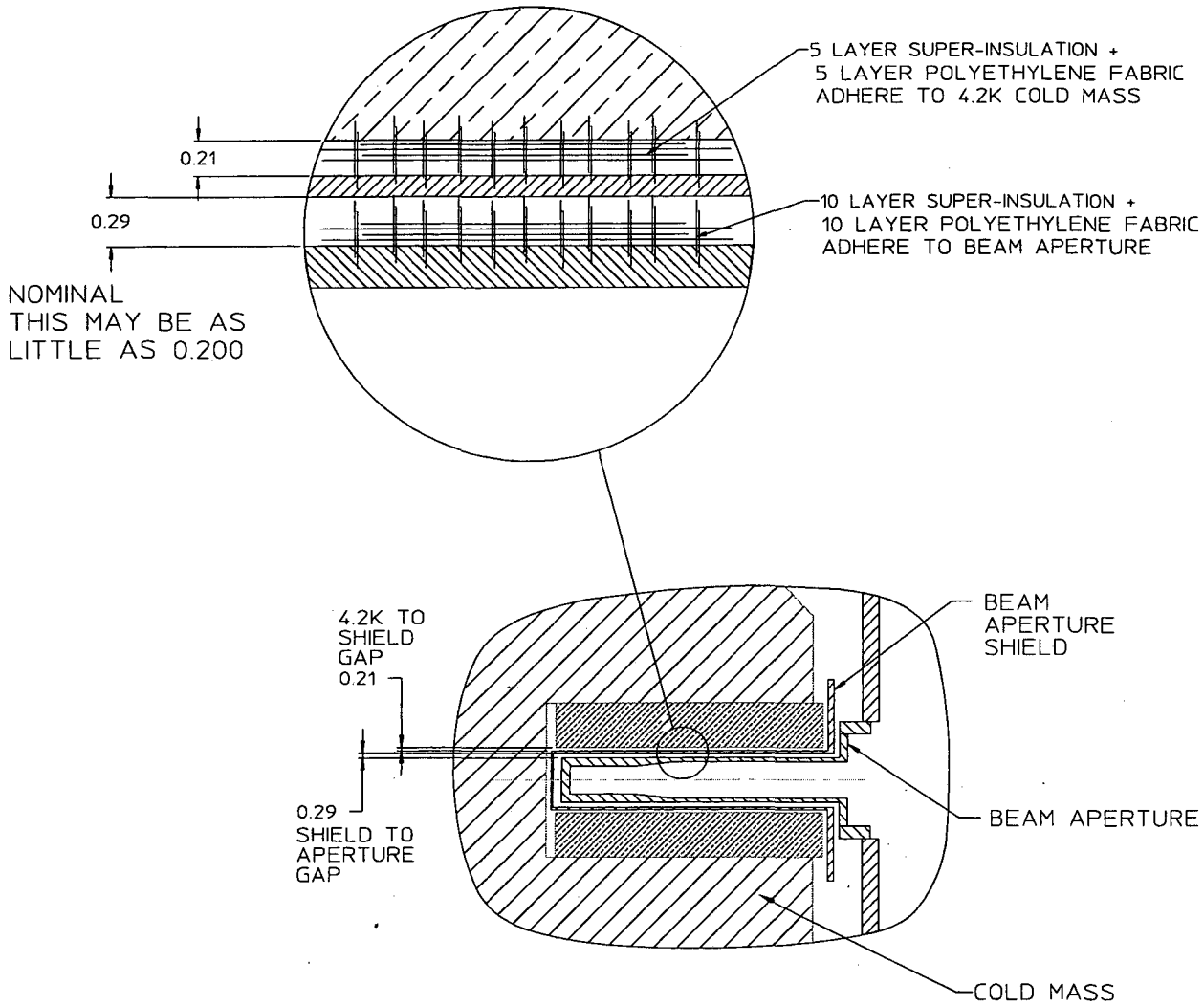

Figure 10. Vacuum vessel mouthpiece details.

Longitudinal	+/- 0.25 mm
Radial	+/- 0.25 mm
Vertical	+/- 0.25 mm
Pitch	+/- 1.25 mrad (based on a 400 mm fiducial spacing)
Roll	+/- 0.83 mrad (based on a 600 mm fiducial spacing)
Yaw	+/-1.25 mrad (based on a 400 mm fiducial spacing)

The possible motion is much less than the space available for adjustment.

The vacuum vessel must be fabricated such that the ALS Superbend Vacuum Chamber Alignment Fixture can be inserted into the mouthpiece and aligned so that the fixture is positioned symmetrically about the Superbend Magnet vacuum chamber gap.

During assembly of the Superbend Magnet, the internal cold mass must then be positioned (aligned) such that the center of the iron cold mass is coincident with the defined center of the ALS Superbend Vacuum Chamber Alignment Fixture. This is to be accomplished with optical tooling viewing the fiducials on the magnet yoke and the ALS Superbend Vacuum Chamber Alignment Fixture. Estimated accuracy of this alignment is tabulated below:

Magnet core fiducial – vacuum chamber alignment fixture (measuring) error (at atmospheric pressure and 300 degree K):

Longitudinal	+/- 0.100 mm
Radial	+/- 0.100 mm
Vertical	+/- 0.100 mm
Pitch	+/- 0.33 mrad (based on a 600 mm fiducial spacing)
Roll	+/- 0.25 mrad (based on a 800 mm fiducial spacing)
Yaw	+/- 0.25 mrad (based on a 800 mm fiducial spacing)

After the Superbend Magnet internal cold mass is aligned with the ALS Superbend Vacuum Chamber Alignment Fixture, then the magnet core fiducial positions must be transferred to the external fiducials on the Superbend Magnet vacuum vessel. Estimated accuracy of transferring the fiducial information is tabulated here:

Magnet core fiducial –Superbend vacuum vessel alignment (measuring) error (at atmospheric pressure and 300 degree K):

Longitudinal	+/- 0.100 mm
Radial	+/- 0.100 mm
Vertical	+/- 0.100 mm
Pitch	+/- 0.33 mrad (based on a 600 mm fiducial spacing)
Roll	+/- 0.25 mrad (based on a 800 mm fiducial spacing)
Yaw	+/- 0.25 mrad (based on a 800 mm fiducial spacing)

Vacuum vessel deflections were estimated with the vessel under vacuum [8]. The side plates, 1.0-inch thick by 1.47 m by 0.90 m, deflect 1.2 mm which corresponds to a natural frequency of 18.4 Hz. The top plate, 0.75 inch thick by 0.90 m by 0.65 m, deflects 0.25 mm. The mouth piece plates, analyzed as uniform

0.25 inch thick plates, with maximum lateral dimensions of 0.42 m by 0.57 m, deflects 1.3 mm. However, the design is now a variable thickness plate, 0.50 inch thick at the inner radius and tapering down to 0.25 inch at the outer portion of the chamber, so the actual deflection should be less.

A modal analysis was carried out with the Superbend Magnet assembled, i.e. the cold mass was supported via the 8 straps from the vacuum vessel which in turn was supported by the external strut system from the storage ring girder [9]. Using the following reference system; pitch defined as rotation about a radial axis, roll defined as rotation about a longitudinal (beam direction) axis and yaw defined as rotation about a vertical axis, the lowest resonant frequencies are given below:

Superbend Magnet Resonant Frequencies

Mode	Freq. (Hz)	Action
1	13	pitch of cryostat
2	14	roll of cryostat
3	15	yaw of core with respect to vacuum vessel
4	17	roll of core with antiroll of vacuum vessel
5	21	pitch of core with respect to vacuum vessel
6	28	vertical motion of cryostat
7	35	pitch of core with anti pitch of vacuum vessel
8	40	roll of core with antiroll of vacuum vessel
9	58	yaw of cryostat
10	74	vertical core motion with opposing vertical vacuum vessel motion

A vibrational analysis was carried out using the above modal analysis and driven by the following power spectral density (PSD) that represents the ALS Storage Ring Girder.

ALS Storage Ring Girder Power Spectral Density

Frequency Peaks	Horizontal PSD (m^2/Hz)	Vertical PSD (m^2/Hz)
6.4	8 x E - 14	1 x E – 15
9.7	1 x E – 14	3 x E – 15
12.7	3 x E – 14	5 x E – 14
15.3	1 x E – 17	1 x E – 17

Results are as follows at the 4.2 deg K core – strap connection points (8):

PSD Excitation	Radial (micron)	Vertical (micron)	Longitudinal (micron)	Roll (microrad)
Vertical	0.06	0.09	0.005	0.33
Horizontal	0.25	0.11	0.01	0.66

The roll motion, for the horizontal PSD, is 1/3 the Superbend Magnet roll tolerance.

Further analysis was carried out to simulate the cryocooler mounted on the cryostat. The top of the cryostat was driven with a 30 N (7 lb) load oscillating at 1 Hz to model the displacer motion of the cryocooler. The analysis shows that the vertical magnet motion is 2.6 microns and the vacuum vessel lid motion is 1.5 micron which corresponds to driving frequencies of 309 Hz and 403 Hz respectively.

4.5.12 External Support

The Superbend Magnet is to be supported with 6 struts from the ALS Sector Girder as shown in Figure 9. Alignment of the Superbend magnet will be similar to the alignment of other magnetic elements on an ALS girder. Estimated alignment accuracy of the Superbend Magnet Vacuum Vessel to the ALS Net is as follows:

Cryostat fiducial – ALS storage ring net errors: (achievable alignment of cryostat with 6 strut system from the cryostat fiducials to the ALS storage ring net)

Longitudinal	+/- 0.05 mm
Radial	+/- 0.05 mm
Vertical	+/- 0.05 mm
Pitch	+/- 0.17 mrad (based on a 600 mm fiducial spacing)
Roll	+/- 0.13 mrad (based on a 800 mm fiducial spacing)
Yaw	+/- 0.13 mrad (based on a 800 mm fiducial spacing)

Since the roll tolerance is 0.17 mrad and the 6 strut system can only achieve +/- 0.13 mrad accuracy, a precision level for roll measurements, with resolution of +/- 0.020 mrad, will be used in its place.

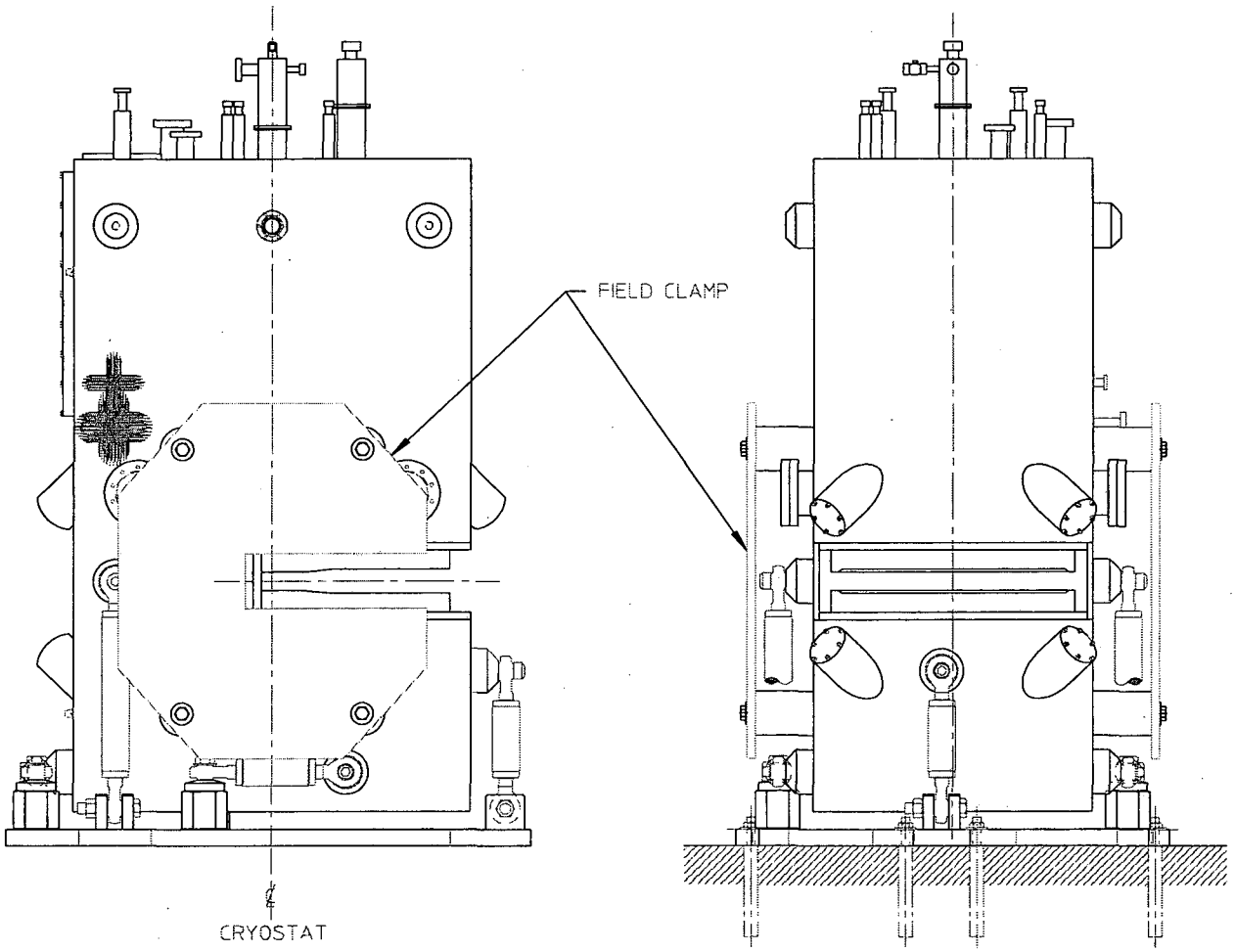

Figure 11. Superbend magnet field clamp configuration.

4.5.13 Field Clamps

Field clamps are required to terminate the field. They are positioned 260 mm from the magnet yoke. Each field clamp is 0.75 inch thick and weighs 145 lbs [10]. The clamps are bolted to the vacuum vessel as is shown in Figure 11.

4.6. References

[1] Hoyer, E., Pole and Coil Dimensional Information, LBNL Engineering Note M7786, August, 1999.

[2] Hoyer, E., Pole Tip and Coil Positional Tolerances, LBNL Engineering Note M7787, August, 1999.

[3] Hoyer, E., Yoke Forces and Deflections, LBNL Engineering Note M7781, April,1999.

[4] Zbasnik, J., Superconductor Specification, LBNL Specification M908, August, 1999.

[5] Hoyer, E., Magnet Straps – Loads and Deflections, LBNL Engineering Note M7783, April,1999.

[6] Hoyer, E., Vacuum Chamber – Preliminary Wall Thicknesses, LBNL Engineering Note M7784, August,1999.

[7] Hoyer, E., Magnet Core – Cryostat Dimensional Budget at R. T., LBNL Engineering Note M7785, August, 1999.

[8] Corradi, C., Cryostat – Vessel Deflection Analysis, LBNL Engineering Note M7854, January, 2000

[9] Corradi, C., Cryostat Modal Analysis, LBNL Engineering Note M7855, January, 2000

[10] Hoyer, E., Field Clamp Sizing & Magnet Fringe Fields, LBNL Engineering Note M7782, July, 1999.

DIPOLE MAGNETIC MEASUREMENTS AND FIDUCIALIZATION

A variety of magnetic measurements will be conducted to assure that the super-bend dipole magnetic field meets the required tolerances for installation into the ring, and to provide fiducials for proper alignment. The program of measurements will include conventional integrated multipole measurements, time dependent measurements of the field fundamental and multipoles during current ramps, and on-axis field mapping.

Section 1.1 below lists the requirements. Section 1.2 discusses the measurements designed to assure the requirements. Section 1.3 discusses the procedures for locating magnet fiducials relative to the magnetic center.

5.1 Field and position tolerances

5.1.1 Integrated multipoles

The following convention is used to represent multipole field components.

$$\overline{B^*} = i\sum\left(\bar{a}_n + i\bar{b}_n\right)\left(\frac{z}{r_0}\right)^{n-1}$$

The $\bar{}$ symbol is used to indicate integrated quantities. The following table lists multipole requirements.

Table 1. Maximum normalized multipole requirements at r = 1 cm

n	$\bar{a}_n/\bar{a}_1$	$\Delta\bar{a}_n/\bar{a}_1$	$\bar{b}_n/\bar{a}_1$
1	1	1×10^{-3}	1.7×10^{-4}
2	---	5×10^{-4}	6×10^{-4}
3	6×10^{-3}	3×10^{-4}	1×10^{-4}
$n > 3$	1×10^{-4}	---	1×10^{-4}

The Δ symbol indicates a requirement on magnet-to-magnet reproducibility. The requirement on b_1 corresponds to a magnet roll requirement; Δa_1 corresponds to a requirement on the transfer function reproducibility. The Δa_2 requirement is based upon the β-beat tolerance. The a_3 and Δa_3 requirements are based upon simulations.

5.1.2 Magnet position

The following table lists the dipole position tolerances along with the driver, or reason for, the requirement. Due to the presence of a large sextupole component and the resulting feed-down into the quadrupole due to a position error, the requirements for the quadrupole components listed in Table 1 have their counter part in Δx and Δy position tolerances. The sextupole feed-down is explained in detail in Section 1.2.1.3.

Table 2. Alignment requirements

Position	Tolerance	Driver
Longitudinal	$\|\Delta z\| < 1$ mm	Horizontal orbit distortion
Horizontal	$\|\Delta x\| < 0.5$ mm	β_x beat
Vertical	$\|\Delta y\| < 0.4$ mm	β_y beat
Roll	$\|\Delta\varphi_y\| < 170$ μrad	Vertical orbit distortion

5.1.3 Transfer function

The transfer function, T, is the measure of integrated field as a function of input current.

$$T = \frac{1}{I}\int B_y dz$$

The requirement on the resolution and repeatability of T, based upon the tolerable horizontal orbit distortion for storing beam, is

$$\frac{\Delta T}{T} < 1 \times 10^{-3}$$

5.2 Magnetic measurements

A variety of magnetic measurements will be performed in order to assess each super bend dipole relative to the magnet tolerances stated in Section 1.1 above. Table 3 below summarizes the type of measurements that will be done to address each category of requirement. This will be followed by a description of the measurement system, and then by a detailed analysis of each type of measurement with an evaluation in terms of the expected resolution and error and the resulting level of measurement uncertainty relative to the corresponding magnet tolerance.

Table 3. Measurement type

Requirement	Measurement
Integrated Multipoles	Rotating Integral Coil
Transfer Function	Rotating Integral Coil
Hysteresis Loop	Rotating Integral Coil
Horizontal, Vertical Magnetic Center	Rotating Integral Coil
Longitudinal Magnetic Center	Hall Probe Scan
Roll	Rotating Integral Coil
Field Shape	Hall Probe Scan
Calibrate Embedded Hall Probes	Rotating Integral Coil

A rotating search coil will be used to measure the integrated fundamental and integrated multipole values. The integrated quadrupole measurement will be used to determine the transverse and vertical magnetic center position for fiducialization. The integrated fundamental measurements will also be used to calibrate and test repeatability of two Hall probes that will be embedded in the cryostat wall that will be used to provide a field measurement for control feedback and diagnostics that is independent of current. A Hall probe system will be used to acquire a field scan along the magnetic axis. This will determine the peak field and field shape and be used to locate the effective longitudinal magnetic center for fiducialization.

5.2.1 Magnet measurement system

The magnetic measurement system instrumentation is schematically illustrated in Figure 1 below.

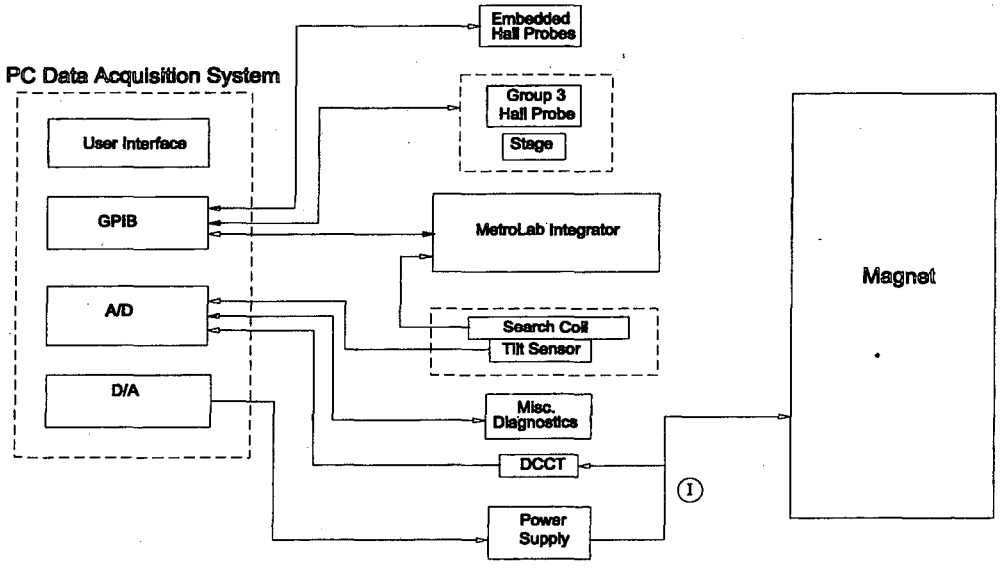

Figure 1. Magnetic measurement system instrumentation.

The full system includes rotating integral coil and Hall probe scanning subsystems. The user and instrumentation interface is through a PC-based data acquisition system. The rotating coil subsystem consists of multi-channel coil, described in Section 1.2.2 below, a Metrolab dual channel digital integrator to process the coil voltage signals and an Applied Geomechanics precision tilt sensor to provide an absolute angle reference for the coil. The Metrolab integrator interface to the computer is via GPIB. The tilt sensor signal is read through an A/D board installed in the computer.

The Hall probe subsystem consists of Group 3 Hall probe and Tesla-meter, and a simple track to position and locate the probe along the magnetic axis. The Hall probe system is interfaced to the computer through GPIB.

Auxiliary instrumentation includes analog power supply control, through a D/A channel, current transducer monitoring (DCCT) through an A/D channel, a Hall probe embedded in the cryostat wall, interfaced through GPIB, and a provision for monitoring of other miscellaneous voltage signals using A/D channels. Figure 2 shows the rotating coil installation setup. This setup provides a basis for relating the magnets fiducials to the magnetic center and for checking for vacuum chamber clearance at the properly aligned location. Fiducialization will be described in detail in Section 1.3.

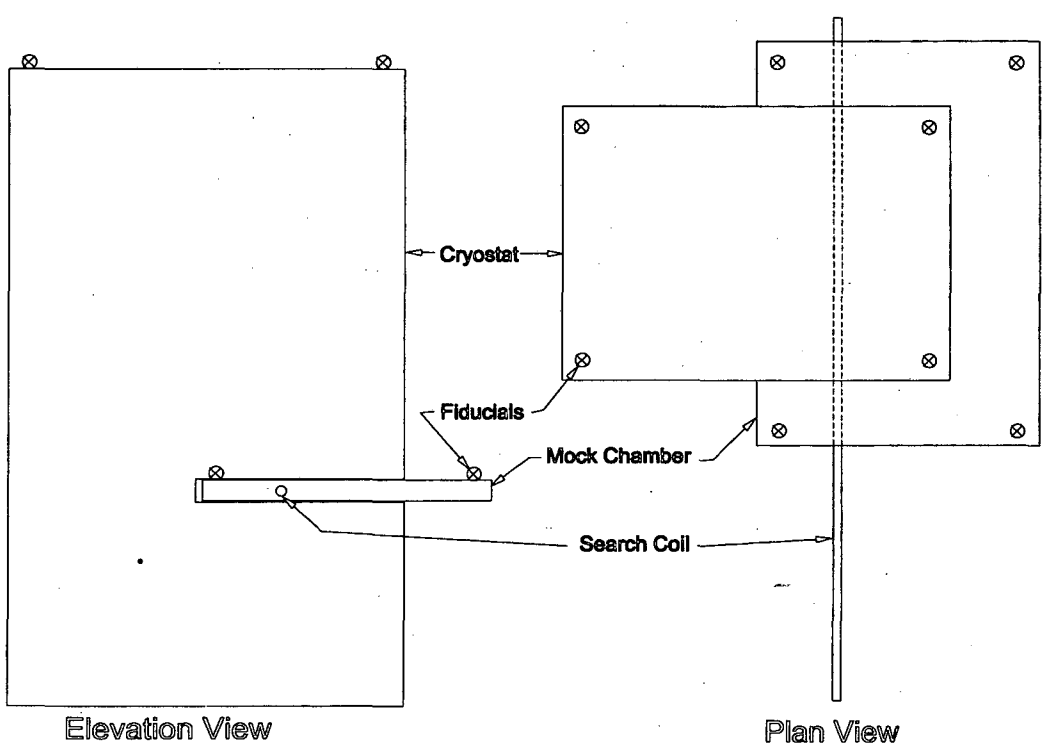

Figure 2. Rotating integral coil setup.

5.2.2 Search coil measurements

The search coil system consists of a 1 m long tangential search coil assembly with a nominal radius of 1 cm, and a PC-based data acquisition system utilizing the Metrolab digital integrator for acquiring and processing coil voltages. The coil assembly includes a set of coils that can be configured for bucked and unbucked dipole measurements. The unbucked configuration will be used to measure the integrated fundamental. The bucked configuration will be used to measure higher order integrated multipoles.

Figure 3 below illustrates the dipole search coil. The primary coil, used for fundamental measurements, connects TW1 and TW2. The two bucking coils connect DW1 and DW3, and DW2 and DW4, respectively. The coil geometry is summarized in the table.

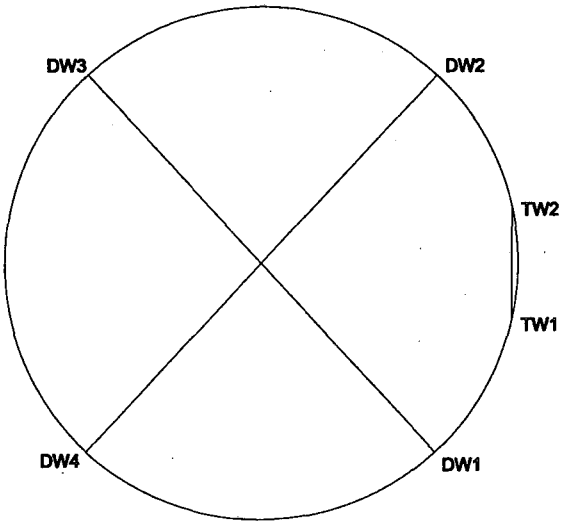

	Turns	Polarity	Angle (deg.)	Radius (cm)
TW1	40	+	12.88	1.166
TW2	40	-	-12.88	1.170
DW1	6	-	47.75	1.180
DW2	6	+	-47.87	1.179
DW3	6	+	-131.89	1.181
DW4	6	-	131.82	1.178

Figure 3. Rotating integral coil geometry.

The following equation is used to represent the relationship between flux, multipoles and coil geometry.

$$\Phi(\Theta) = \mathrm{Re}\left\{\sigma_n \overline{c_n}\left(\frac{r_1}{r_0}\right)^n e^{in\theta}\right\}$$

Where $\Phi(\theta)$ is the flux intercepted by the coil array at the angle θ relative to its θ = 0 reference. The terms σ_n are sensitivity coefficients that represent the coil geometry. The terms $\overline{C_n}$ are multipole coefficients for the integrated complex potential, and are related to the field multipoles by the following equation

$$i\overline{c_n} = i\left(\overline{a_n} + i\overline{b_n}\right) = \frac{\overline{nc_n}}{r_0}$$

The two radii in the equation, r_1 and r_0 are the coil reference radius and multipole normalization radius, respectively.

Sensitivity coefficients for a coil assembly are calculated from the following equation

$$\sigma_n = \sum_{ij} N\rho_j^n\left[\left(\cos n\theta_{j+} - \beta_j^n \cos n\theta_{j-}\right) + i\left(\sin n\theta_{j+} - \beta_j^n \sin n\theta_{j-}\right)\right],$$

where summation subscript j represents the terms for each coil in the assembly. The terms in the equation are defined below.

$N_j \equiv$ number of turns.
$\rho_j \equiv$ ratio of positive terminal radius to r_1.
$\beta_j \equiv$ ratio of negative terminal radius to positive terminal radius.
θ_{j+}, $\theta_{j-} \equiv$ angular position of positive and negative terminals, respectively.

5.2.2.1 Fundamental and transfer function measurement

The full-field integrated dipole, required for 1.9 GeV operation, is 1.1 T-m. This value corresponds to the value $\overline{c}_0/r_0$, therefore $\overline{c}_0 = 0.011\,\text{T-m}^2$ at r_0 = 1 cm. The unbucked dipole sensitivity $\sigma_1 = i17.86$. So the corresponding signal level is

$|\Phi_1| = |\sigma_1||\overline{c}_0| = 0.2$ V-s (T-m^2).

The Metrolab's specified resolution and noise level are 0.1 μV-s and 0.3 μV-s, respectively for the appropriate gain settings. To assure transfer function repeatability to 1×10^{-3}, we want to resolve signals to 1×10^{-4}. Based upon this, we can measure a signal 100 times smaller before being limited by the integrators resolution and noise level. We must also measure current to determine the transfer function. This will be done using a Danfysik DCCT which resolve current to 1×10^{-6}.

5.2.2.2 Multipole measurements

The required signal resolution is determined by examining the signals corresponding to the terms in Table 1. So $|\bar{c}_{n-1}|/|\bar{c}_0| = n|\bar{C}_n|/|\bar{C}_1|$ = (smaller of a_n or b_n in Table 1). The value for $\bar{C}_1$ corresponds to the 1.9 GeV integrated dipole value of 1.1 T-m^2. The values for σ_n in the table correspond to the bucked coil configuration. All quantities are calculated in the appropriate SI units.

Table 4

n	$\lvert\bar{C}_n\rvert$	$\lvert\sigma_n\rvert$	$\lvert\Phi_n\rvert = \lvert\sigma_n\rvert\lvert\bar{C}_n\rvert$
1	0.011	0.22	2.4×10^{-3}
2	3.3×10^{-6}	34.9	1.2×10^{-5}
3	2.2×10^{-5}	35.6	7.8×10^{-5}
4	2.8×10^{-7}	62.8	1.7×10^{-5}
5	2.2×10^{-7}	94.7	2.1×10^{-5}
6	1.8×10^{-7}	78.9	1.5×10^{-5}
7	1.6×10^{-7}	91.6	1.4×10^{-5}
8	1.4×10^{-7}	79.7	1.1×10^{-5}
9	1.2×10^{-7}	48.0	5.9×10^{-6}

The quantities in the right hand column correspond to signal levels (in V-s) and should be compared to the resolution and noise specification values of 0.1 μV-s and 0.3 μV-s. All measurements must be corrected for integrator drift. The drift must be stable at about the same level as the noise specification over the approximately 1 second coil revolution time. According to the Metrolab specifications, the expected drift rate, following offset adjustment, for a gain setting of 200, appropriate for these measurements, is 0.7 μV. The specified stability is 0.07 μV/°C. This drift rate and stability is more than sufficient for measurements spanning several seconds.

5.2.2.3 Time dependent measurements

When boosting the electron energy from 1.5 GeV to 1.9 GeV following injection, the currents for all magnets are ramped over a period of about one minute. We must measure the ramp rate dependent transfer function to assure that stored beam can be maintained during this ramp. We must also measure the ramp dependent multipoles, in particular the quadrupole and sextupole components, to assure that they remain within the tolerance.

Changes in the fundamental transfer function can be measured using the unbucked coil configuration while the coil is in a static position. Alternatively, the absolute transfer function can be measured using the conventional unbucked coil

rotation method. Bucked rotating coil measurements will be used to measure multipoles. Since the coil rotation time will not be sufficiently fast during the ramp, all data values within a single rotation must be normalized by current.

These measurments must be drift corrected. For the conventional rotating coil measurements, the drift compensation can be calculated for each revolution, since the last value repeats the first. No value is repeated during a ramp, so drift rate must be determined before the ramp is started and after the ramp is complete for comparison. Since these measurements span about a minute, the drift stability requirement is more challenging than that for the conventional measurements. If the drift stability is as good as specified for the Metrolab, this is sufficient. We can also use the pre-calibrated embedded Hall probes as a cross check on the drift correction.

5.2.2.4 Transverse and vertical magnetic center determination

The transverse and vertical magnetic center is defined as the center of the sextupole component. This is the location where the quadrupole component is zero. An apparent quadrupole term appears due to an offset of the magnetic center by an amount Δz in the presence of a sextupole. This can be seen from the following equation for the sextupole.

$$\overline{B_3^*} = \overline{c_3}\left(\frac{z+\Delta z}{r_0}\right)^2 = \overline{c_3}\left(\frac{z^2+2\Delta z z+\Delta z^2}{r_0^2}\right)$$

The apparent quadrupole component is

$$\overline{c}_2 = 2\frac{\Delta z}{r_0}\overline{c}_3 .$$

So the magnetic center offset, $\Delta z = \Delta x + i\Delta y$, is determined from

$$\Delta z = \frac{1}{2} r_0 \frac{\overline{c}_2}{\overline{c}_3} .$$

The tolerances on Δx and Δy are 0.5 mm and 0.4 mm, respectively. The ratio of $\overline{c}_1/\overline{c}_2$ must be resolved to 0.008 to insure a resolution of Δy to 0.04 mm. The integrator's noise and resolution specification are more than sufficient for this requirement.

The error in locating the magnetic center will be dominated by the mechanical alignment accuracy that is common to all magnets in the ring. The expected accuracy for transferring coil fiducials to magnet fiducials and for final a magnet alignment is about 0.05 mm.

5.2.2.5 Roll measurement

The magnet's roll about its axis will be determined from

$$\phi_z = \frac{B_x}{B_y}.$$

An absolute angular reference will be provided for the measurement by an Applied Geomechanics model 756 tilt sensor attached directly to the coil. The sensor has a 5 μrad resolution. The full strength signal for B_y is 0.011 V-s, so if B_x is resolved to 1×10^{-7} V-s, corresponding to the integrator's specified noise level, then the roll, will be resolved to 10 μrad. Both resolution limitations are small compared to the 170 μrad requirement.

Again, the actual roll accuracy of the magnet when placed in the ring will be limited by the mechanical alignment accuracy common to placement of all ring magnets.

5.2.3 Hall probe measurements

Point field measurements will be taken to provide the on-axis field profile. The primary purpose is to locate the axial magnetic center for fiducialization. This will also provide a measurement of the peak field and field values at the effective photon source locations. A Hall probe calibrated up to 6 T will be used for field measurements. A manual stage will be used for probe positioning.

5.2.3.1 Axial field profile and magnetic center

A tolerance of 1 mm has been placed on the longitudinal, or axial, positioning of the dipole. This is determined from the requirement on the maximum tolerable horizontal orbit distortion. Let us examine the orbit distortion mechanism in order to understand the measurement requirements.

The Figure 4 below illustrates the nominal electron trajectory through the magnet, shown as the solid line, and a perturbed trajectory, shown as the dashed line.

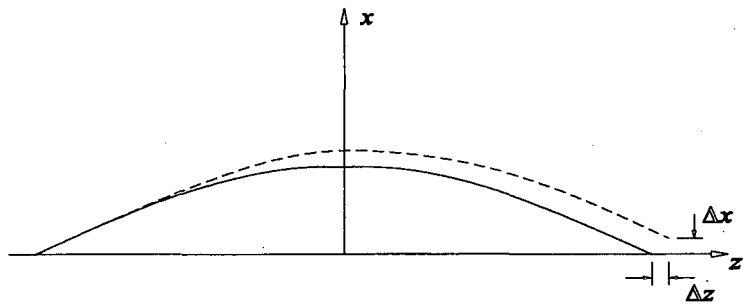

Figure 4. Electron trajectory distortion.

The electron beam enters the magnet at an angle of +5° relative to the magnet's axis. It is constrained to bend through 10°, and thus leave at -5°. However, if the magnetic field profile differs from the nominal profile, the trajectory exit will be offset from the nominal exit by Δx and Δz, where $\Delta x/\Delta z = \tan 5°$. The horizontal orbit distortion at this location is perpendicular to the trajectory and equal to $\Delta z \sin 5°$. Since a field distortion produces the same affect on beam orbit, as an axial shift of the nominal field, the Δz position tolerance must be evaluated in terms of the shift in trajectory exit position. The axial magnetic center should be defined such that this trajectory shift is zero.

We can represent the trajectory passing through the magnetic field in terms of the position $x(z)$ and angle $x'(z)$.

$$x'(z) = \frac{1}{B\rho}\int_{-\infty}^{z} B(\varsigma)d\varsigma$$

$$x(z) = \frac{1}{B\rho}\int_{-\infty}^{z}\int_{-\infty}^{\varsigma} B(\xi)d\xi d\varsigma$$

The axial field distribution, $B(z)$, will be measured as set of discrete data (z_l, B_l). Measurement errors, δz or δB, will result in an uncertainty in the trajectory, and thus Δz. We can evaluate δz or δB on the same basis using the following relationship

$$\delta B = \frac{dB}{dz}\delta z .$$

For a discrete set of N measurements at equal intervals over the length l, having an RMS error of ε_B, the expected trajectory uncertainties, δx_e and $\delta x_e'$, are given by

$$\delta x_e' = \frac{1}{B\rho}\varepsilon_B \frac{l}{\sqrt{N}}$$

$$\delta x_e = \frac{1}{B\rho}\frac{2}{3}\varepsilon_B \frac{l^2}{\sqrt{N}}$$

We need to evaluate δx_e relative to the specified tolerance on Δz. Using the criteria that the measurement uncertainty should be no more than 10% of the tolerance

$$\delta x_e < 0.1\Delta z \tan 5^\circ .$$

Use the following values to determine the requirements for δz and δB: N = 50, l = 500 mm, and $B\rho = 6.3\times10^7$ G-mm, corresponding to 1.9 GeV.

$$\delta B < 24\,\mathrm{G}$$

$$\delta z < 0.1\,\mathrm{mm}$$

The evaluation of δz is based upon an average dB/dz = 240 G/mm. Hall probe measurements better than 1 G are routine. Probe placement to 0.1 mm can easily be done with reasonable care.

5.3 Magnet fiducialization

Fiducials, consisting of tooling balls placed upon the superbend cryostat, will be used for placement and alignment of the magnetic center within the ring to the tolerances specified in Section 1.1. The measurement procedures described in Section 1.2 will be used to locate the magnetic center relative to the measurement system fixtures. Fiducials attached to the measurement fixture must be located relative to the magnet fiducials in order to locate the magnetic center for magnet placement and alignment.

The search coil fixture will consist of a mock vacuum chamber section that will center the search coil axis within the vacuum chamber beam aperture. As part of the measurement procedure, the coil will be moved so that its axis is coincident with the magnetic center. This will insure that the cryostat will fit around the vacuum chamber when it is located within the ring.

The fixture for Hall probe scanning system will place the scanning axis on the same vacuum chamber aperture center. It must also have a fixed z reference that can be located relative to the magnet fiducials.

VACUUM CHAMBER MODIFICATIONS

6.1 Storage Ring Vacuum Chamber Machining

The existing storage ring vacuum chamber has sloped machined surfaces that provide clearance for the existing Gradient magnet pole tips and coil. See figure 1 for an isometric view of a section of vacuum chamber at the central gradient magnet.

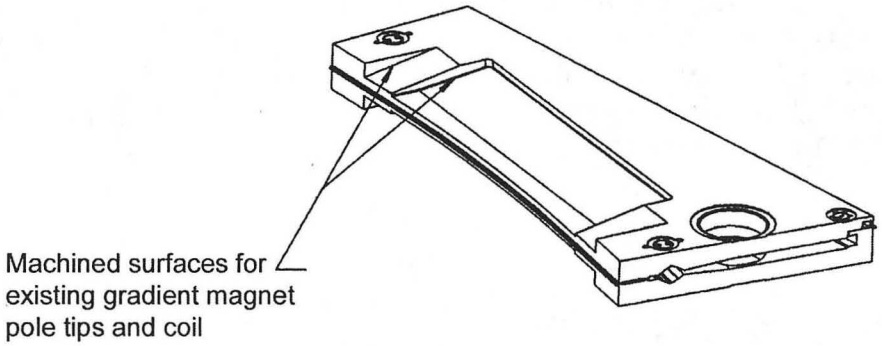

Figure 1. Existing Storage Ring Vacuum Chamber

The Superbend magnet will have parallel pole tips spaced at 100mm (3.937in.). The opening in the cryostat that will fit around the vacuum chamber will have parallel surfaces 54.8 mm (2.157in.) apart. To provide installation and alignment clearance for the Superbend, the storage ring vacuum chamber will be machined to a nominal height of 51.6mm (2.031in.). This will provide a nominal installation and alignment clearance of 1.6mm (.063in) top and bottom. It is planned that components will be toleranced so that the minimum space between the storage ring vacuum chamber and the cryostat will be 1.5mm (.060in). See figure 2.

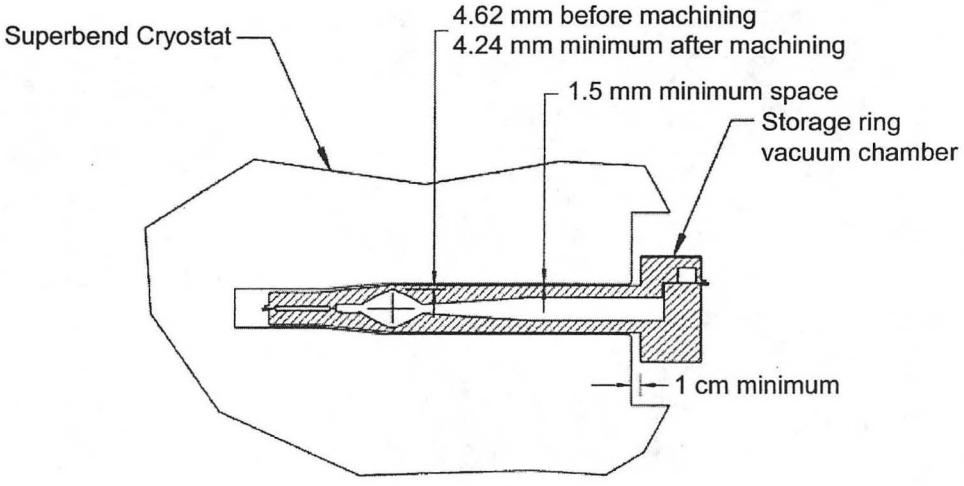

Figure 2. Cross-section Storage Ring Vacuum Chamber and Superbend

Figure 3 shows an isometric view of a section of the storage ring vacuum chamber after machining. The tooling necessary to machine the chamber in place has been developed. This tooling consists of a milling head mounted on a transverse slide which is in turn mounted to a rotary table. See figure 4. These components are mounted to a plate which has 4 legs that provide a means of mounting and aligning the tooling assembly onto the chamber. The tooling in figure 4, is shown in the orientation that it would be in to machine the bottom of the chamber. Thick aluminum plates are clamped onto both sides of the chamber and the above described tooling is mounted to these plates. Figure 5 shows the tooling mounted to the top of the vacuum chamber in sector 4 during the machining of this chamber in place. The vacuum chamber in sector 4 has been successfully machined. The dimensions after machining have been recorded on drawing 25D8294. The vacuum chambers in sectors 8 and 12 are planned to be machined in February 2000.

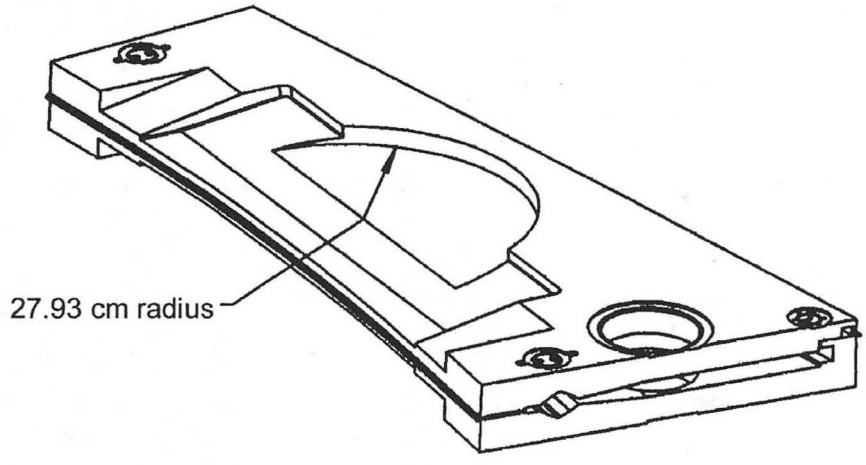

Figure 3. Storage Ring Vacuum Chamber – After Machining

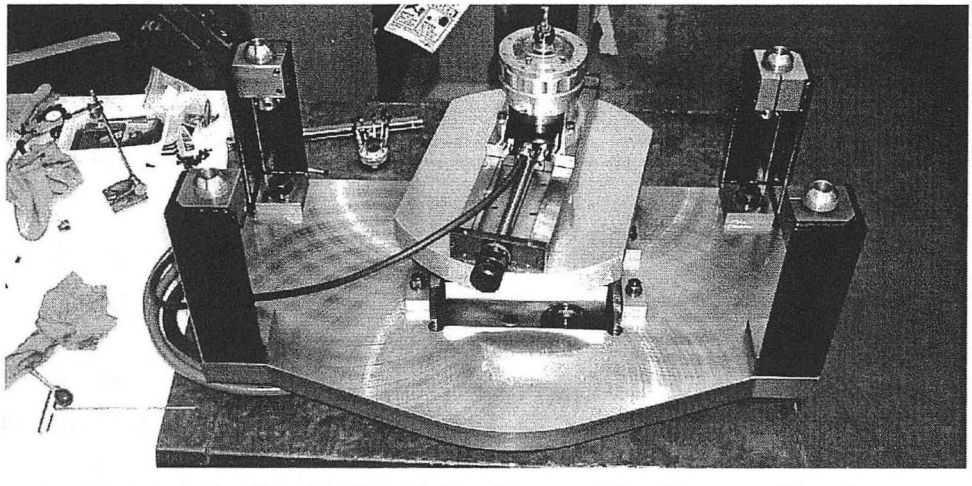

Figure 4. Tooling for Machining Storage Ring Vacuum Chamber

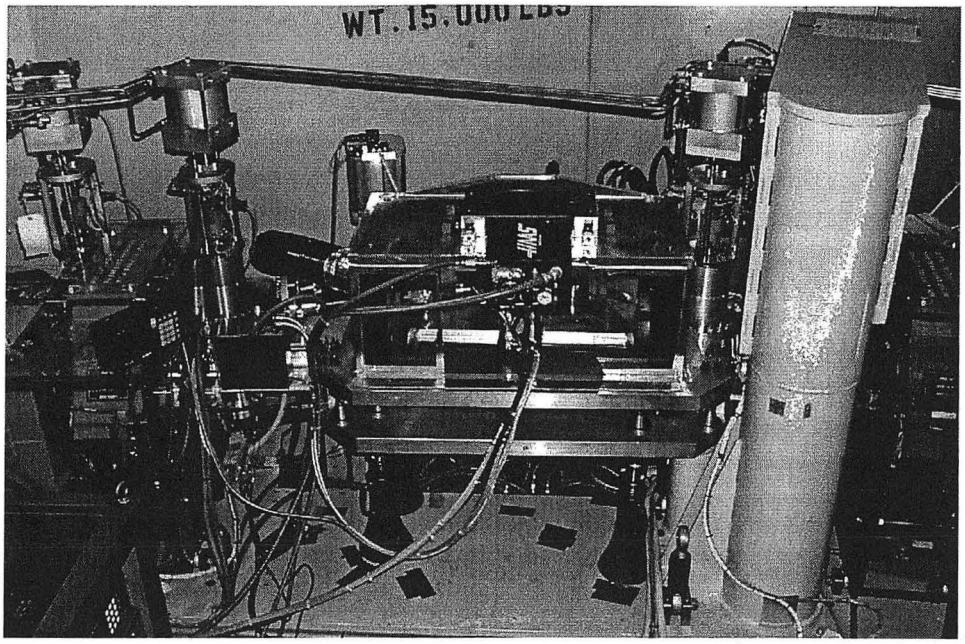

Figure 5. Machining Sector 4 Storage Ring Vacuum Chamber

6.2 Storage Ring Photon Stops

The Photon beam from existing Bend Magnets in the Storage Ring is intercepted by a combination of Photon Stops and water cooled blank off flanges when there are no Beam Lines connected to the Storage Ring .The Photon Stops are fabricated from Oxygen Free Copper, Photon Stops 4, 5, and 6 along with a water cooled flange at the X.3 port will intercept beam from the new Super Bend Magnet. See Figure 1. There is a Titanium Sublimination Pump (TSP) at each Photon stop location. See Figure 2.

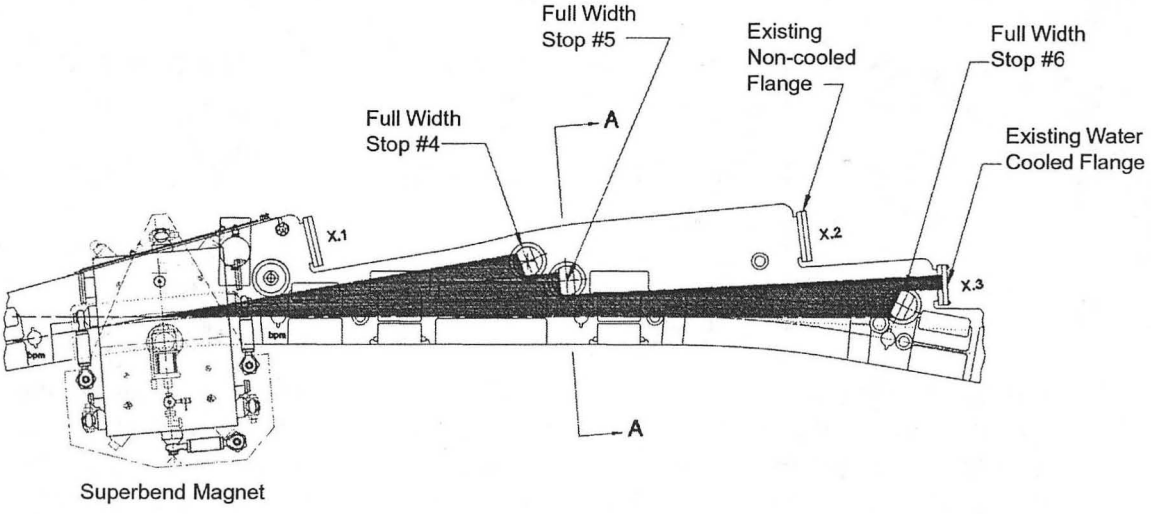

Figure 6. Superbend Full Width Photon Stops – Plan View

Due to the increased heat load from the Superbend beam, the following changes are planned:

Photon Stop 4	Replace with Glidcop, increase water flow to 1 gpm
Photon Stop 5	Replace with Glidcop, increase water flow to 1 gpm
Photon Stop 6	Use existing, increase water flow to 1 gpm
X.3 Blank off	Increase water flow to 1 gpm
TSP 4,5 & 6	Water cool, 1/2 gpm

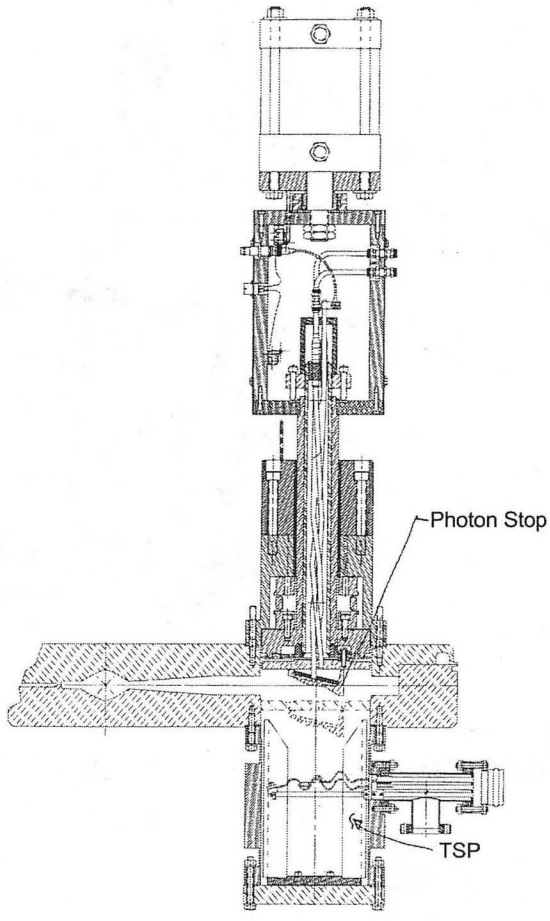

Figure 7. Photon Stop/TSP Section AA

The described changes to Photon Stops, Blank Flanges and TSP's have been shown to be necessary by calculations. See the following Engineering notes:

> "Superbend - Photon Stops/Blank Flanges - Thermal and Structural Analysis," Engineering Note M7823A.
>
> "Superbend - Photon Stops/Blank Flanges - Reflected Photon Stop Power on TSP," Engineering Note M7869.
>
> "Superbend - Photon Stops/Blank Flanges - TSP cooling tests," Engineering Note M7872.

So that the Photon Beam can exit the Storage Ring and enter a beam line, it is planned to provide Cut Photon Stops 4, 5 & 6. It is planned that Stops 4 and 5 will be fabricated from Glidcop and Stop 6 will be fabricated from Oxygen Free Copper. All three stops in each Super Bend Sector will have their water flow increased to 1gpm. It is planned that there will be Flow Switch interlocks on these water circuits.

CONTROLS

Controls in this project include:

- Superbend Power Supply Controls
- Superbend Magnet Monitoring
- Superbend Cryosystem &Quench Monitoring
- QFA Quadrupole Controls
- QDA Quadrupole Controls

The controls content of the superbend project includes controls for the new superbend magnet power supplies, diagnostic monitoring for the cryosystems and magnet, and controls for the new and repowered quadrupole magnet supplies.

7.1 Requirements categories

7.1.1 Standard requirements

- Safety, Equipment protection
- Reliability, maintainability
- Readout & control rates
- Ramping not controls-limited
- Compatibility with existing applications
- Utilize off the shelf, Standards

The standard requirements are the ones that the ALS was built with, so we must follow for compatibility. Safety and Equipment protection must, as always, not be subject to the potential failures of Controls hardware and software.

The reliability and maintainability of the controls must meet the high needs of the accelerator. With beam life of 4 hours it is important to avoid interruptions of the system by any source, and the controls must abide by this. In event of a failure the time to diagnose and repair should be relatively short and it should be possible for the staff on hand to accomplish the task with minimal coaching from the development staff (who may be home asleep at the time).

We need to meet the long established 10 hz readout and control rates.

It is important that the ramping rates not be controls limited.

Insofar as meaningful, the new systems should be compatible with the existing software applications.

Wherever practical commercial hardware and software is to be employed.

7.1.2 Evolutionary requirements

Using Compact PCI

- Developed for controls expansion, upgrade
- Already in use on Third Harmonic Cavity

Settable Ramping Rate Control

- Existing ramping rates are static

The evolutionary requirements represent a small change from the existing work we have done. Compact PCI hardware has been developed as an expansion and upgrade path for legacy controls. This equipment has been installed in the Third Harmonic Cavity system. Only small changes to this existing design are planned for this project.

The power supply controls existing in the Legacy Controls have ramp rates that are relatively static. They can be changed only by reloading software. Smooth ramping of the machine is difficult because these parameters must be selected for some average situation (including magnet cycling) and not tailored to the actual ramp in use. It is planned to make these ramps adjustable on the new systems in Superbend.

7.1.3 New requirements

Resolution, Setability

-1 part in 60,000

Stability and Noise

-1 part in 60,000 long term
-1 part in 200,000 short term

The New requirements imposed by the Superbend Controls are stiff based on the physics requirements for beam location and stability. This led us to consider a digital interface to the supplies since routing analog signals of this type between systems is problematic and might lead to difficulty fixing the source of problems. With a digital interface it is up to the supply (one vendor) to perform once the command has been digitally sent.

7.1.4 Power supply review

- Recommended using 18-bit DAC
- Validated our proposal to use embedded controller in supply

A review of the power supply for the Superbend was held prior to the procurement going to the vendor. Action items from the review included moving to an 18 bit DAC (exceeding our 1:60,000 requirement slightly) and using digital controls to the supply.

7.2 Superbend supply controls design

-18-bit DAC (existing design)

- Embedded PLC in supply
    - Commercial hardware
- Standard Field Bus interface
    - DeviceNet (superset of CANBus)
- 10 hz control/readout

    50 hz loop, ramping step

The Superbend power supply vendor has an existing 18 bit design that exceeds our requirements at reasonable cost, we have specified that. They proposed an Allen Bradley embedded PLC in the design to implement the required DeviceNet. We chose DeviceNet after some research and discussion with others in the controls business. The DeviceNet consortium, led by Allen Bradley, has many hundreds of manufacturers, and many products are available. Our choice was not solely for the Superbend project, as we are seeking standards for access to I/O for many future projects and DeviceNet appears to meet that need.

The 10 hz readout and control is the standard capability of the ALS control system, so we require it here even though the Superbends cannot respond that quickly.

The 50 hz ramp rate was proposed by an AB engineer and our PLC programmer indicated this was a typical looping rate for a PLC of this type. The ramp step will make small cumulative changes to the DAC input according to the ramp rate set into the control registers. This will facilitate smooth ramping. As other magnet controls are upgraded they will all have the additional capability to set the ramp rate dynamically.

7.2.1 Scope of new controls

- DeviceNet
    - use commercial hardware and software
    - start this early

- PLC embedded software
    - work with vendor, get source code
- Superconducting/Cryo User Interfacing
    - alarm issues

To minimize the risk of delay associated with the unknown (to us) DeviceNet interfacing we are starting this work early (already). We will use commercial hardware and software for most of this effort, but it will require some software to interface with our EPICS based controls core. The developer is scheduled for training and we are proceeding to procure a DeviceNet Bus Analyzer to shorten our development times.

The PLC embedded software will be handled by the power supply vendor. They will supply us with source code but we do not plan to work at that level. We will work with the vendor to avoid surprises in the delivered system.

The User Interface will consist of a new application for the Superbends that folds the available controls information into one set of displays. There are many channels and relating them in a custom display is the most effective way for operations to work with them. Alarms are under discussion. Temperature trends could be alarmed since detection precedes beam loss and notification could be used to take action that could preclude beam loss.

7.3 ALS Superbend controls

7.3.1 Controls scope of work

- Step cPCI I/O card, chassis
- Superbend Power Supply Controls
- Superbend Diagnostic Controls
- Quadrupole Controls
- Control Room Application
- Systems Integration

The scope of controls work in the Superbend project includes work in six areas shown here. The actual I/O card is a slightly improved model of the one developed for Controls Expansion and Upgrades that is currently employed in the Third Harmonic Cavity system. The changes are primarily adding a serial eeprom memory to store calibration information onboard. This work is already underway. Parts procurement has begun even before the design changes are complete due to the lead times involved and the small design changes planned.

The superbend power supply controls will be a joint effort between us and the power supply vendor. This contract is already out, and we have already begun

developing our end of the DeviceNet interface. We expect to work closely with the vendor as he ramps up the PLC programming.

Superbend diagnostics include standard analog and digital inputs and outputs, and GPIB I/O. The one new item is the fast data acquisition for cryo monitoring. A number of channels will be monitored into a circular buffer 1024 in size at 1 to 10 hz. Receipt of a post-trigger will stop the data collection and subsequent readout will display trends immediately prior to the event.

Quadrupole controls are conventional for the control system but this will be the first time we have controlled quads with the new control hardware. Some software that currently exists on the ILC will have to be converted to run in the cPCI.

A Superbend Control Room Application is planned that will integrate the channels into coherent operator and engineering displays in the control room. Alarms are under discussion that would alert operations staff to dangerous trends in the cryo temperatures long before they endangered the stored beam in the machine.

Systems Integration is an important and significant piece of work that is always required to effectively commission the hardware and software.

7.4 Ramping the (Super) ALS storage ring

Ramping is done in small steps, currently 600 are used. These steps are defined to be small enough that any combination of supplies can be on either the pre- or post- step value without losing the beam. There is NO REQUIREMENT for synchronism within the step, only that all supplies are done at the start of the next step. At the current time (4/00) we are ramping in approximately 50 seconds across a hybrid of legacy (ILC) and new (IOC) controls without appreciable loss of beam.

The step rate requirement for the overall control system is 10/second.

The ramp time requirement for Superbend is NOT LONGER than pre-Superbend. This could be taken as 200 seconds (pre-fab), or 50 seconds (post-fab).

All new controls are capable of exceeding the 10/second rate (latency typically 2-10ms). The legacy controls have shared buffers that saturate depending on the number of updates required on a particular link, which is difficult to accurately predict, but they are handling the current rate.

Superbend Controls Ramping and Communications - The Superbend power supplies are to be controlled via DeviceNet. The conversion from ethernet (EPICS CA protocol) to DeviceNet occurs in the Compact PCI chassis, so the la-

tency to the power supply includes the 2-10 ms to reach the cPCI chassis, a couple msec CanBus latency, and then the 50 hz scan time of the power supply controller dominates the delay budget. The overall estimated latency is 5-30 ms for the Superbend supply. This can be somewhat mitigated by the ramping software sending the bend supply commands first. (Legacy controls take even longer, so an optimum order is legacy, Suberbend, new controls.)

7.5 ALS Superbends diagnostic monitoring

Diagnostics Signal and Bandwidth Specs
10 second 500 hz quench buffer proposed (7/99 review)

The new controls are already used in several applications that require 100 hz update. One is the Elliptical Polarization Undulator which requires 100 hz interpolated updates based on the positions of the Y and Z motions to two pairs of corrector magnets. The other 100 hz application is power supply ramping and filtering, implemented on new controlled power supplies including Main Bend, Main QFA, three Superbend QFAs and six SuperBend QDAs.

The plan for the SuperBend Diagnostic fast monitoring is to utilize this existing 100 hz capability to gather six signals - upper and lower coil voltages, and lead one and two voltages, with two spares. These will be gathered in a 5 second deep fifo continuously, and a post-quench trigger will trigger a delayed save to disk, producing a 5 second data window around the quench.

If it is found that higher bandwidth is required the Instrumentation group plans to attach a portable multi-channel system. Additionally, the control system data acquisition could be expanded to higher rates and more channels. The ADCs are 40 khz conversion so each set of four is converting at 10 khz in a cycle. Sampling these channels at 500 hz would require modest changes in the software.

7.6 ALS controls expansion

Significant Controls expansion is required for new projects such as Third Harmonic Cavities, and the Superbend project. The existing controls (ILC, CMM, DMM) are difficult to extend significantly - due to unavailability of components, limitations of the original design and obsolescence of the commercial subsystems (Intel Multibus). Various methods of controls extension have been employed in the past (VME, EPICS) so interoperation of this hybrid system had largely been addressed previously. The requirements for the expansion were chosen to also address the expected replacement of legacy systems at some future time, therefore the 3U rackspace density requirement was maintained, and compatible or readily adaptable cable plant as well. The ALS controls cable plant was required to enter the 3U chassis from the rear for serviceability, while cards are removable from the front. VME 3U chassis were investigated, and several

prototypes constructed. I/O density and rear cabling was problematic, and Compact PCI was found to be a better choice due to the availability of more than 220 pins for I/O to the rear. Commercially available Industry Pack (IP) rear pinout I/O cards were selected to allow flexibility in I/O board selection. IP cards are bus independent, with carriers available for VME, VXI, ISA, PCI, and other busses. A search of available I/O boards did not turn up a solution for our combination of I/O requirements that fit within the packaging density, so they were fabricated.

The legacy system consists of a 3U chassis that holds up to 6 each ILC modules (Intelligent Local Controllers), and each of those has four analog inputs and outputs, and 3.5 bytes of digital I/O. The Analog I/O is 16 bit, monotonic, and has tight temperature stability and linearity requirements (see spec.). An IP card was developed by Mike Chin to exceed these requirements for our use. (Mike was one of the developers of the ILC). Four of these IP I/O cards fit on a cPCI carrier board, and each has four analog inputs, two analog outputs, and two bytes of digital I/O. A rear transition PCB was developed to bring the signals out to the rear connectors, and the standard ALS controls connectors were used, with a small change to a compatible type for the booleans. Due to the size of these connectors only three rear transition modules will fit in a 3U chassis, but this provides more I/O than a full ILC chassis (except for serial and GPIB which are being handled separately).

In a 3U chassis there are 6 slots, one for the CPU, three for the transition modules. This leaves 2 slots free, however the rear panel space is full so I/O for these slots will be more problematic. Still, we have doubled the analog input capacity while meeting the analog controls and exceeding the digital I/O of the ILC chassis. This more than meets requirements.

The GPIB requirements for expansion are met with a different solution. The original ILC has a space for a piggyback module that can be either serial or GPIB. To handle new GPIB based instruments we employ a GPIB to ethernet adapter manufactured by HP. This unit was selected due in part to available software and is employed currently for a number of I/O devices including the main frequency synthesizer.

Serial I/O expansion is planned using an IP based octal-serial card. Software is in planning to support this card. It can be sited in either VME or cPCI, depending on the available slot proximity. The first use, in sector 11, will be in VME. This card can be installed on either a front or rear I/O transition card as needed.

Controls expansion has been developed and tested on a number of systems including the Third Harmonic Cavity, the Main Bend, the Main QFA, the three SuperBend QFAs, and (very soon) the Superbend QDAs. Ramping performance, noise and temperature stability are all acceptable and Accelerator Physics has been satisfied with the upgrade.

POWER SUPPLIES

8.1 Suberbend power supply requirements and specifications

8.1.1 Description

8.1.1.1 General

The power supply for the ALS super bend magnet requires high stability and repeatability performance compared to other existing power supplies at the ALS. These requirements are spelled out in the specifications. The specifications include a description of the normal operation and an appendix describing the digital interface requirements. In addition to regular power supply components, the supply includes current down circuitry. This circuitry ramps the magnet coil current down in a controlled fashion when an interlock chain is broken

8.1.1.2 Current ramp down

The Interlock chain consists of two independent circuits. A simplified diagram of these circuits is shown in the power supply specifications as figure 2. One circuit is a general interlock chain input circuit to the power supply. A breakage of this chain, or an AC line power failure results in a slow magnet coil current ramp down into a 30 milli-Ohm resistor. The rate of this current ramp has a maximum of ~3A/sec and is determined by the circuit L/R time constant. This time constant is 100 seconds, based on the calculated coil inductance of 3 Henry. A second interlock chain circuit is connected to the HTC lead over temperature and over current detection circuit. When this circuit detects a HTC lead condition that exceeds a preset threshold value, then a generated output command breaks the second interlock chain. This disconnect also results in a AC power down condition to the power supply. The coil current is ramped down into a 200 milli-Ohm resistor, resulting in a faster ramp down time constant of 15 seconds. In this case the voltage across the super conductive coil due to the Ldi/dt will exceed the internal super conductive quench protection circuit voltage and actually diminishes to the current ramp down time.

8.1.1.3 Magnet current

The Power Supply (PS) will be used to power a super conductive magnet. The PS is required to deliver a maximum current of 350A into an inductive load. The current is to be ramped positive or negative causing the PS output voltage to reverse in direction. The PS will operate in the first and fourth quadrant. The required output current is variable from 0 to 300A. The rate at which the current is

changed during normal operating conditions is about 1A/sec, while the maximum rate is 3A/sec. The operating current ramp shape is shown below in Figure 1.

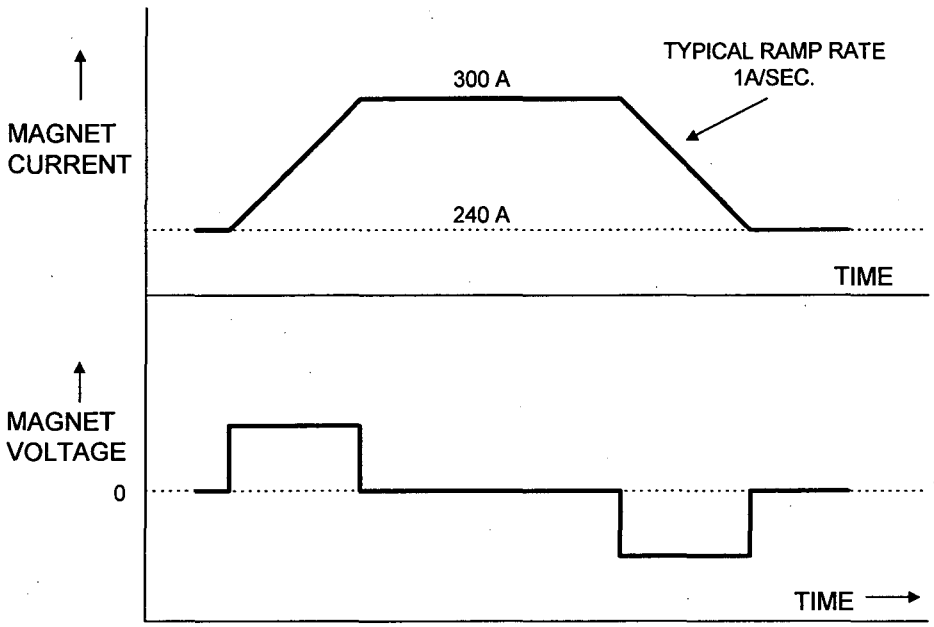

Figure 1. The operating current ramp shape and PS voltage is shown verses time.

8.1.1.4 Magnet inductance

The magnet coil inductance is variable and dependent on the magnet current. The magnet inductance is defined in a dynamic and static region. The dynamic inductance is present in the magnet current range of a few amps to about 40-50 amps, peaking at an inductance of 7H around 10 amps and dropping rapidly to 3.5H at about 50 Amp. In the static range of 50 to 300A the inductance is practically a straight line connecting the 3.5H point at 50A to 2.5H at 300A.

8.1.1.5 Magnet current ramp down

In case of a AC power interruption, the power supply current ramps the magnet current down via a resistor built into the power supply. The magnet coil current is diverted into the resistor via a relay-contactor. During normal operation, the maximum allowable current ramp down rate is 3A/sec. The voltage across the coil (due to -LdI/dt) at the high current levels, will be no more than 10 Volt. At the time the current has decayed to a value where the coil inductance is 7H (peak inductance) the coil voltage is a low value. A second ramp down circuit, shown in figure 2, with a current ramp down of 20A/sec is activated when a HTC over current or over temperature has been detected.

8.1.1.6 Power supply

The PS unit will be designed as a 6 pulse forced air-cooled, precision power supply with premium components to ensure excellent overall performance and high reliability. The units will be designed as a thyristor controlled precision unit which includes a single power transformer which feeds an individual 6 pulse thyristor bank consisting of six (6) devices arranged in a six phase star configuration. The output will be filtered via a 90 Hz filter to reduce the output ripple. The output of the assembly will pass through Zero Flux Current Transformer (ZFCT) as the current monitoring element to provide 0 to 350 Amperes, 0 to ± 15Volts DC output.

8.1.2 Specifications (apply after a 30 minute warm-up period)

Function	Specification	Comments
OUTPUT VOLTAGE RANGE	+/- 15V	Two quadrant supply (1 & 4)
OUTPUT CURRENT RANGE	0 to 350A	
ACCURACY	1 part in 1000 FS	Absolute accuracy of output current
REPEATABILITY / SETABILITY	1 part in 60,000 FS	The repeatability of the required output current
STABILITY or DRIFT	1 part in 60,000 FS	Time domain from 1 minute to 8 hours (ambient temperature is 22 degree C +/- 5 degree C)
RIPPLE OF OUTPUT CURRENT	1 part in 200,000 FS	Time domain to 1 minute for high frequencies
LINE REGULATION	1 part in 60,000 FS	Output current dependency on input voltage variation
LOAD REGULATION	1 part in 60,000 FS	Output current dependency on load variation
LINEARITY	<0.1 % of input control voltage	Output current versus input voltage
PROTECTION CIRCUIT REACTION TIME	<100 milliseconds	Time available for the internal PS protection circuit to react
QUENCH PREVENTION CIRCUIT	Contactor Activated	Actives during AC power interruption and HTC lead fault detection
SLEW RATE	3A/second	Current regulator (or program) response time
CURRENT RAMP-DOWN RATE (L/R=100Sec or 15 sec dependent on the cause)	3A/sec or 20A/sec	Slow ramp down after power interrupt detection. Fast ramp down after HTC lead over current or over temperature detection
CURRENT RAMP TRACKING ERROR 125-300A	<0.1% of FS (0.3A)	Error exist as a following offset error during current ramp in the range from 125A to 300A
STATIC MAGNET COIL INDUCTANCE	2.5 to 3.5 Henry	The static inductance is present in the current range of 50 to 300 A
DYNAMIC MAGNET COIL INDUCTANCE	7 Henry	The dynamic inductance is present in the current range of a few amps to about 40-50 amps
EXTERNAL LINE RESISTANCE	600 micro Ohm	Resistance includes the HTC maximum resistance
MEAN TIME TO REPAIR (after FAILURE)	<4 hours down time per failure	Power supply quality and reliability requirements affects price & performance
MEAN TIME BETWEEN FAILURE	5 YEARS	
CONSTRUCTION REQUIREMENTS	Modular construction	Modular construction for maintainability and reparability considerations

8.1.3 AC Input

208 Volts +/-10%, 3 Phase, 60 Hertz,

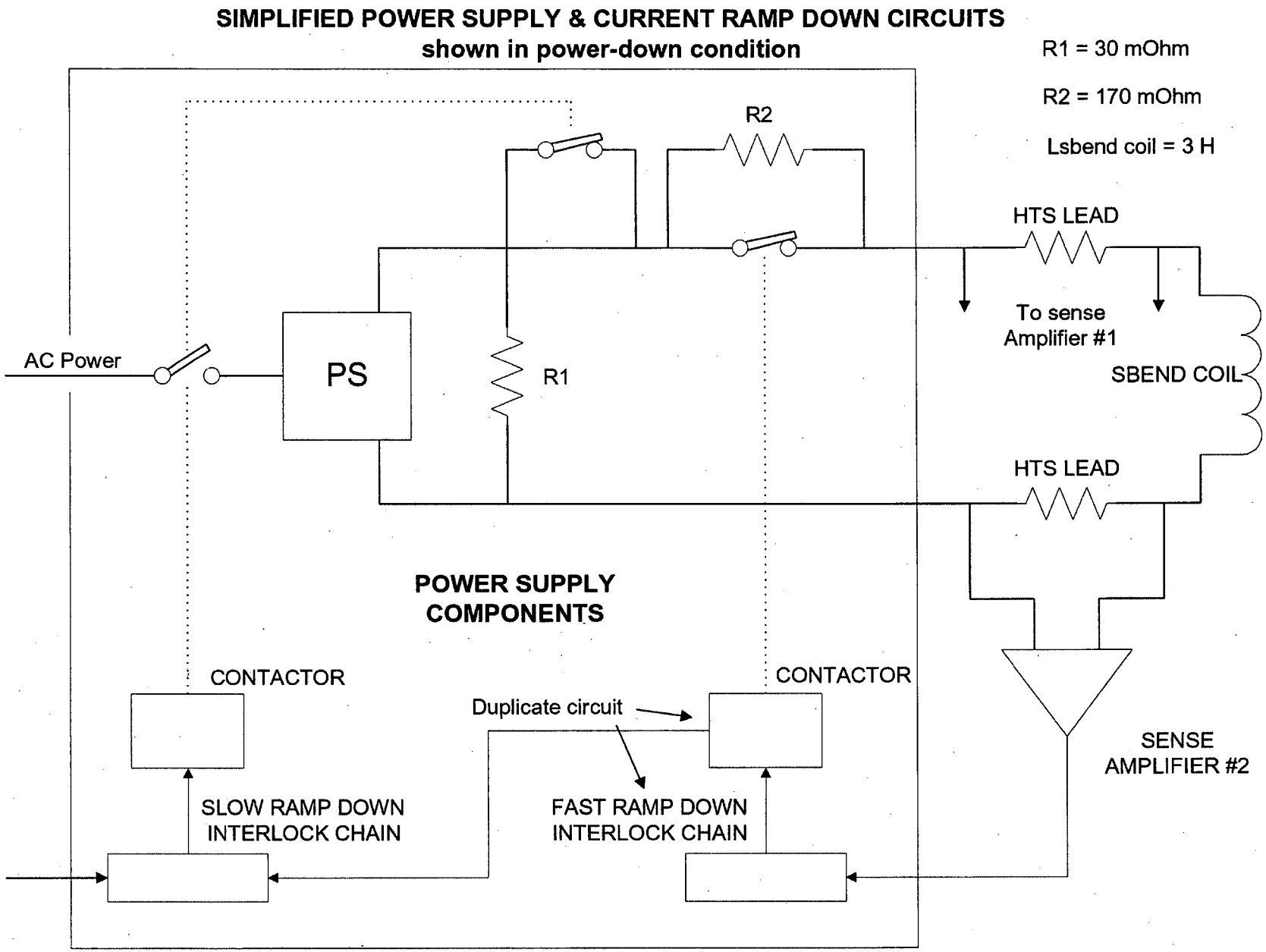
SIMPLIFIED POWER SUPPLY & CURRENT RAMP DOWN CIRCUITS
shown in power-down condition
R1 = 30 mOhm
R2 = 170 mOhm
Lsbend coil = 3 H
R2
HTS LEAD
To sense
Amplifier #1
SBEND COIL
AC Power
PS
R1
HTS LEAD
POWER SUPPLY
COMPONENTS
CONTACTOR
CONTACTOR
Duplicate circuit
SENSE
AMPLIFIER #2
SLOW RAMP DOWN
INTERLOCK CHAIN
FAST RAMP DOWN
INTERLOCK CHAIN

8.1.4 DC output

0 to +/-15 Volts, 0 to 350 Amperes

The power supplies will be designed to provide a constant current controlled output into the load specified in this specification. The output current is controlled locally with a zero to 10 Volt analog signal, or remotely with a digital control signal. The output over current trip level shall be adjustable inside the power supply. This adjustment shall be easily accessible to maintenance technicians or engineers. The PS will have a current monitor (read-back) with a range of zero to 10V. This signal will be short circuit proof and isolated from the PS internal electronics, thus when this monitor signal is shorted or grounded the PS operation will not be affected. This monitor signal is to be available on the rear and front panel. In the front panel this monitor signal will be available on a standard or floating BNC connector.

The unit will be designed to provide an envelope of uncertainty in the flattop of less than 1 part in 200,000 (5 ppm) encompassing ripple, Periodic And Random Deviations (PARD) and stability (for Line variance of +/-10% or Load resistance change of +/-10%) frequencies higher than 0.01666H (period <1 minute). Stability of the output current in the range of frequencies less than 0.01666Hz (period >1 minute) is specified as 1 part in 60000.

8.1.5 Ambient temperature

The power supply as specified will be operating in a controlled environment where the temperature is 22°C ±5°C. The power supply shall perform within the specifications over this temperature range. The unit will operate without failure within a temperature range of 10 to 40°C.

8.1.6 Rectifier components

The rectifier components are rated for 100% continuous full load service for a 10 to 40°C ambient, 5-95% relative humidity.

8.1.7 AC power switch

The units will be equipped with an electromagnetic contactor. The electromagnetic contactors will be employed to turn the units On/Off locally or remotely. A three position switch, "Local," "Remote" or "Off" selects PS control mode. In the local mode the power supply shall be controlled manually from the front panel or externally with voltage source of zero to 10V control. The ON/OFF operation shall be performed with front panel push buttons.

8.1.8 Main power transformer

All transformers are computer designed to provide optimum performance. The design of these units will incorporate a single main power transformer manufactured in the following manner:

Winding Material	Splice-free, electrolytically pure copper.
Core Material	Low loss, high quality, grain oriented silicon steel provides good flux transfer and low eddy current losses.
Insulation Material	220°C class insulation incorporating glass, fiberglass, and NOMEX insulation.
Process	The coils are vacuum impregnated by varnish and then baked to cure. Varnishing provides additional electro-mechanical strength and protection from the operating environment.

All coils are wound for stress distribution under fault conditions to provide superior mechanical strength.. Thermal switches will be supplied to trip the power supply off in the event of an overheating condition in the power supply.

8.1.9 Secondary thyristor regulation/rectification

The units will be designed as filtered secondary thyristor 6 pulse power supplies which feed an output filter. The bandwidth of the current loop is 5Hz and the corner frequency of the output filter is 90Hz. These characteristics will meet the 300 ppm tracking error specified on the ramp-down .The thyristors will be operated at extremely conservative values. The unit will enter the Fault state in the event of an over-temperature condition. Each pair of devices is protected by a snubber network to limit the voltage transients across the devices. Thermal switches will be employed to shut the unit off if the thyristors experience an overheat condition. After an over temperature condition has been detected, the shut off condition will be latched until the PS has been reset.

8.1.10 Power supply controls

8.1.10.1 Electronic controls

The current measuring device will be a Zero Current Flux Transformer (ZFCT) and will be used as the current feedback element. The electronics are equipped with the following features:

a) Automatic current control (ACC). Continuous output control, from 0% to 100% of the power supply current rating is provided. Regulation of better than 5ppm is supplied from 10% to 100% of the power supply current rating.

b) Thyristor firing indication. The hard fire gate pulses to the thyristors also drive LED's mounted next to the gate terminals. This convenient feature is used as a troubleshooting aid to indicate the presence of gate signals.

8.1.10.2 Electrical controls

The output current level will be set as proposed in this offer via a 0 to 10 Volt analog signal for use in local control mode, or with a digital control signal for use in remote control mode. The digital control is specified in the appendix of this document. The analog signal input is a differential input with a common mode rejection of at least 90dB. The analog control signal may or may not be connected to the local common ground or chassis ground.

The additional manual control instrumentation includes local (front panel) analog Voltmeter and Ammeter as well as ten turn potentiometers for local setting of the output current and voltage. Additional diagnostic pilot lights are provided for local annunciation of power supply status. The unit will be supplied with a current ramp down (spin down) resistor assembly to allow the magnet to re-generate into the resistor load in the event of a main power failure or an external interlock chain disconnect shown in the simplified circuit (figure 2). The unit will be equipped with contactors such that the input to the power supply is disconnected from the AC supply lines and the resistor (30 mOhm) assembly is connected across the PS output terminals upon the loss of power (or interlock chain breakage). In addition to the power-failure-current-ramp-down resistor, a ramp down resistor of the value 170 mOhm shall connected in series with the 30 mOhm in case of a HTC lead fault is detected. The ramp down circuits (excluding the resistors) shall be independent; Two HTC lead interlock input connectors and contactors shall be installed (with the contact switches connected in series. The stored energy ((1/2)*I^2*L) in inductance of the super conductive magnet is ~185kJ, based on the value of 3 Henry and a maximum current of about 350 A. The ramp down resistor R1 duty cycle will be no more than 10%, which means that the power supply will not be turned back on for 15 minutes, after a power interrupt has occurred. A PS internal timer shall be installed to prevent the PS to be turned back on within this 15 minute resistor cool down period. The ramp down resistor R2 duty cycle is 1% or less, no internal watchdog timer is required for this duty cycle factor.

8.1.10.3 Digital monitor & indicators

In addition to the standard, supplied by the manufacturer, a number of digital monitor channels and interlock chain connectors are required as well as front panel light indicators. These are shown below:

Function	Digital data link	FP LED indicator	Comments
Power Supply Ready	YES	YES	
Power Supply ON/OFF	YES	YES	
Transformer Temperature monitor		YES	
SCR temperature monitor		YES	
AC over current		YES	
DC over current		YES	
Ground fault detector		YES	
Door interlock		YES	If applicable
Interlock chain detector		YES	2 RP connectors

8.1.11 Sound level

Less than 75 dB at full load measured on an "A" weighted scale, three feet from equipment.

8.1.12 PS construction

The DC output terminals will terminate inside the enclosure. The AC input power and DC current output terminals, mounted inside the power supply, shall be accessible with a removable panel for installation, maintenance or repair service. Lifting lugs or crane hooks, connected to the structures frame, shall be provided.

The output terminals shall not be grounded and not connected to the control electronics common.

All 208 V or 110 V line power wiring shall be kept separate from the lower voltage wiring.

The exterior of the cabinet shall be painted with a good grade of paint of color Federal Standard Color number 23578 (beige). All external meters, connectors and breakers shall be labeled according to their function with black silkscreen lettering.

The PS shall be manufactured according to the standards published in and defined by the American National Standards Institute (ANSI), The National Electrical Manufactures Association (NEMA) and the Institute of the Electrical and Electronic Engineers (IEEE).

A nameplate with the following information shall be attached to the front of the PS:

Manufactures Name
Serial number
Date of Manufacture
LBNL specification number
KVA rating
Input AC Voltage
Output DC Voltage
Output DC Current
Weight

8.1.13 Air cooling

Air-cooled units use totally enclosed ball bearing motors to drive shrouded fan blades, delivering a maximum volume of air over the heat sinks and transformer. An internal sub-panel separates electrical control components such as contactors, relays and electronics from the air stream. The resistor assembly will be rated for convection cooling. Overheating detection devices shall turn off the PS when component overheating occurs.

8.1.14 Safety & interlock

The PS shall be constructed in accordance to industry safety standards. Interlock connectors (Burndy type) shall be provided on the rear panel to provide for three external PS interlock capability. One connector shall be labeled "slow ramp down interlock", while a second pair of connectors shall be labeled "fast ramp down Interlock" The interlock circuit shall require an external relay contact closure that, when closed, will allow AC line power to be connected to the PS. The operational interlock chain voltage shall be in the range of +12V to +24V.

8.1.15 Testing & documentation

The power supply will be designed to provide the highest in reliability and production. The units will adhere to the ISO 9001 certification and will employ the standards outlined and required by ISO 9001 in the production of these units. Complete testing documentation will be supplied and LBNL will be advised of the testing milestones to allow for witnessing of said tests if desired.

The testing procedure for these units will be submitted by the manufacturer prior to commencing the testing for LBNL's review. The manufacturing facility will be open for review during the entire scope of the project for LBNL inspections and

witness testing. At LBNL the unit may be tested into an inductive load or a resistive load. The load condition is predetermined with a jumper connection on the regulator board to ensure the regulator to be stable under both load conditions. This connection will be clearly marked.

Operating & Instruction manuals will be supplied which will include the installation instructions, performance parameters, maintenance procedures, spare parts list and circuit diagrams. All PS components mounted on printed circuit boards, components mounted individual and modules shall be labeled, corresponding with the parts on the drawings and spare part lists for easy troubleshooting and maintenance. All cables and cable harness shall be labeled. One set of drawings and manuals will be provided as hard copies and one set on 3.5 inch floppy disks of which the format is acceptable to the Lawrence Berkeley National Laboratory.

The documentation shall include:

Installation instructions
Theory of operation
Recommended test procedures
Signal waveforms time diagrams for testing troubleshooting purposes
Routine maintenance schedules
Data sheets of crucial unorthodox parts
Data sheets of the semi conductors used
Factory test procedures and results

Acceptance tests: The unit(s) will be shipped after having been completely tested in accordance with the requirements and specification of this document.

8.1.16 Superbend power supply controls specifications

The current control digital to analog converter shall meet the following specifications:

18 bits precision
0.5 LSB linearity
monotonic to 18 bit level
settle to ½ LSB within 50uS
0.25 ppm per degree C (Temperature controlled unit)

The analog monitor of actual power supply current (from DCCT signal) shall meet:

16 bits precision
monotonic to 16 bit level

0.01% maximum nonlinearity
5 ppm per degree C temperature stability

The interface between the control system and the power supply shall meet:

DeviceNet 2.0 specifications

The parameters of the interface shall include (details below):

current control register
current ramp rate control register
maximum current limit control register

DAC input readout register
actual current readout register (from DCCT ADC)

supply ON boolean control
supply OFF boolean control
supply RESET boolean control
supply REBOOT boolean control

supply READY boolean monitor
supply ON boolean monitor
supply REMOTE boolean monitor
supply RAMPING boolean monitor

supply ERROR CODE multibit boolean monitor
other miscellaneous supply status boolean, multibit, etc. monitors...as available

Control rates and throughput

The control interface will be cycled at up to 10 Hz. A cycle is to include:

read status booleans
read DAC input
read actual current
set ramp rate limit
set current

Interface PLC characteristics

The interface PLC is to scan inputs and outputs and perform control computations at 50 Hz. The timing of this loop is to be consistent within 10% due to the ramping rate control requirement.

Ramping is implemented by the power supply PLC. At each iteration through the control loop it calculates the new DAC output based on the previous setting, the desired setting, the ramp rate limit, and the maximum current limits, apply the result to the DAC.

A watchdog reset is to be generated by hardware if rounds not completed on schedule. This will cause power supply shutdown and controller reset and will leave a code in the error register that indicates a watchdog timeout occurred.

Documented PLC source code in machine-readable format and on paper is to be included in the deliverable.

Safety issues

The power supply can only energize when:

1. the supply is READY (all subsystems ready including external interlock inputs).
2. a supply ON boolean control command is received (if it fails to energize at this moment, or trips off for any reason, it can not come back on without a RESET and a new ON command).

When the supply trips off it requires RESET before becoming READY again, either via the interface or via a front panel RESET button.

Miscellany

There must be no date dependence for correct operation. Any dates used in the system must include a four-digit year, and algorithms must be correct for 1999-2100 period.

This specification is the controls part of the complete Power Supply Specification.

8.1.17 Superbend control parameters details

The interface parameters are a combination of booleans and multibit values up to 18 bits in precision. Due to the values exceeding 16 bits in size, 32 bits were chosen for all values for consistency. These may be signed or unsigned (vendor choice) but should be consistent (and all should be signed and all should be unsigned).

Due to the control loop performance, the status booleans should be grouped such that they can be read efficiently with a minimum of network transactions.

The reading and writing of the parameters is specified from the network perspective.

Interface parameters detailed (DeviceNet application object attributes)

Current control register

32 bit
readable and writable (from network perspective)
power-on default: 0

The current control register is et by the main control system to the final current desired of the main power supply. The supply will ramp to this current (subject to the constraints of ramp rate and maximum current). This value can be changed while ramping is in progress, affecting the next 50 Hz ramping computation.

Current ramp rate control register

32 bit
readable and writable
power-on default: 0

The current ramp rate control register set the maximum change in the current control DAC input that the controller may make during each 50 Hz update cycle. This value may be changed during ramping, affecting the next 50 Hz ramping computation.

Maximum current limit control register

32 bit
readable and writable
power-on default: 0

The maximum current limit control register sets the maximum value that will be allowed to the current control DAC input. Requested values greater than the maximum will result in the maximum value.

DAC input readout register

32 bit
readable
power-on default: 0

The DAC input readout indicates the actual value the DAC is converting to analog.

Actual current readout register

32 bit
readable

Reads actual current reported by ADC from the DCCT.

Supply ON boolean control

control strobe
writable
power-on default: OFF

The supply on control sets supply ON mode and requested current to zero if all conditions are met.

Supply OFF boolean control

control strobe
writable
power-on default: OFF

Clears supply ON mode, setting supply to OFF.

Supply RESET boolean control

control strobe
writable
clears error status bits (if conditions have been corrected)
returns supply to READY state (if conditions have been corrected)

Supply REBOOT boolean control

control strobe
writable
returns supply and controller to power ON sequence

Supply READY boolean monitor

readable
true indicates supply subsystems and external interlock inputs are all ready to turn on

Supply ON boolean monitor

readable
true indicates supply is ON and ramping or delivering the requested current

8.2 QFA and QDA power supplies

Item	QFA	QDA
Required current stability	(+/-) 0.01% or 1 part in 10,000	(+/-) 0.01% or 1 part in 10,000
Feedback element	Resistor	Resistor
External current sense	DCCT	DCCT
Output voltage & current	35V, 550A	55V, 130A
Power supply connections	2 magnets per PS	1 magnet per PS
Number of PS to be ordered	4	6
Preliminary quotation	$31,000	$13,000

8.3.1 Sector 4 layout

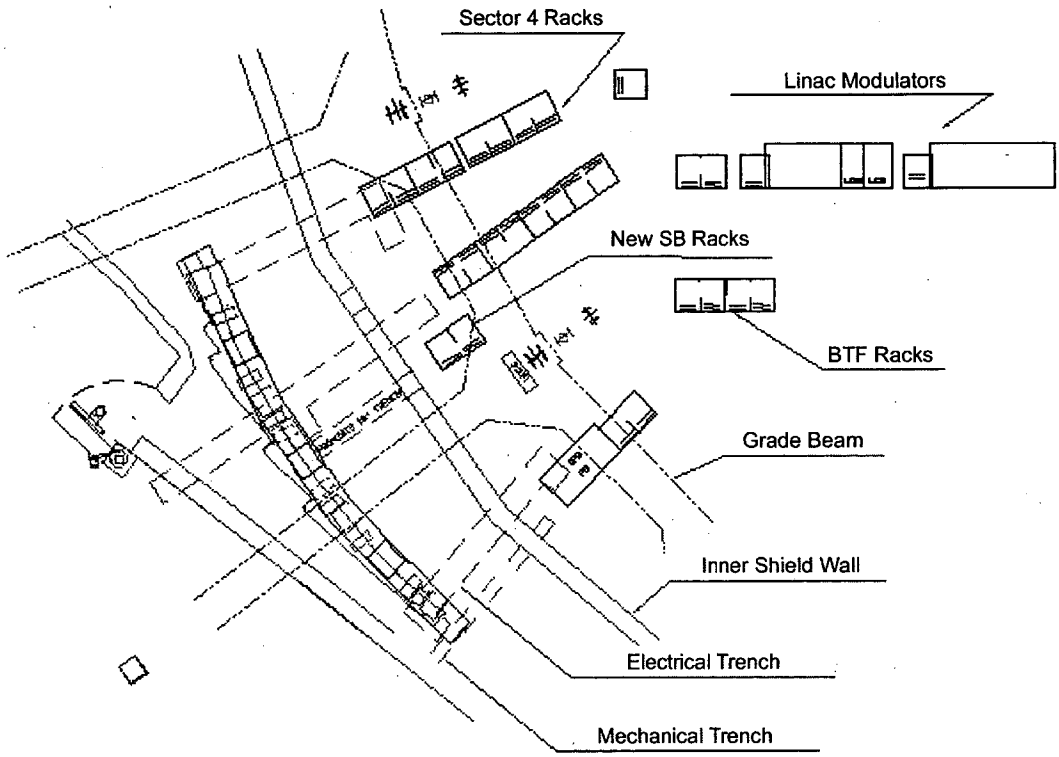

8.3.2 Sector 8 layout

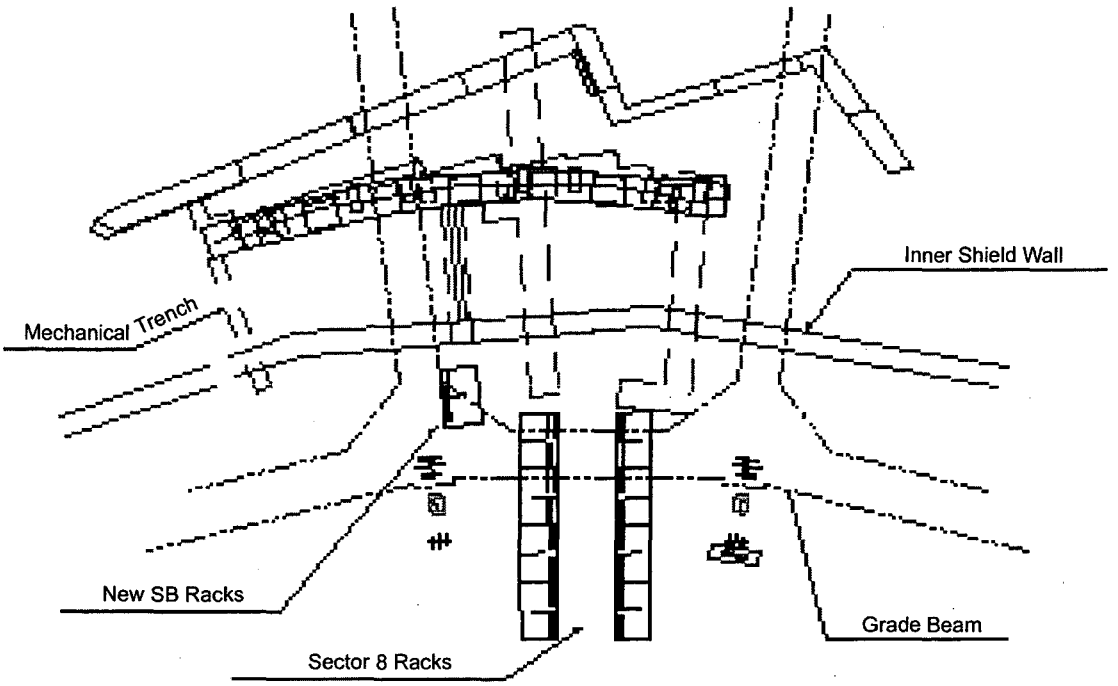

8.3.3 Sector 12 layout

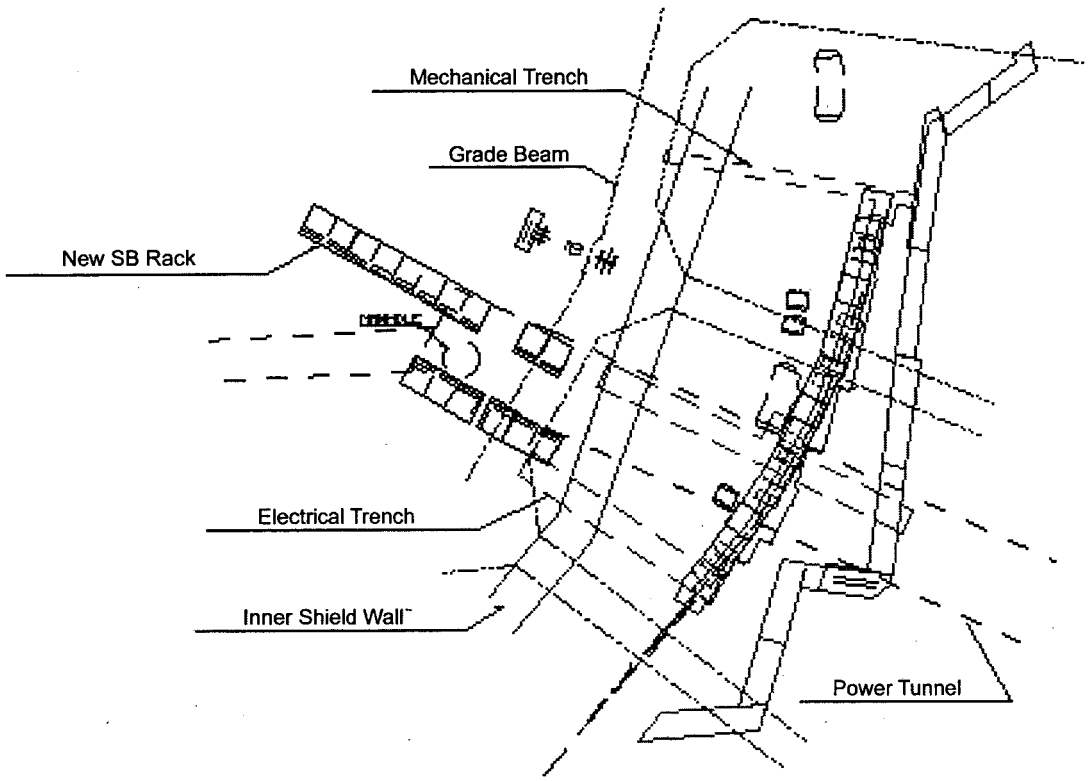

MAGNET AND CRYOSTAT DIAGNOSTICS

Superbend magnet reliability is critically important to the successful operation of the Advanced Light Source. Accordingly, several diagnostic systems are installed in the magnet cryostat to monitor Superbend system performance, to warn of potential problems, and to aid in diagnosis of a faulty cryostat or magnet.

9.1 Quench Management

Superbend magnet coil and high temperature superconductor (HTS) lead quenches are expected to occur rarely. If a coil does quench during high current operation, its stored energy must be safely dissipated, and coil voltages must be limited to non-destructive levels. Vendor supplied voltage clamps internal to the cryostat limit coil voltage to about 30 V per coil. Several silicon diodes in series establish the clamping level. At room temperature the voltage required to forward bias a silicon diode into conduction is about 0.7 V. At 4° K this voltage rises to approximately 5 V. In normal circumstances the magnet power supply cannot deliver sufficient voltage to forward bias the cold diodes, so no current is expected to flow in the diodes as the magnet is charged and discharged. However, during a quench coil voltage will rise above the clamp potential and cause substantial current to flow in the diodes. This current flow heats the diode junctions, and as they are heated, their forward voltage drop falls to less than 1 volt each. This is an avalanche condition that will disable a Superbend magnet for many hours before it can be cooled and operated again.

The HTS leads bridge the thermal gap between the 4° K coils and the 70° K power supply input leads. Normally the voltage drop across these leads is much less than 1 mV at full current. If the HTS leads become normal, the magnet current will destroy them if it is not quickly shut off.

Quench detection electronics external to the cryostat monitor voltages developed across the coils and HTS leads. If the difference between coil voltages exceeds approximately 1 volt, a quench is assumed to be in progress and the power supply is shut down. If voltage across an HTS lead exceeds approximately 1 mV, the lead is assumed to be going normal, and the power supply is shut down. In addition to turning off the power supply, the quench detection electronics control switches in the power supply. These switches insert resistors in the magnet current path providing a load for energy discharge. Additional voltage monitors across the clamp diodes and resistors permit monitoring of quench protection circuit current.

The quench detection electronics are critically important and must be as fail-safe as possible. To insure that the voltage monitor circuit path is continuous, a small bias voltage is applied to each monitor wire. If a cryostat lead should fail or if the

cable connecting the quench detection electronics to the cryostat should be disconnected, the power supply will be disabled.

See Fig. 1 for a simplified diagram of the power supply, magnet, and quench detection electronics. Table 1 explains the various quench scenarios and normal magnet energy management.

9.2 Magnet Field Monitoring

Two Hall probes capable of measuring 6 T fields are installed in each cryostat. The function of the probes is to provide an absolute field reading, which is scaled to the maximum field in the center of the magnet. The field reading is used rather than the magnet current for the operating set point because of the effects of magnet field hysteresis and remnant field.

The probes are mounted in a machined groove in the outer cryostat wall. Two probes are used for redundancy since removal of a cryostat for probe replacement is not desirable. Each probe has a sensitive area of 1 x 0.05 mm. The probes are not positioned in the area of maximum field. They are under the magnet pole tip in a field of 4.5 T at 1.9 GeV. The probe is a Group 3 model MPT-141 which is connected to the Group 3 DTM-151 Teslameter. Absolute accuracy of the magnet field reading is ± 0.01% of the reading plus 0.006% of full scale at 25° C. Resolution is 2 μT to the accelerator control system. The data rate is 10 Hz via the IEEE 488 bus. Temperature stability of the probe is ± 10 ppm of the reading per °C maximum. The temperature in the storage ring tunnel is very tightly controlled, so the probe temperature coefficient does not contribute a significant error.

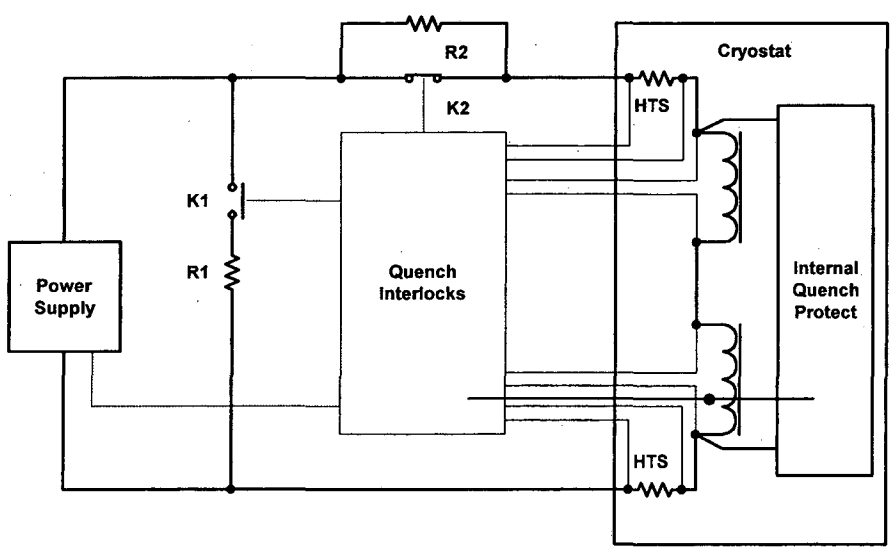

Figure 1 Magnet quench circuits. Contactors shown in normal, running positions.

Condition	Power Supply	Shunt Switch K1	Series Switch K2	di/dt	Magnet Quench
Superbend Off	Off	Close	No change	-3A/sec	No
AC Power Loss	Off	Close	No change	-3A/sec	No
HTS Quench	Off	Close	Open	-20A/sec	Yes
SB Quench	Off	Close	Open	-20A/sec	Yes
SB Coil Temp.	Off	Close	No change	-3A/sec	No
HTS Temp.	Off	Close	No change	-3A/sec	No
Compressor Off	No change	Open	No change	NA	No
Crash Off	Off	Close	No change	-3A/sec	No
Cryostat Pressure	On	Open	No change	NA	No

Table 1. Quench scenarios.

9.3 Magnet Temperature

Several Lakeshore Cernox temperature sensors are attached to the magnet core, HTS leads, and the cold cryostat components. Cernox sensors are used because of low sensitivity to ionizing radiation and magnetic field. Redundant sensors on the core indicate the temperature of the superconducting magnet coils. The sensors are biased and read out by a Lakeshore model 218 scanner. This instrument has adjustable set points for relay actuation. The Superbend magnet power supply is interlocked with magnet temperature via the scanner relays. The interlock set point is 4 °K. The power supply may not be operated unless the magnet coils are in a superconducting state.

9.4 HTS Lead Temperature

The upper (warmer) ends of the HTC leads are monitored with Cernox temperature sensors identical to those near the coils. The sensor scanner interlock relays are set to trip at 80 °K. These relays are in the magnet power supply external interlock chain and will trip the power supply off if the leads become too warm.

9.5 Magnet Coil Voltage Monitor

Normally the magnet coil voltage is zero, even with full current. If the current is changed, a voltage is developed,

$$V_{coil} = -L\,di/dt$$

where L is the coil inductance. By carefully controlling the current rate of change and measuring the instantaneous coil voltage one may obtain a measure of dy-

namic coil inductance. If a coil develops shorted turns, this measurement will be useful in diagnosis.

9.6 Cryogenic Level Measurement

American Magnetic Inc. cryogenic level sensors are installed in the cryostat. The LN sensor is a capacitance-based measuring device. The LHe sensor is superconducting. An AMI model 186 Liquid Level Instrument measures the level of LN and controls filling valves. The AMI model 136 Liquid Helium Level Controller measures the superconducting probe resistance and also controls filling valves. Both instruments are connected to the accelerator control system for data collection.

9.7 Errant Photon Beam Protection

The powerful photon beam created in the Superbend magnets is hazardous to the vacuum chamber when the beam orbit is vertically offset by more than 3 milliradians from the mean orbit. Electron beam position monitors (BPM) approximately ½ meter on both sides of the magnets continuously monitor horizontal and vertical beam position. Interlock electronics trip the accelerator RF off, aborting the electron beam if the vertical beam position changes by more than 1 mm in either BPM. This interlock is automatically activated when stored beam exceeds 200 mA average current.

9.8 Cryostat Pressure Monitoring

An ion gauge pressure monitor continuously monitors cryostat pressure. If the pressure rises above 1 e-4 Torr, the ion gauge controller trips off creating an alarm.

9.9 Cryostat Heaters

Two 5 W (100 V, 0.05 A) resistive heaters are installed on the cryogenic cooler. They are periodically used to heat the cooler as a method to prolong its life.

ACCELERATOR TEST PLANS

10.1 Introduction

For the accelerator physics test the goal is to minimize the commissioning and subsequent "teething" time that the users experience after the Superbends are installed. Therefore it is important to identify and attempt to study as many of the possible issues prior to installation as possible. In this section we discuss the accelerator physics studies that we expect to perform in preparation for operation of the ALS with Superbends. First we will discuss the installation plan. Next we will outline the issues that we wish to test. Finally we will discuss the detailed test plan.

10.2 Installation plan

There will be two major shutdowns of the machine in preparation for Superbends. The first will occur in February and March of 2000 and the second will occur in mid 2001.
Except for the Superbend magnets that will be installed in the 2001 shutdown, many of the other systems will already be installed in the 1999 shutdown or in two-day shutdowns in between the major shutdowns:

- The QDA quadrupoles will be installed.
- The QFA quadrupoles surrounding the Superbends will be decoupled by adding new power supplies and moved to the new control system.
- The 18 remaining QFA quadrupoles will be powered on the old supply but will be moved to the new system
- The normal bending magnets will be moved to the new control system
- New BPM buttons and electronics surrounding the Superbends will be installed.

10.3 Accelerator physics concerns

What are the concerns when operating with the Superbends? In general operation with the Superbends will be more complicated than present operation. In particular

- The bends will be decoupled which can give rise to larger orbit motion and distortion. We are particularly concerned with the impact on injection, ramping and orbit stability (See section 3).

- We will have more "knobs" to adjust. There will be 3 additional bend power supplies and 9 more quadrupole power supplies
- Periodicity breaking will reduce the stable operational region in tune space. We are particularly concerned with the impact on injection, ramping, and lifetime (See section 3).
- We have limited experience operating the machine with nonzero dispersion in the straight section. We would like to experimentally quantify the impact on emittance, lifetime, injection and ramping.
- The BPM system maybe necessary to detect and abort missteered beam in the Superbends. We have yet to use the BPM interlock system during operation.

We can only know the "actual" effects of the Superbends for certain after they have been installed (such as the effects on orbit jitter and whether the control system performs sufficiently well). However many of the other issues can be tested earlier.

10.4 Accelerator physics tests (prior to commissioning)

10.4.1 Stability of the normal bend magnetic field

As mentioned in section 3 the field jitter in the normal bend needs to be sufficiently small in order to have acceptably small orbit jitter. The tolerance on the field jitter for the normal bends is the same as that for the Superbends, which is 1 part in 160,000 at 1.9 GeV. There was a concern that the normal bend power supply, which was specified at 1 part in 50,000 would not be sufficiently good.

In order to determine if we had sufficiently small field jitter, a measurement was made of the power supply [1]. The actual field jitter (especially at high frequencies) would be less than the power supply jitter due to induced eddy currents in the beam chamber. So the power supply jitter measurement was considered a conservative number. The measured power supply jitter from 0.01 to 100 Hz was +/- 0.0056 Amps at 900 Amps (Bend current is about 900 Amps at 1.9 GeV) or 1 part in 161,000 which was much better than the specifications and sufficiently good for Superbend operation.

10.4.2 Reproducibility of the normal bend

As mentioned in section 3 it is important for ramping between 1.9 and 1.5 GeV that the bend field is reproducible to 1 part in 1000. If the reproducibility is worse than this it is difficult to ramp the magnets based

solely upon a lookup table and one has to use another scheme - possibly use field measurements or orbit feedback.

With all bends on one power supply (the condition without Superbends) non-reproducibility in field results in changes in beam energy but not changes in orbit. So one method to measure the field reproducibility would be to measure the reproducibility in beam energy from fill to fill.

The beam energy is measured in the machine to very high precision (2 x 10^{-5}) through resonant depolarization [2]. This technique relies on the following principle: The electron beam tends to naturally become polarized over time due to the emission of synchrotron radiation in the bends. The Moller or intrabeam scattering cross section is a function of the degree of polarization of the beam. Thus when the beam becomes depolarized there is a change in the lifetime. This change in lifetime can be more than 10%. By resonantly driving the beam transversely at different frequencies and precisely determining at which frequency the beam becomes depolarized, allows one to determine the energy of the beam (since the spin precession frequency only depends on the beam energy).

In the experiment the beam was depolarized using the transverse feedback kickers and both the lifetime as well as count rates in beam loss monitors were measured to detect the precise driving frequency at which the beam became depolarized. The relative energy change

- $< 2 \times 10^{-5}$ fill to fill
- $< 5 \times 10^{-5}$ within a day
- $< 2 \times 10^{-4}$ within a week

These changes are small compared with 10^{-3} that is required for Superbend operation.

10.4.3 Hysteresis loop for the normal bend

In order that the orbit excursions are sufficiently small during ramping it is important to know precisely the current to field transfer function for the normal bends so that they can be matched to the Superbends. For the final operation this match will probably be done empirically by ramping the beam and adjusting the Superbend fields to minimize the orbit distortion. However it is important to have a good first guess for the map before hand.

Extending the energy measurement method in section 11.3 measuring the energy of the beam at different points along the ramp we hope that it is possible to map out the hysterisis curve rather precisely.

10.4.4 Ramping with the new control system

As discussed in section 3, energy ramping in with the Superbends will become more complicated than without Superbends. In addition to the larger number of families and the decoupling of the dipoles the ALS will be in the middle of moving to a new control system (see section 7). In the February 2000 shutdown, 5 power supplies will be moved from the old to the new control system – Normal Bends (1), QFAs (4). Shortly after the shutdown the 6 QDA's will be connected and controlled by the new control system. The rest of the magnets will remain on the old control system. With the exception of the 6 QDA power supplies (which can be switched off during operation), the new control system has to immediately work in concert with the old control system if we are to ramp the machine and run at 1.9 GeV for users. It should be noted that the new control system has already been used to control the third harmonic cavities.

Therefore the initial tests of the new control system with beam will occur just following storage ring startup after the February shutdown. There will be more than a week scheduled for startup. It is important that we know within a time span of 4 or 5 days that we can inject, store and ramp the beam with the new control system in place. If we encounter problems at that time we will still have enough time to switch back to the old control system and to come back for users.

Due the fact that QDAs are not an integral part of operation, we can always commission them at our leisure during accelerator physics shifts in 2000.

Thus in 2000 we will have experience running the machine with many of the magnet families of magnets on the new control system. The only remaining magnet families to be commissioned will be the Superbends.

10.4.5 Characterizing the zero dispersion lattice with 3 fold periodicity

One of the issues of concern is the impact on the dynamics reducing the storage ring's natural 12-fold periodicity down to 3. It is possible to use the new QFA and QDA families to artificially perturb the ring's natural 12-fold periodicity to approximate what operation will be when running with the Superbends. We will initially need to determine through modeling how the quadrupole fields need to be adjusted to best approximate the conditions with the Superbends.

One method for determining this is to start with a Superbend lattice and compute a response matrix. Then one takes a lattice without Superbends and adjusts the QDA and QFA quadrupoles in such a way as to minimize

the difference in response matrices between the lattice without Superbends and the lattice with Superbends. This is one possible method. There are certainly other ways to adjust the magnets.

After choosing some values for the quadrupoles one needs to see how well this artificial case actually approximates the nonlinear dynamics case with Superbends. A good way to compare the dynamics is through simulated frequency map analysis [3]. By numerically generating and comparing frequency maps of a lattice with and without Superbends one sees the generation of resonances and can determine how well the two will actually compare. Hopefully it is possible to end up with a model whose dynamics is similar to the Superbends.

Up to this point all the work has been done on paper. Now it is possible to simulate operation with the Superbends on the ALS. The first experiments would involve adjusting the quadrupoles to the desired values, checking that one has actually gotten the proper values through response matrix characterization [4], and experimentally measuring a frequency map and comparing it to the model frequency map[5].

One can then make other tests of the machine performance. The horizontal aperture can be measured. This is important for injection and we can determine what kind of margin exists. We can ramp the machine with these detuned quadrupoles and see how difficult it is. We can try to characterize the impact on lifetime and dynamic momentum acceptance and see whether the results are in agreement with predictions. We can also observe the possible impacts if insertion devices further perturb the periodicity.

10.4.6 Characterizing machine performance with nonzero dispersion

One interesting possibility is to operate the ALS with some finite positive dispersion in the straight sections in order to reduce the emittance and dispersion in the arcs. As discussed in section 3 operating with finite dispersion reduces the horizontal emittance (close to a factor of 2). It is important to characterize the performance of the machine in that operational mode. We need to look at the reduction in emittance and the impact on injection and lifetime. Also with the new power supplies it is possible to see if there is an impact when the periodicity is perturbed.

10.4.7 Betatron tune feed forward compensation for the insertion devices

As mentioned in Section 3, the stable operational region in tunespace will be reduced when operating with the Superbends. Presently we experience

large tuneshifts when the insertion devices move. This is already undesirable since tune changes translate into beam size changes as the tune moves closer or further from the linear coupling resonance. These tune changes may become more serious with the Superbends because the reduced operational region in tunespace.

There is a known relation between gap and tune change for each insertion device. Since the total tune change will be sum of the tune change from each of the insertion devices one can calculate the total tune change by knowing only the gap changes. So one can read the gap positions, determine the tune change and adjust quadrupole magnets to compensate the tune. This is called tune feed forward compensation.

There are two possible difficulties with feedforward compensation. The first is that the quadrupoles can cause orbit changes in addition to tune changes. If the quadrupoles move slow enough the orbit changes will be compensated with the global orbit feedback system that was commissioned in 1999. So this problem may not be too serious.

The second possible problem has to do with tune drifts. It may be possible that over a long 1.5 GeV run where the quadrupoles are frequently adjusted up and down the tunes slowly drift away. Since we are feeding forward on the tunes and not feeding back, we would not take care of this. (Because the present tune measurement system perturbs the beam it is not desirable to measure the tunes during normal user operation.) This is something that can be tested in a physics shift by artificially moving the insertion devices very quickly over wide ranges and feeding forward on the tunes. We can see how much the tunes move. If necessary the development of a new tune measurement schemes will be sped up to enable tune feedback.

We should commission a tune compensation feed forward system prior to the Superbends being installed in the storage ring.

10.4.8 Preparation for difficulties establishing stored beams

When the Superbends are first turned on it may be difficult to capture the beam. This was the case when the storage ring first turned on. It will be important to gain additional practice with the turn-by-turn beam position monitors (FADs) which are in the ring in the event that we have trouble. We may want to artificially put in errors in the machine and see if we can diagnose them with the FADs in the event that there is trouble.

10.4.9 Preparation for accurate alignment of the orbit

The ideal orbit of the beam will pass through the center of the QFA and QDA quadrupoles both on the upstream and downstream sides of the Superbends. Therefore it is necessary to determine the position of the center of the QFA and QDA quadrupoles. This is done through beam-based alignment of the QFA and QDA magnets. For beam-based alignment of the QFAs we need to finish commissioning of the QFA shunts. Each QDA quadrupole can be individually adjusted so there is no need for shunts for beam-based alignment. In doing this we will be able to put the beam through the center of the QFAs and QDAs in the Superbend sectors simultaneously and determine the best position for the orbit in the Superbends.

10.4.10 Test the Superbend EPBI system

It is most likely that we will require the BPMs surrounding the Superbends to limit the maximum excursion of the beam to prevent excessive heating of the beam chamber. Therefore we will need to test the beam abort system when using the BPMs surrounding the Superbends. This can only be done after the new buttons and electronics are installed.

10.4.11 References

[1] G. Portmann, M. Chin, J. Hinkson, D. Robin, "Bend Magnet Power Supply Stability," LSEE 127 (June, 1999)

[2] J. Byrd, P. Kuske, and C. Steier, "Precision beam energy measurement using resonant depolarization in the Advanced Light Source," work in progress

[3] J. Laskar and D. Robin, "Application of Frequency Map Analysis to the ALS," Particle Accelerators 1996, Vol. 54. pp. 183-192

[4] D. Robin, J. Safranek, and W. Decking, "Realizing the benefits of restored periodicity in the Advanced Light Source," Phys. Rev. Special Topics – Accelerators and Beams, Vol. 2 (1999)

[5] D. Robin, C. Steier, J. Laskar, and L. Nadolski, "Global Dynamics of the ALS Revealed Through Experimental Frequency Map Analysis," LBNL-44760 (2000)

UTILITIES

11.1 Utilities - General

The primary access route for utilities associated with the Superbend storage ring modifications is shown in Figure 1. Magnet power cables, signal cables, and the cryocooler compressor lines will enter the storage ring through 6 inch diameter holes drilled through the storage ring inner radius shielding wall at each Superbend sector. The utilities will then lay in a 24-inch wide by 6-inch high tray near the shielding roof. Magnet power cabling will be routed from the tray to the magnets on the outer radius side of the electron beam center line to avoid blocking lines of sight for survey and alignment. The holes through the inner radius shielding wall will be located to avoid the internal re-bar and spaced at least 24 inches from any pin location on the inner radius shielding wall. The tray will span the distance between the inner and outer shielding walls and be supported at the ends only, so that the shielding roof can be removed without disturbing the utilities in the tray. The trays will be positioned approximately 24 inches down stream from the Superbend and will have dividers separating the magnet leads, low voltage control wiring and the lines from the cryocooler compressor.

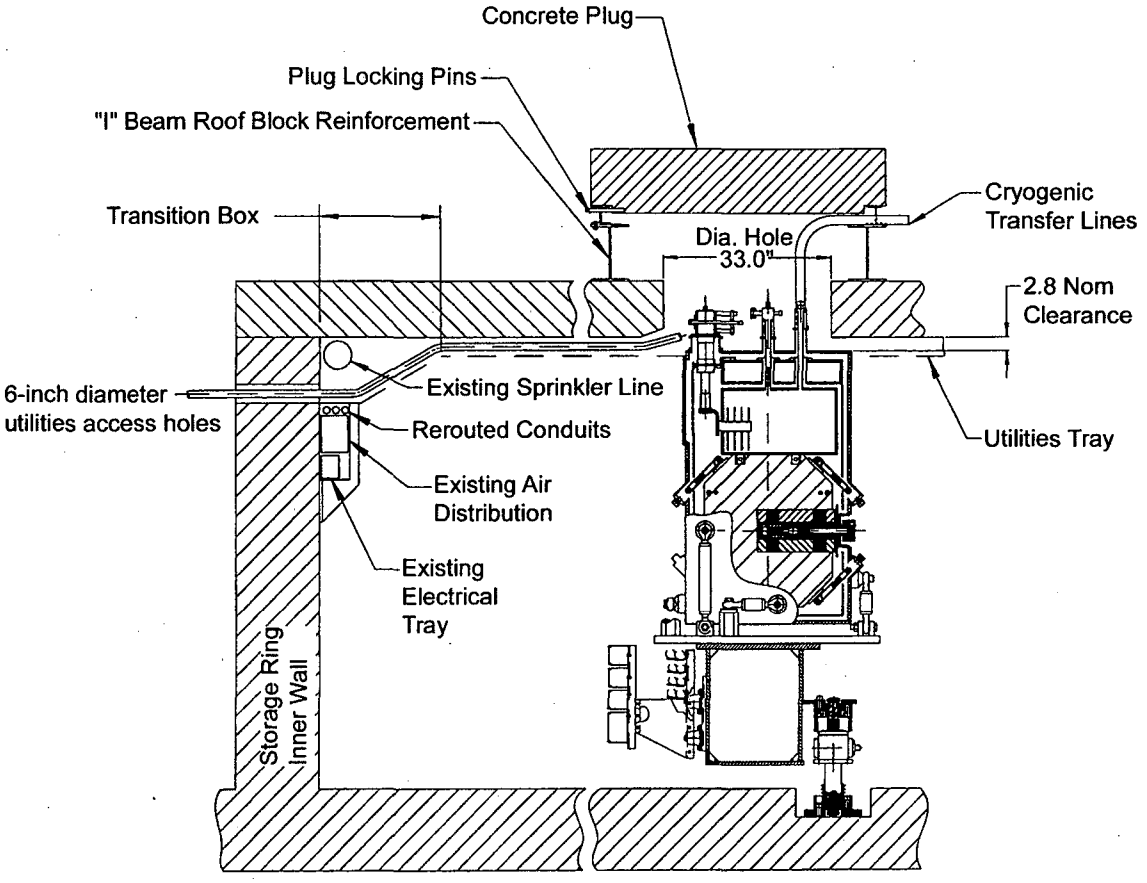

Figure 1. Storage Ring Cross-section at Superbend Magnet

A 33-inch diameter hole will be drilled through the existing roof shielding to provide access to the connections on the top of the Superbend cryostat. The roof shielding block will have a reinforcement frame around the 33-inch diameter hole to provide adequate strength to the roof shielding block as drilling the 33-inch diameter hole will cut through existing internal re-bar. There will be a removable spacer on top of the reinforcement frame to provide space for cryogenic transfer lines to exit the storage ring. There will be a Concrete Plug over this hole to provide adequate radiation shielding. See Figure 1.

11.2 Utilities - Quadrupoles QFA

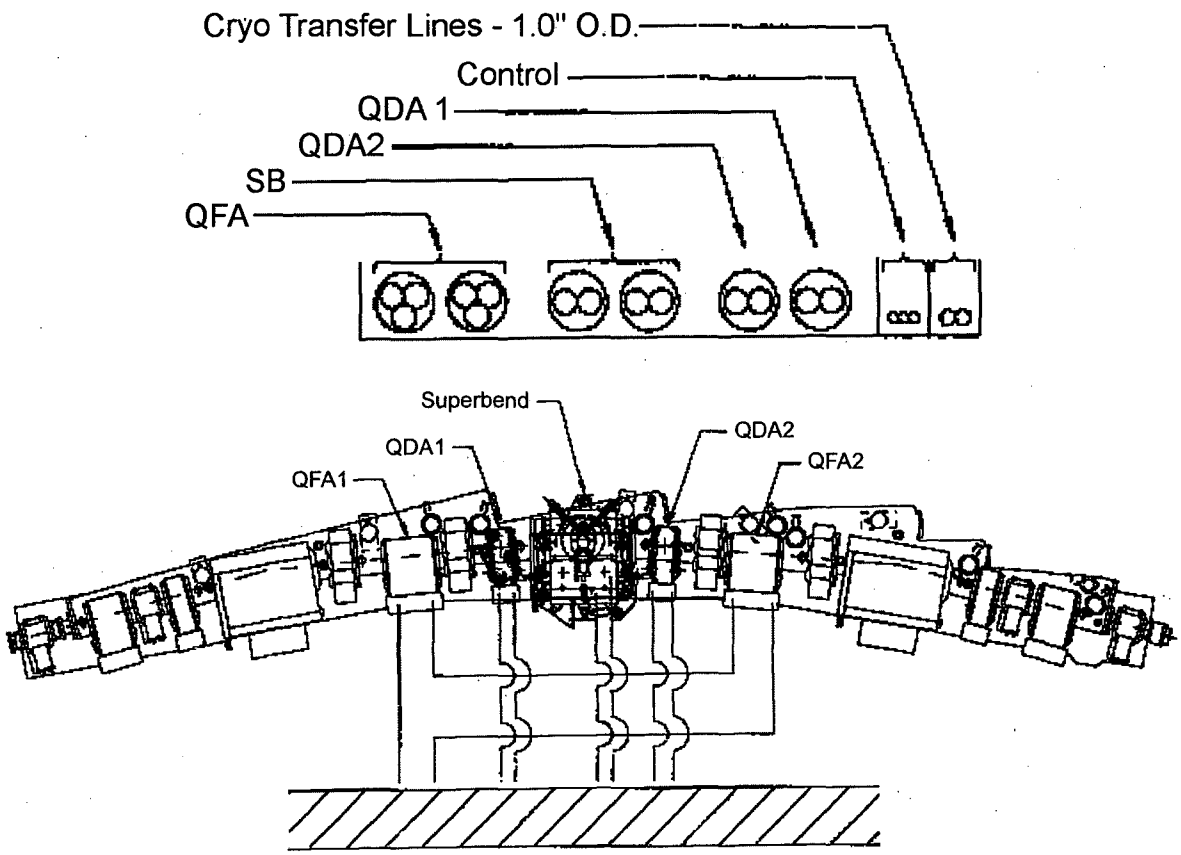

Magnet	Number of conductors in cable	Conductor gauge	Cable O.D. inches	Cable Type	Cable lbs/ft.	Cable Current Rating Amps	Cable Voltage Rating Volts
QFA1 & QFA2	3	#3/0	1.45	TC	1.988	600	600
QDA1 & QDA2	2	#2/0	1.09	TC	0.810	130	600
SB	2	#1/0	1.26	TC	1.144	350	600

Figure 2. Cross-section through Superbend Utilities Tray

The two existing Quadrupoles, QFA1 and QFA2, at each Superbend sector will be removed from the existing series wiring of all storage ring QFAs. The existing

wiring will be jumpered at each Superbend sector to remove these two quadrupoles and to leave the remaining storage ring QFA Quadrupoles in series. QFA1 and QFA2, at each Superbend sector, will be wired in series to a single power supply. See Figure 2.

The power supply for these two QFA Quadrupoles will be located in a rack inside the inner radius shielding wall of the Storage ring. The conductors from power supply to Quadrupoles will enter the storage ring through 6-inch diameter holes drilled through the storage ring inner radius shielding wall. See Figures1 & 2.

11.3 Utilities - Quadrupoles QDA

The two new Quadrupoles, QDA1 and QDA2, at each Superbend sector will each be powered by a separate power supply. See Figure 2.

The power supplies for these two QDA Quadrupoles will be located in a rack inside the inner radius shielding wall of the Storage ring. The conductors from power supply to Quadrupoles will enter the storage ring through 6-inch diameter holes drilled through the storage ring inner radius shielding wall. See Figure1.

11.4 Utilities - Superbend

Each Superbend Magnet, will be powered by a separate power supply. See Figure 2. The existing gradient magnets will be removed from the series wiring of all gradient magnets and the existing cables will be jumpered to preserve the series wiring of the remaining gradient magnets.

The power supplies for the Superbend Magnets will be located in a rack inside the inner radius shielding wall of the Storage ring. The conductors from power supply to Quadrupoles will enter the storage ring through 6-inch diameter holes drilled through the storage ring inner radius shielding wall. See Figures1 & 2.

11.5 Utilities - Cryogenic

Each Superbend Magnet will be cooled by a cryocooler. The compressor for the cryocooler will be located inside the inner radius shielding wall of the Storage ring. The supply and return compressor lines to the cryocooler will enter the storage ring through 6 inch diameter holes drilled through the storage ring inner radius shielding wall. See Figures1 & 2.

Each Superbend Magnet will be capable of being rapidly cooled by use of liquid Helium and liquid Nitrogen. Each magnet will also be capable of running on liquid cryogens in the event of cryocooler failure. The Helium and Nitrogen transfer

lines will be routed from the top of the cryostat, through the new 33-inch diameter hole in the shielding roof and to appropriate dewars on top of the roof shielding. See Figure 1. Bayonet type connections will be used at the Cryostat to transfer line interface so that the transfer lines and the main roof shielding block can be removed without warming of the cryostat or loss of insulating vacuum.

11.6 Utilities - Miscellaneous

Control and signal wiring will enter the storage ring through 6-inch diameter holes drilled through the storage ring inner radius shielding wall. See Figure1.

Control and signal wiring include: Hall probe signals, Cryostat heater signal wiring, Interlock wiring, and cryostat ion gauge wiring.

Ernest Orlando Lawrence Berkeley National Laboratory
One Cyclotron Road | Berkeley, California 94720

Prepared for the U.S. Department of Energy under Contract No. DE-AC03-76SF00098